NASA CONTRACTOR REPORT 177426

Passive Orbital Disconnect Strut (PODS-IV) Development

I. Spradley

Prepared for
Ames Research Center
Under Contract NAS2-11946
September 1986

National Aeronautics and
Space Administration

Ames Research Center
Moffett Field, California 94035

FOREWORD

This work was conducted for the National Aeronautics and Space Administration (NASA) through the Ames Research Center, Moffett Field, California, Dr. Peter Kittel, Program Manager.

The Lockheed Research & Development Division conducted the program within the Cryogenic Technology Group of the Thermal Sciences Laboratory. Key individuals who contributed to this program are:

- A. Holmes - Designed filament assembly stand
- R. Gardner - Performed load-deflection testing and data reduction
- J. Nickel - Assembled PODS-IV support

I. E. Spradley
Principal Investigator

PRECEDING PAGE BLANK-NOT FILMED

CONTENTS

Section		Page
	FOREWORD	iii
	ILLUSTRATIONS	vi
	TABLES	viii
1	INTRODUCTION AND SUMMARY	1
	1.1 Introduction	1
	1.2 Summary	1
2	PODS-IV DESIGN CONCEPT	4
3	TASK 1 - PODS-IV DESIGN	7
	3.1 Design	7
	3.2 Structural Analyses	7
	3.2.1 Structural Model	23
	3.2.2 Strain Limitations	27
	3.3 Thermal Analyses	29
	3.4 Side Load Resistance	30
4	TASK 2 - FABRICATION	33
	4.1 PODS-IV Components	33
	4.2 Filament Assembly	34
	4.3 Nut/Collar Assembly	38
	4.4 Strut Assembly	39
5	TASK 3 - TESTING	42
	5.1 Test Articles	42
	5.2 Nut/Collar Testing	42
	5.2.1 Test Article and Setup	42
	5.2.2 Nut/Collar Test Procedure	46
	5.2.3 Nut/Collar Test Results	46
	5.3 Single Strut Side-Load Testing	49
	5.3.1 Side-Load Tests	49

CONTENTS (Cont.)

Section		Page
	5.3.2 Test Setup	50
	5.3.3 Single Strut Test Results	50
6	CONCLUSION AND RECOMMENDATIONS	58
	6.1 Conclusions	58
	6.2 Recommendations	59
7	REFERENCES	60
Appendixes		
A	LOAD-DEFLECTION TEST RESULTS	61
	DISTRIBUTION LIST	76

ILLUSTRATIONS

Figure		Page
2-1	PODS-IV Support Concept	4
2-2	PODS-IV Modification Concept	5
3-1	Support Strut Assembly	8
3-2	Filament Support Ring	9
3-3	Collar	10
3-4	Launch Tube	11
3-5	Orbit Tube	12
3-6	Body, Cold End	13
3-7	Body, Warm End	14
3-8	Stem	15
3-9	Nut	16
3-10	Adjustment Bushing	17
3-11	Length Adjustment	18
3-12	Large Clamshell	19
3-13	Small clamshell	20
3-14	Jam Nut	21
3-15	Radiation Shields and Spacers	22
3-16	PODS-IV Side-Load Mechanism	23
3-17	Comparison of Composite and Invar Thermal Expansion Values	25
3-18	PODS-IV Cooldown	25
3-19	PODS-IV System Displacement Due to Load F	26
3-20	Predicted Strand Resistance at Operating Temperature	27
3-21	Maximum Strand Shorting Strain	28
3-22	Maximum Resultant Strand Shorting Force	28
3-23	Filament Size for a 10% Increase in PODS-III Heat Rates	31
3-24	Effect of Filament Size on Heat Rates	31
3-25	Side-Load Resistance for a 10% Increase in Heat Load	32
3-26	Side-Load Filament Sizing	32

ILLUSTRATIONS (Cont.)

Figure		Page
4-1	Filament Assembly Stand	35
4-2	Whiffle-Tree Schematic	36
4-3	Load Cell	36
4-4	Actual Whiffle Tree Assembly	37
4-5	Filament Assembly	38
4-6	Nut/Collar Assembly	40
4-7	PODS-IV Support	40
4-8	PODS-IV Side-Load Mechanism	41
5-1	Load-Deflection Test Setup	43
5-2	Nut/Collar Assembly in Hex Holder	44
5-3	Filament Ultimate Load Test Setup	45
5-4	Filament Load Versus Displacement Results (290 K)	48
5-5	Filament Load Versus Displacement Results (77 K)	49
5-6	Length Adjustment Bar	50
5-7	Side-Load Test Setup	51
5-8	Test Setup With PODS-IV Installed	52
5-9	PODS-IV Support Side-Load Mechanism	52
5-10	Shorting Side Loads as a Function of Location and Angle	55
5-11	Shorting Side Loads Model-Data Comparison	56
5-12	Side-Load Shorting for a Six Support System	57

TABLES

Table		Page
3-1	Typical Properties of Filaments	24
3-2	Composite Elastic Modulus Values GN/m^2 (10^6 psi)	24
5-1	Nut/Collar Load-Deflection Data	47
5-2	PODS-IV Side-Load Data	53

Section 1
INTRODUCTION AND SUMMARY

1.1 INTRODUCTION

The Passive Orbital Disconnect Strut (PODS) support system was developed under contract NAS2-10848 (Refs. 1,2,3,4). Struts were analyzed, designed, fabricated, and tested structurally and thermally. Tests on a single strut included thermal conductance to helium temperature, thermal expansion data, loads to thermally short out the strut, ultimate loads, evacuation rates, and fatigue tests at liquid-nitrogen temperature. Load tests on a set of six struts included axial and side-load tests and the effect on strut shorting of simulated asymmetric temperatures of the vacuum shell. Modal vibration tests were performed at frequencies consistent with Space Transport System (STS) qualification requirements and principal resonant modes of the strut system.

The major shortcoming of the PODS-III design is lack of side-load resistance to thermal shorting. A conceptual PODS-IV design to increase this resistance was previously described (Ref. 3). The objective of this program was to further develop this design and build and structually test a PODS-IV support. The test data were then compared to previous data and predicted performance to verify the improvement in side-load resistance.

The PODS-IV support is the current selection for supporting the 1580-1 superfluid helium tank on the Gravity Probe-B program and the Lockheed Superfluid Helium Independent Research Dewar. Other missions where the PODS-IV supports may be used include SIRTF, LDR, OTVs, Space Station, and other NASA and DoD missions.

1.2 SUMMARY

The objectives of this program were:

(1) to design structurally and thermally a mechanism to increase PODS resistance to side loads
(2) to fabricate the mechanism and modify a PODS-III support into the PODS-IV configuration
(3) to structurally test both the side-load mechanism and strut to determine improvement in side-load resistance.

TASK 1 - DESIGN

A mechanism was designed to support the launch tube cold end against side loads due to vapor-cooled shield shrinkage and MLI weight. The design considered consists of a invar collar, a invar filament support ring, and graphite filaments. The filament support ring is pressed onto the existing PODS-III nut, and the collar is slid over the cold-end stem. The filaments are wrapped around the collar and support ring tangs.

TASK 2 - FABRICATION

Four test specimens were assembled. The first was a nut/collar assembly wrapped with 700-fiber filaments. The other specimens were constructed from a PODS-III support built under contract NAS2-10848 modified to the PODS-IV configuration using different bonding techniques on 700-fiber and 1000-fiber filaments. (The 700-fiber filaments were hand separated from supplied 3000-fiber filaments, while the 1000-fiber filaments were used as supplied by the manufacturer.) An assembly stand was constructed to wrap the filaments by loading the filaments equally through a whiffle-tree arrangement of pulleys, ball joints, and sliders.

TASK 3 - TESTING

Initial load tests were conducted on the nut/collar assembly as a function of nut displacement with respect to the collar. These deflections were conducted at 30-deg intervals around the nut circumference and ranged between ±0.030 cm (0.012 in.). One ultimate load test was conducted on the filaments at

liquid-nitrogen temperature. Side-load tests were conducted on the PODS-IV support using the test apparatus built under NAS2-10848 for single struts. Side loads were measured as a function of placement along the launch tube and inclination angle of the strut. Placement side loads were also measured around the support circumference to determine concentricity and uniformity in filament side-load resistance. The results of these tests were compared to PODS-III results (Ref. 3) and predicted values based on strut dimensions and properties.

Section 2
PODS-IV DESIGN CONCEPT

Figure 2-1 presents the PODS-IV support concept. A minimum of six struts (three pairs) is required to support a cryogen tank. (Six struts provide a statically determinate support system in all axes.) As the tank diameter changes due to cooldown or pressurization, the angled pinned-end struts are free to move in and out as the tank moves up or down slightly a value of H. A similar adjustment occurs automatically as the vacuum shell changes diameter in orbit due to temperature changes.

For purposes of installation, the warm end of the strut provides a length adjustment feature. The threads on the rod-end fitting and length adjustment are a different pitch; consequently, by rotating the adjustment hex, precise length adjustments can be made during strut installation without rotating the

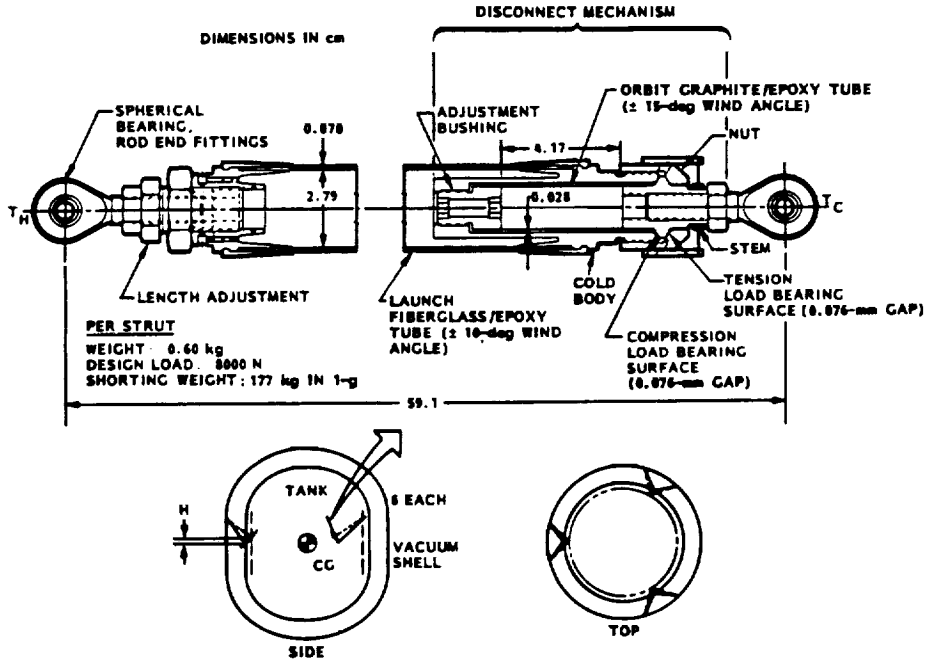

Fig. 2-1 PODS-IV Support Concept

strut. This feature allows length adjustments after the vapor-cooled shields are attached to the struts.

The cold end of the strut provides the passive orbital disconnect feature. The cold rod end fitting/stem is connected to the body by a thin-wall fiberglass or graphite/epoxy orbit tube and adjustment bushing. A collar is slipped over the stem and is connected to the nut by fiberglass or graphite filaments shown in Fig. 2-2. The collar is designed to have a 0.0025-cm (0.001-in.) gap with the stem at ambient temperature. The conical stem load-bearing surfaces are separated from the nut (tension) and body (compression) by an axial gap of 0.0076 cm (0.003 in.) at operating temperature. At ambient temperature, the gaps are set to take into account the differential shrinkage between the various parts. During one-g thermal test or orbital flight, the conical surfaces are prevented from touching by this spacing and the filaments. Consequently, heat is transferred from the body to the cold rod end fitting/stem subassembly by radiation and by conduction along the orbit tube and filaments.

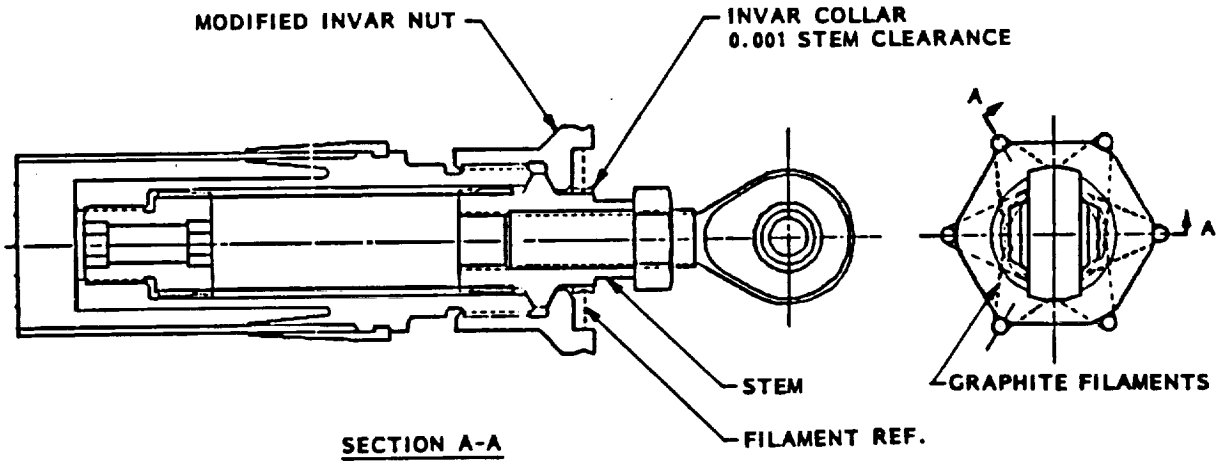

Fig. 2-2 PODS IV Modification Concept

During launch, the g-load elastically deforms the orbit tube along its axis; the conical shoulder of the stem rests hard on the body (compression) or nut (tension). The load path bypasses the orbit tube. The major thermal resistance and load path during launch are now the launch tube. Upon achieving orbit, the conical shoulder of the stem passively disconnects from the body or nut. Side loads on the launch tube due to shield cooldown may or may not engage the side-load resistance mechanism. If the side loads are sufficient enough to engage the mechanism, the collar presses against the stem and the filaments are elastically deformed to resist the load. The major thermal resistance is then the thin-wall orbit tube and filaments. If the side loads are not sufficient enough to engage the mechanism, the collar remains isolated from the stem and the major thermal resistance is again the thin-wall orbit tube.

This design combines the desirable features of a thermal disconnect during ground hold and orbit with the high reliability of a completely passive design. Since the struts do not short out in one-g, the orbital performance of the struts can be demonstrated in one-g thermal qualification tests, and the ground hold heat leak is lower. These are both highly desirable features. References 1, 2, 3, and 4 provide details of prior analyses, design, fabrication, and stuctural and thermal test results.

Section 3
TASK 1 - PODS-IV DESIGN

3.1 DESIGN

Figure 3-1 shows the assembly drawing of the PODS-III support. Figures 3-2 and 3-3 show the two components (filament support ring and collar) required to update the PODS-III support to a PODS-IV. The filament support ring was increased from the three-tang concept shown in Ref. 3 to a six-tang. The reasoning for this change will be discussed in Section 3.2.1. Figures 3-4 through 3-15 present the detail drawings of the remaining parts. The design is identical to that recommended for flight struts except that the filament support ring and nut should be combined into one part.

3.2 STRUCTURAL ANALYSIS

When a side load is applied to the launch tube, it displaces the nut radially toward the stem, effectively decreasing the stem gap until shorting occurs. The PODS-IV mechanism is designed to resist this motion while limiting the increase in heat load through the support. The PODS-IV system includes a nut with tangs, a collar, and filaments. Figure 3-16 shows the system schematic. The collar slips over the stem with a set clearance. The filaments are wound between the tangs and collar. The load is transmitted when the collar bears on the stem, elastically deforming the filaments. The resulting strain places the filaments in tension, resisting the displacement. The filament resistance increases as displacement increases until stem shorting occurs. Filament diameter size is determined by side load and heat load requirements. Filament length is determined by strain limitations.

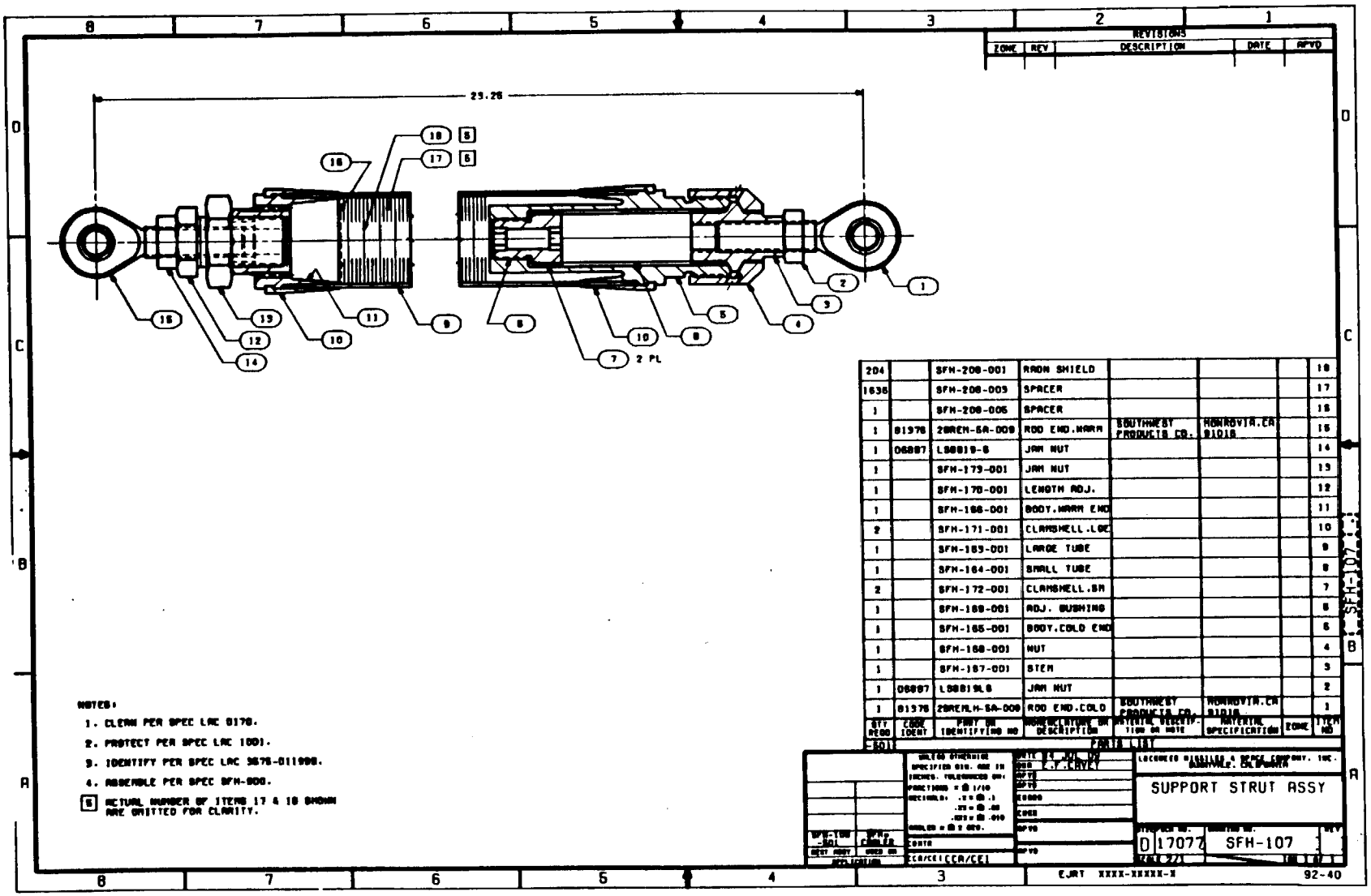

Fig. 3-1 Support Strut Assembly

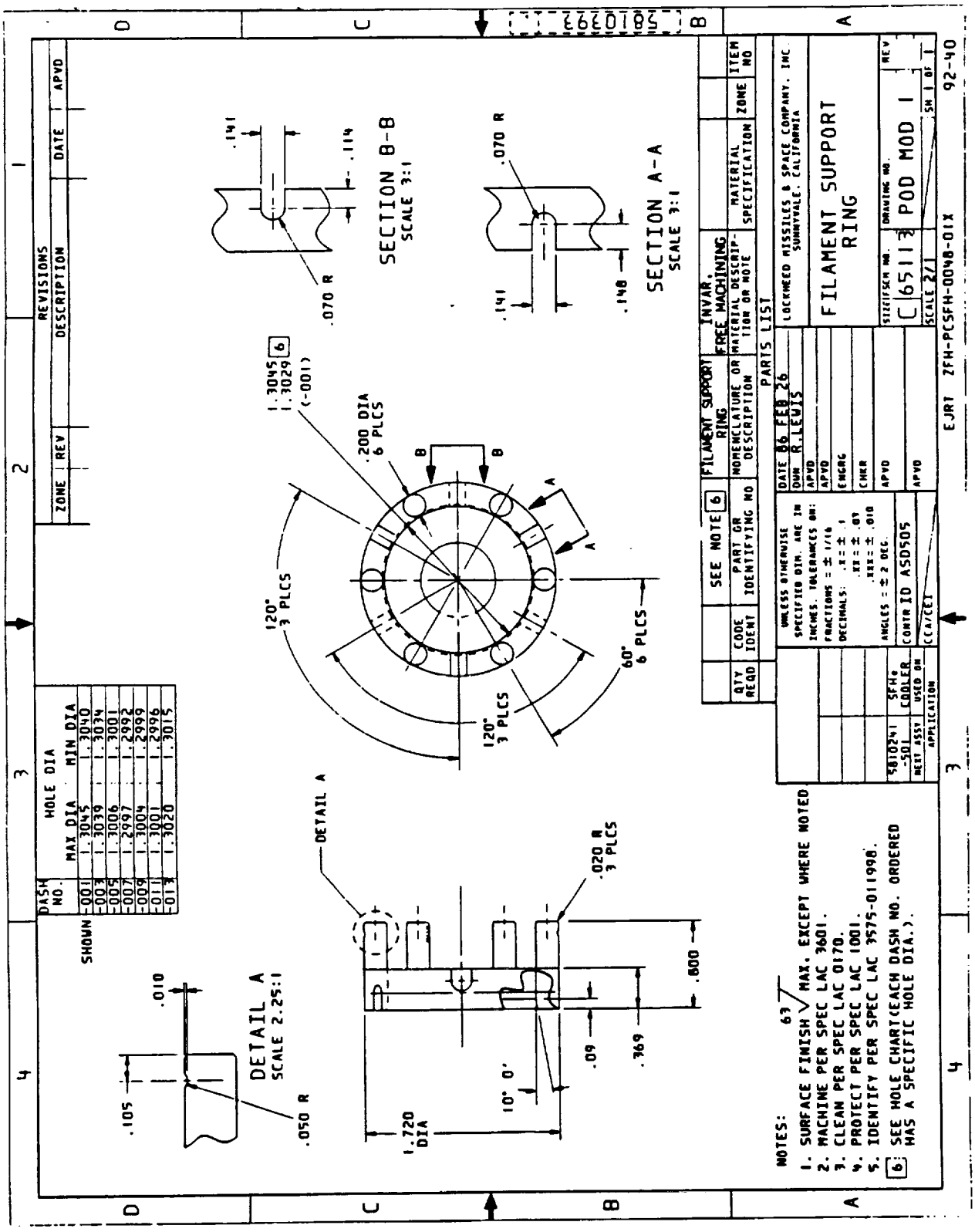

Fig. 3-2 Filament Support Ring

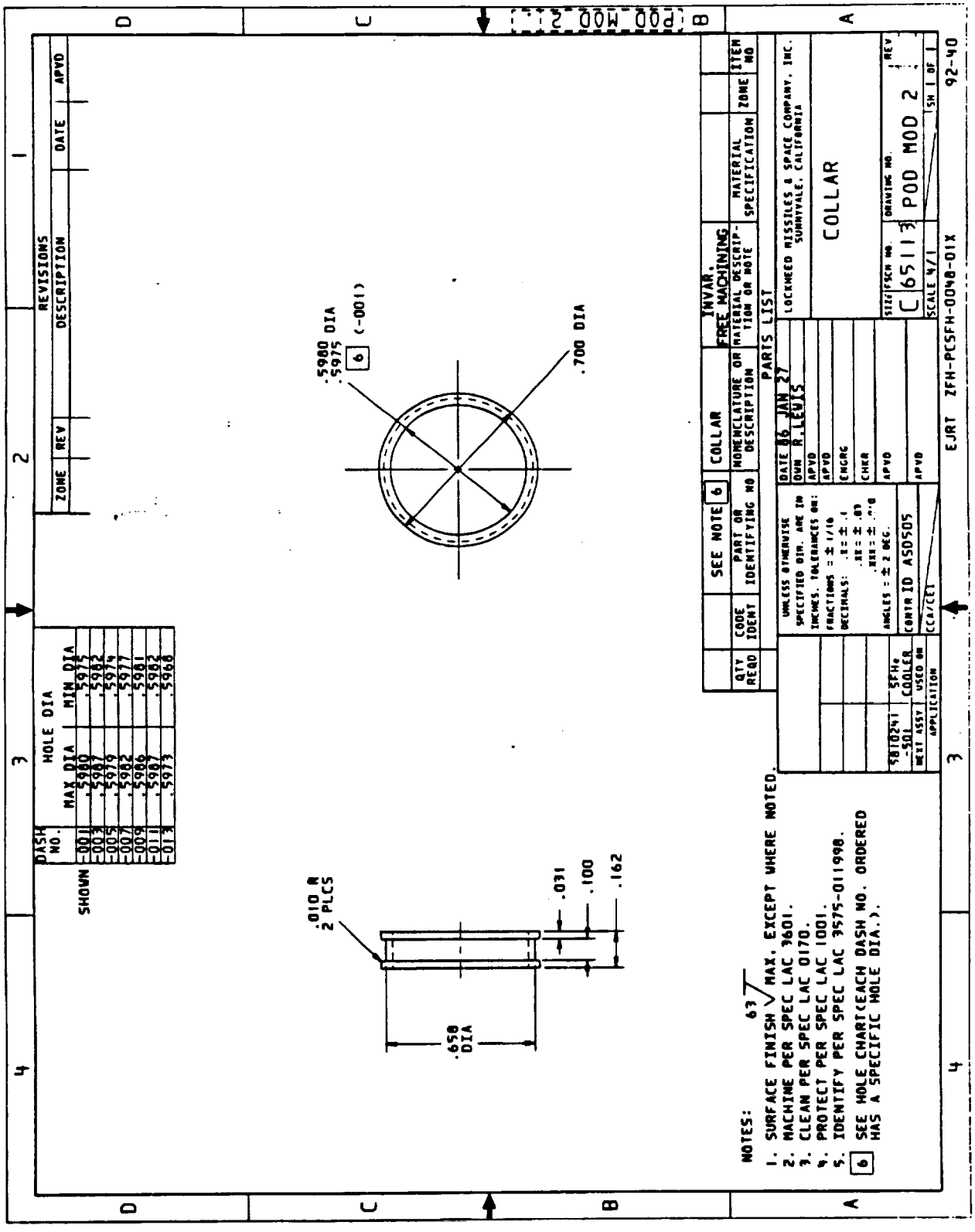

Fig. 3-3 Collar

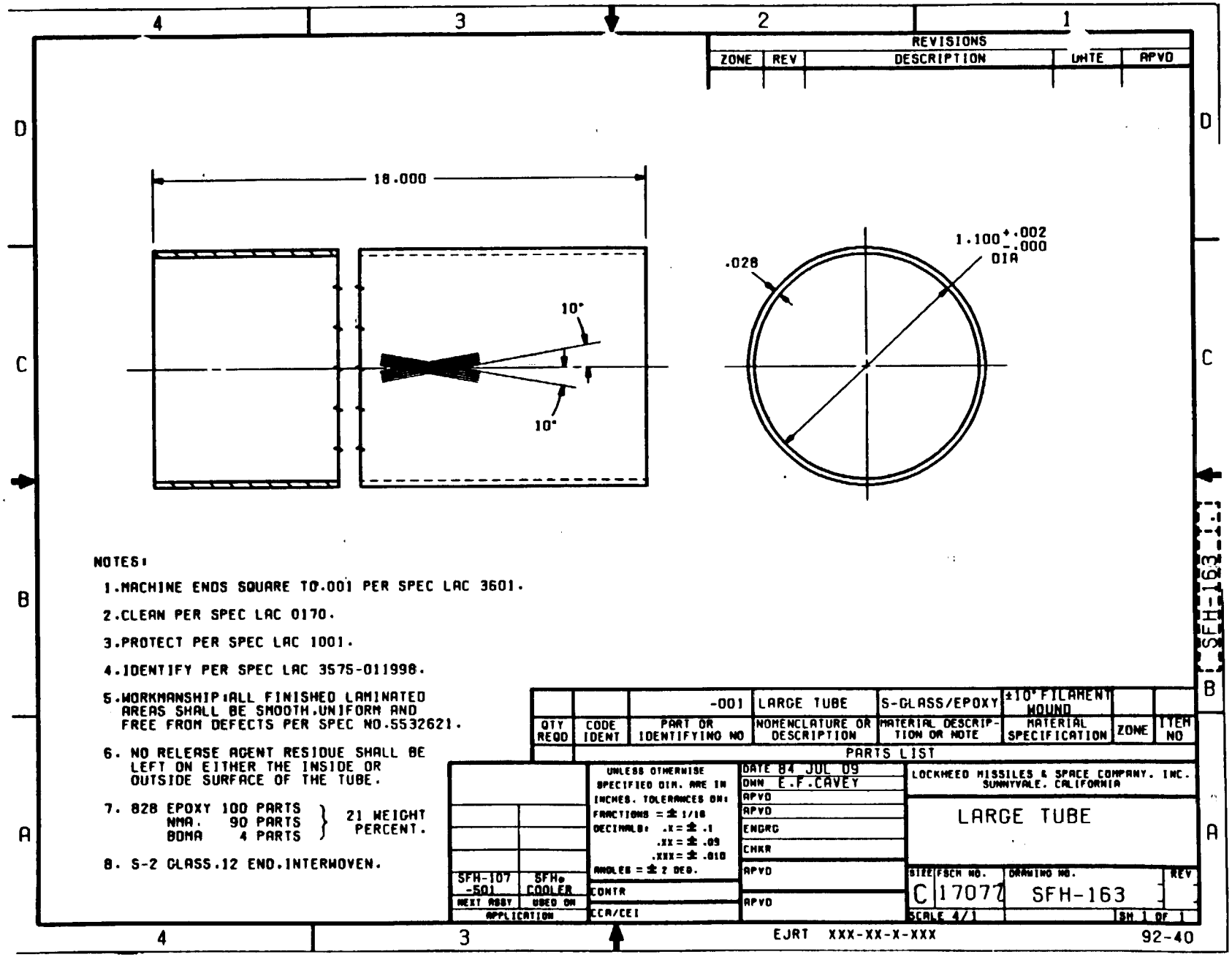

Fig. 3-4 Launch Tube

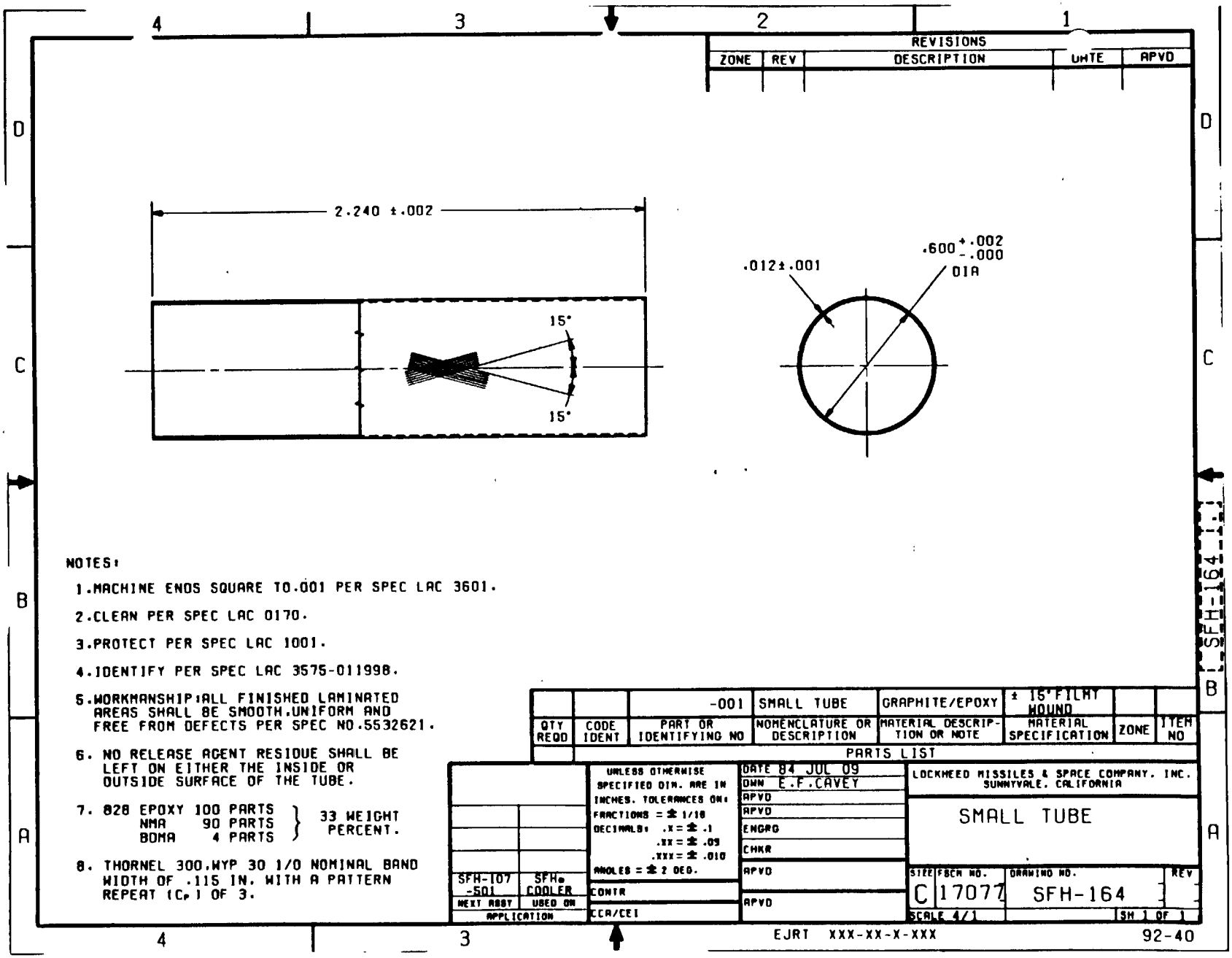

Fig. 3-5 Orbit Tube

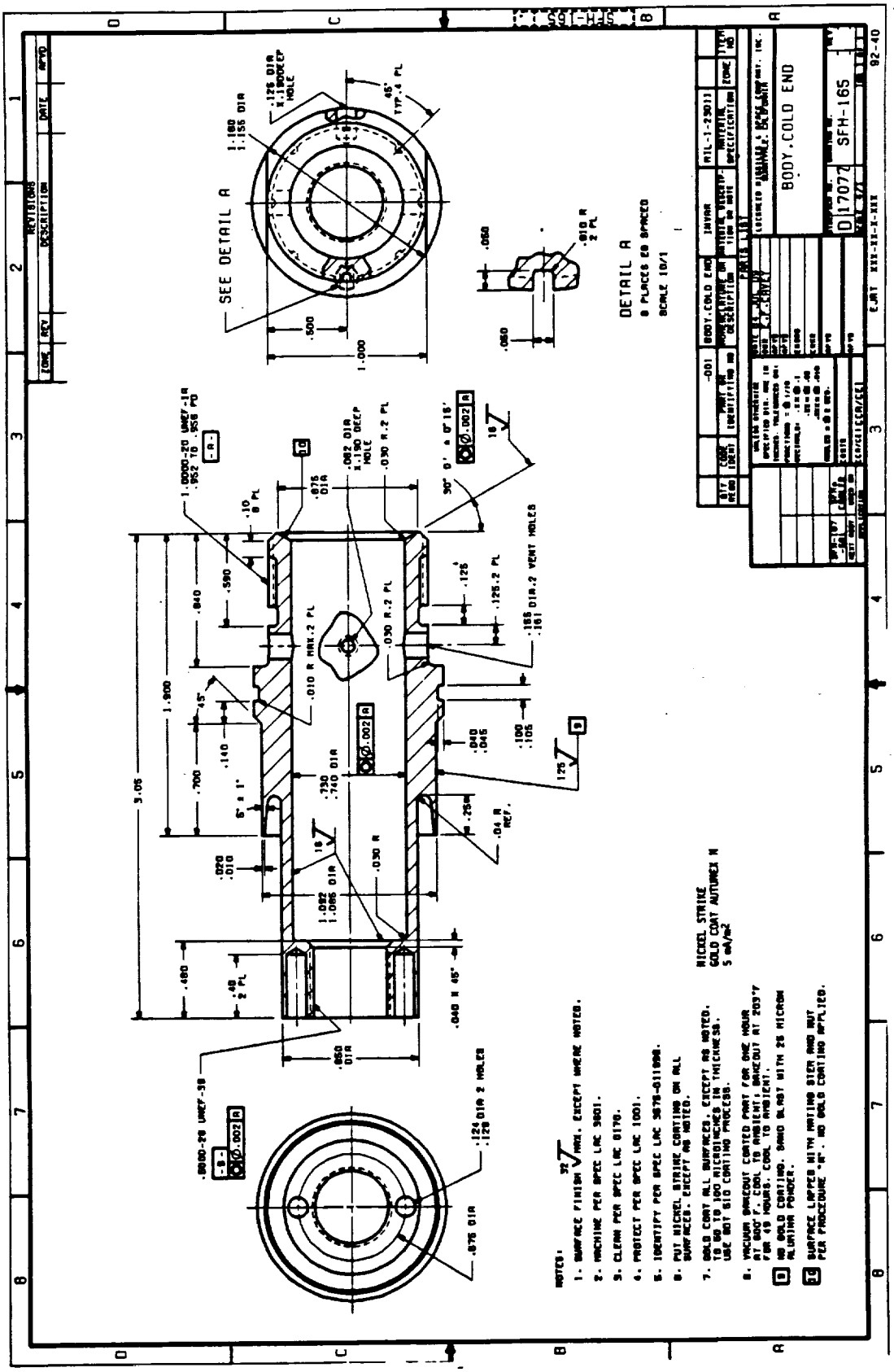

Fig. 3-6 Body, Cold End

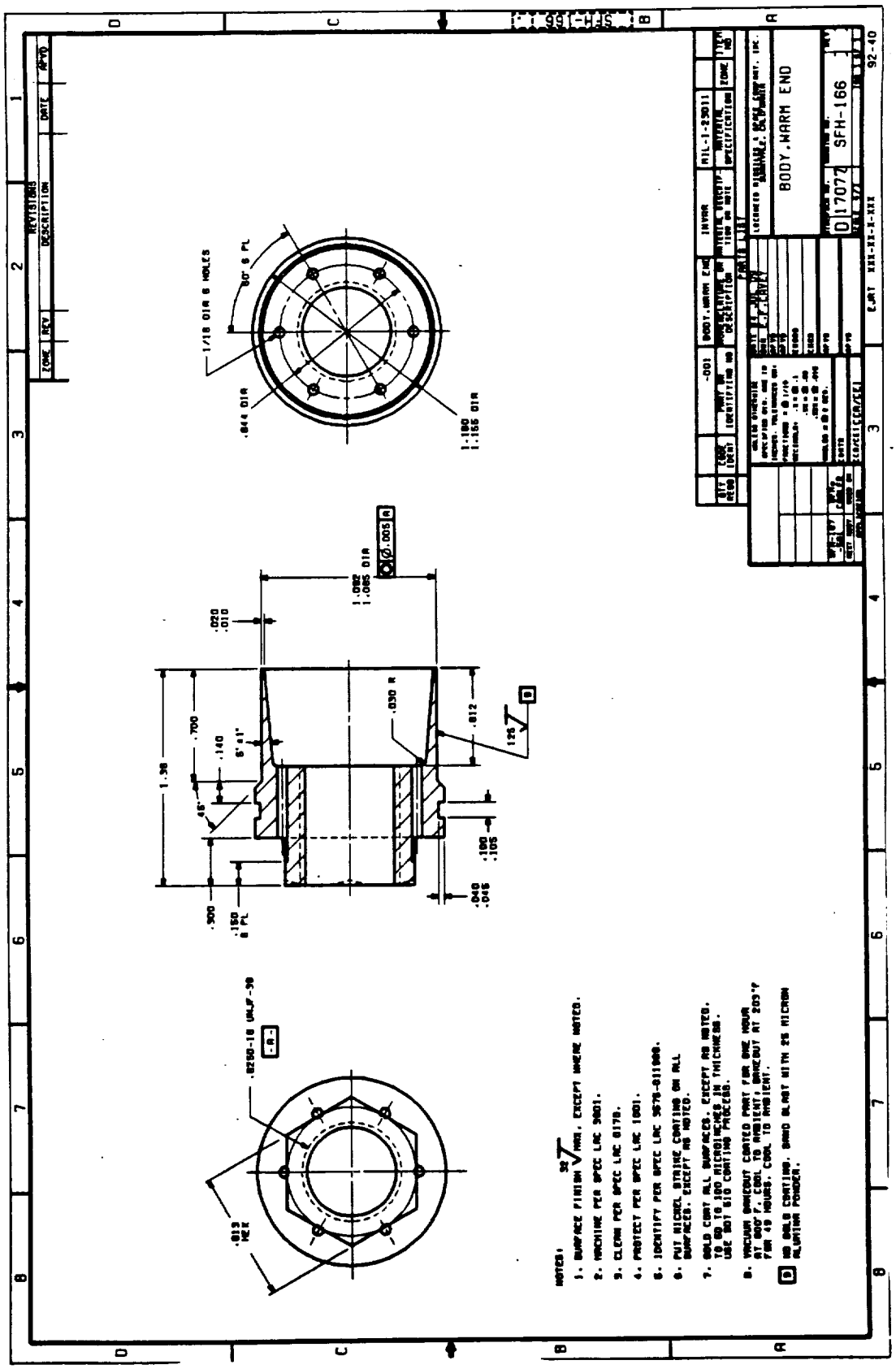

Fig. 3-7 Body, Warm End

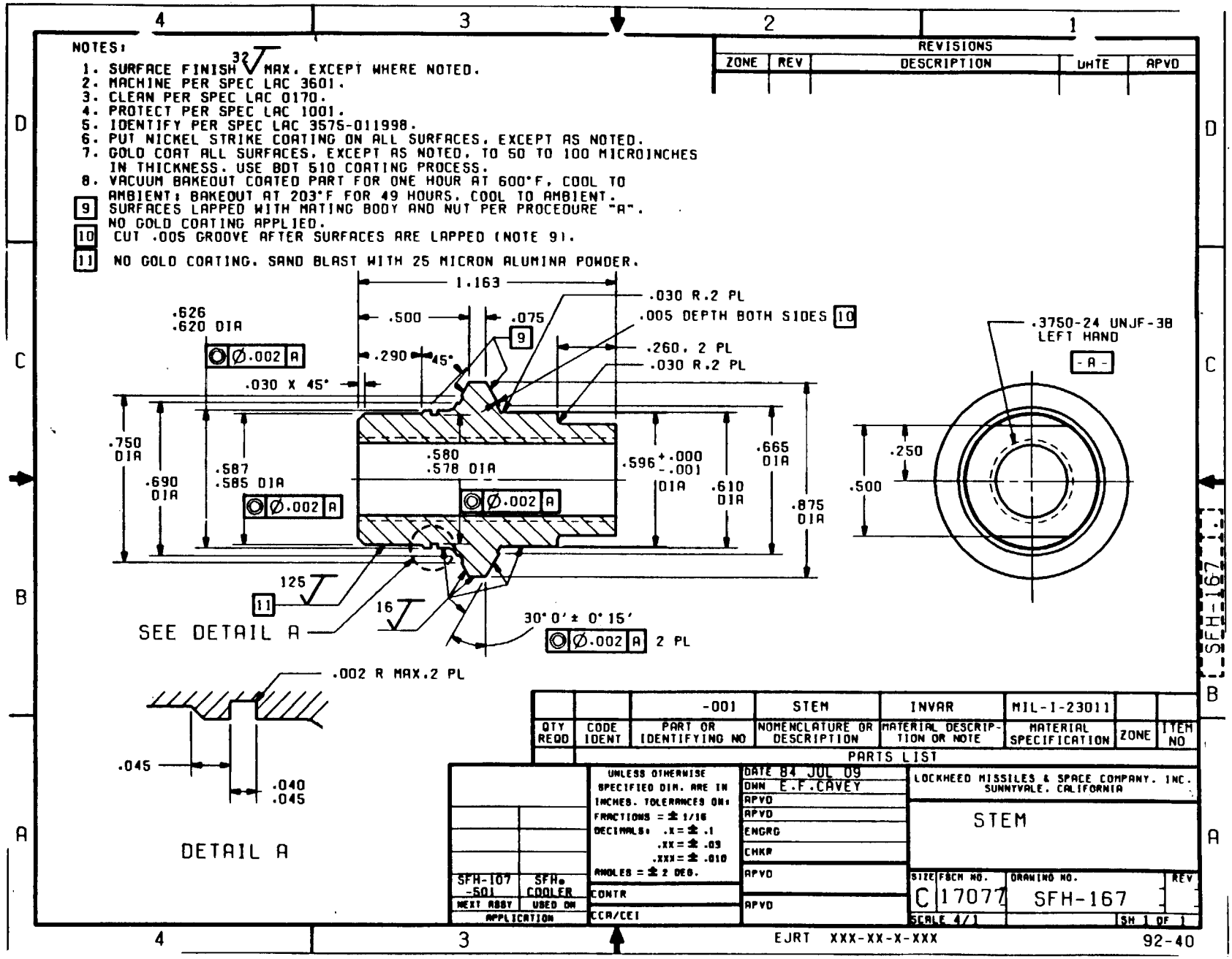
NOTES:
1. SURFACE FINISH 32 MAX. EXCEPT WHERE NOTED.
2. MACHINE PER SPEC LAC 3601.
3. CLEAN PER SPEC LAC 0170.
4. PROTECT PER SPEC LAC 1001.
5. IDENTIFY PER SPEC LAC 3575-011998.
6. PUT NICKEL STRIKE COATING ON ALL SURFACES, EXCEPT AS NOTED.
7. GOLD COAT ALL SURFACES, EXCEPT AS NOTED, TO 50 TO 100 MICROINCHES IN THICKNESS. USE BDT 510 COATING PROCESS.
8. VACUUM BAKEOUT COATED PART FOR ONE HOUR AT 600°F, COOL TO AMBIENT; BAKEOUT AT 203°F FOR 49 HOURS, COOL TO AMBIENT.
9 SURFACES LAPPED WITH MATING BODY AND NUT PER PROCEDURE "A". NO GOLD COATING APPLIED.
10 CUT .005 GROOVE AFTER SURFACES ARE LAPPED (NOTE 9).
11 NO GOLD COATING. SAND BLAST WITH 25 MICRON ALUMINA POWDER.
REVISIONS
ZONE REV DESCRIPTION DATE APVD
1.163
.626
.620 DIA
.500
.075
.030 R.2 PL
.005 DEPTH BOTH SIDES 10
.290
45°
.260, 2 PL
.030 R.2 PL
.030 X 45°
.750 DIA
.690 DIA
.587
.585 DIA
.580
.578 DIA
.596 +.000 -.001 DIA
.610 DIA
.665 DIA
.875 DIA
.3750-24 UNJF-3B
LEFT HAND
-A-
.250
.500
125
11
16
SEE DETAIL A
30° 0' ± 0° 15'
2 PL
.002 R MAX.2 PL
.045
.040
.045
DETAIL A
-001 STEM INVAR MIL-I-23011
QTY REQD
CODE IDENT
PART OR IDENTIFYING NO
NOMENCLATURE OR DESCRIPTION
MATERIAL DESCRIPTION OR NOTE
MATERIAL SPECIFICATION
ZONE
ITEM NO
PARTS LIST
UNLESS OTHERWISE SPECIFIED DIM. ARE IN INCHES. TOLERANCES ON: FRACTIONS = ± 1/16 DECIMALS: .X = ± .1 .XX = ± .03 .XXX = ± .010 ANGLES = ± 2 DEG.
DATE 84 JUL 09
DWN E.F.CAVEY
APVD
APVD
ENGRG
CHKR
APVD
APVD
CONTR
CCA/CEI
LOCKHEED MISSILES & SPACE COMPANY, INC. SUNNYVALE, CALIFORNIA
STEM
SIZE C
FSCM NO. 17077
DRAWING NO. SFH-167
REV
SCALE 4/1
SH 1 OF 1
SFH-107 -501
SFH COOLER
NEXT ASSY
USED ON
APPLICATION
EJRT XXX-XX-X-XXX
92-40
SFH-167 4:1

Fig. 3-8 Stem

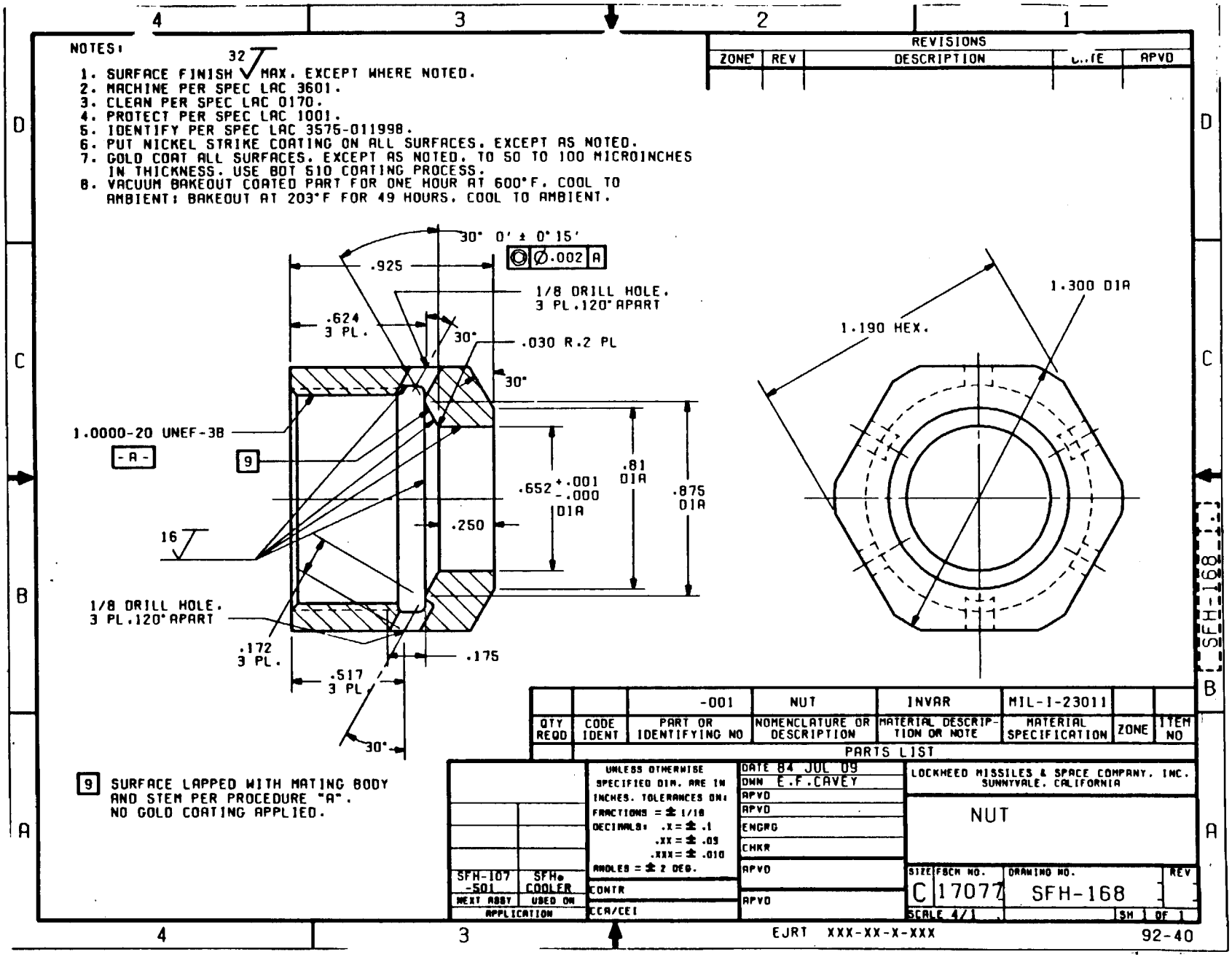
NOTES:
1. SURFACE FINISH 32 MAX. EXCEPT WHERE NOTED.
2. MACHINE PER SPEC LAC 3601.
3. CLEAN PER SPEC LAC 0170.
4. PROTECT PER SPEC LAC 1001.
5. IDENTIFY PER SPEC LAC 3575-011998.
6. PUT NICKEL STRIKE COATING ON ALL SURFACES, EXCEPT AS NOTED.
7. GOLD COAT ALL SURFACES, EXCEPT AS NOTED, TO 50 TO 100 MICROINCHES IN THICKNESS. USE BOT 510 COATING PROCESS.
8. VACUUM BAKEOUT COATED PART FOR ONE HOUR AT 600°F, COOL TO AMBIENT; BAKEOUT AT 203°F FOR 49 HOURS, COOL TO AMBIENT.
REVISIONS
ZONE REV DESCRIPTION DATE APVD
30° 0' ± 0° 15'
Ø.002 A
.925
1/8 DRILL HOLE, 3 PL, 120° APART
.624 3 PL.
30°
.030 R.2 PL
30°
1.0000-20 UNEF-3B
-A-
9
.652 +.001 -.000 DIA
.81 DIA
.875 DIA
.250
16
1/8 DRILL HOLE, 3 PL, 120° APART
.172 3 PL.
.175
.517 3 PL
30°
1.190 HEX.
1.300 DIA
9 SURFACE LAPPED WITH MATING BODY AND STEM PER PROCEDURE "A". NO GOLD COATING APPLIED.
-001 NUT INVAR MIL-I-23011
QTY REQD CODE IDENT PART OR IDENTIFYING NO NOMENCLATURE OR DESCRIPTION MATERIAL DESCRIPTION OR NOTE MATERIAL SPECIFICATION ZONE ITEM NO
PARTS LIST
UNLESS OTHERWISE SPECIFIED DIM. ARE IN INCHES. TOLERANCES ON: FRACTIONS = ± 1/16 DECIMALS: .X = ± .1 .XX = ± .05 .XXX = ± .010 ANGLES = ± 2 DEG.
DATE 84 JUL 09
DWN E.F.CAVEY
APVD
APVD
ENGRG
CHKR
APVD
APVD
LOCKHEED MISSILES & SPACE COMPANY, INC. SUNNYVALE, CALIFORNIA
NUT
SIZE C FSCM NO. 17077 DRAWING NO. SFH-168 REV
SCALE 4/1 SH 1 OF 1
SFH-107 -501 NEXT ASSY
SFH COOLER USED ON
APPLICATION
CONTR
CCA/CEI
EJRT XXX-XX-X-XXX
92-40
SFH-168

Fig. 3-9 Nut

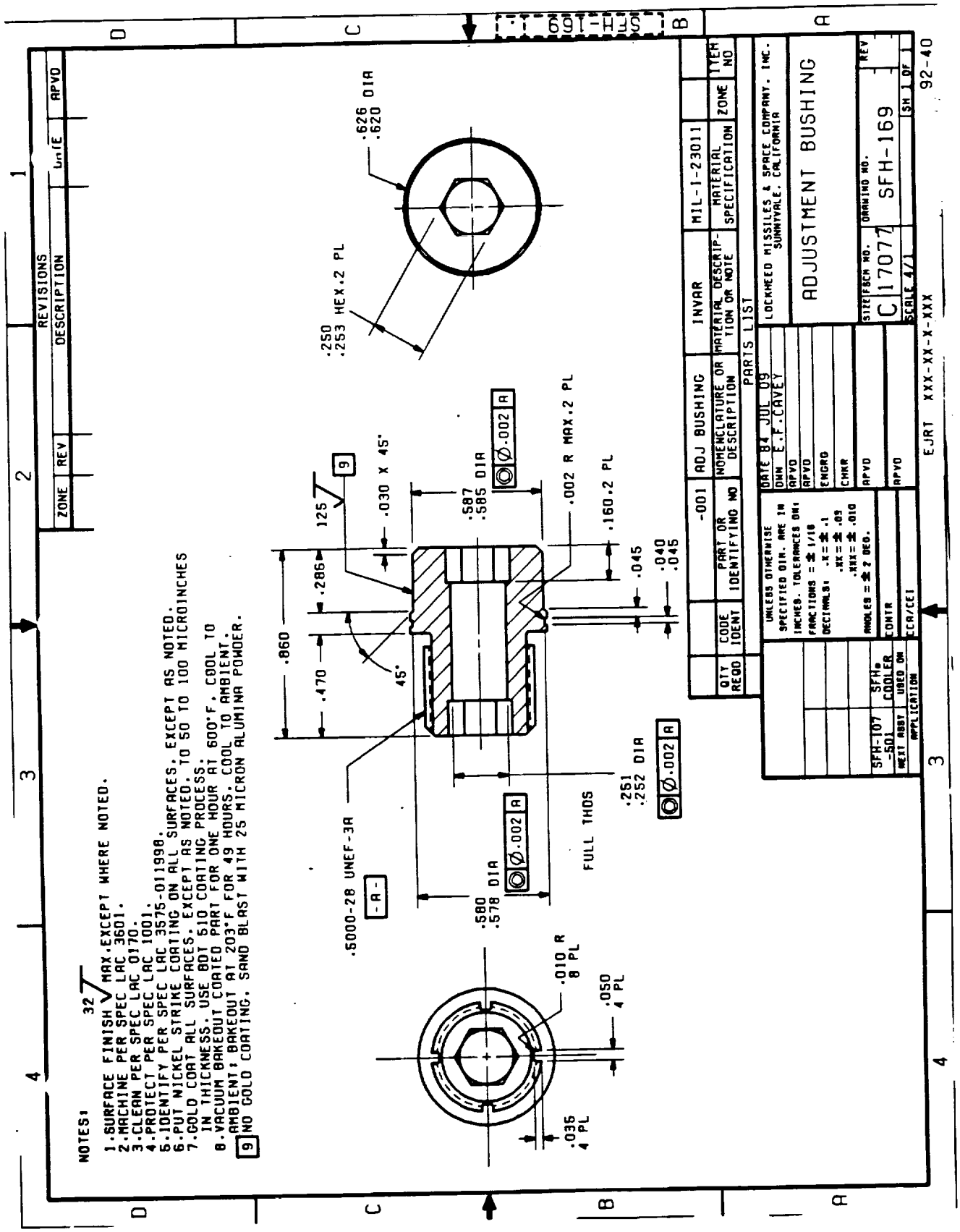

Fig. 3-10 Adjustment Bushing

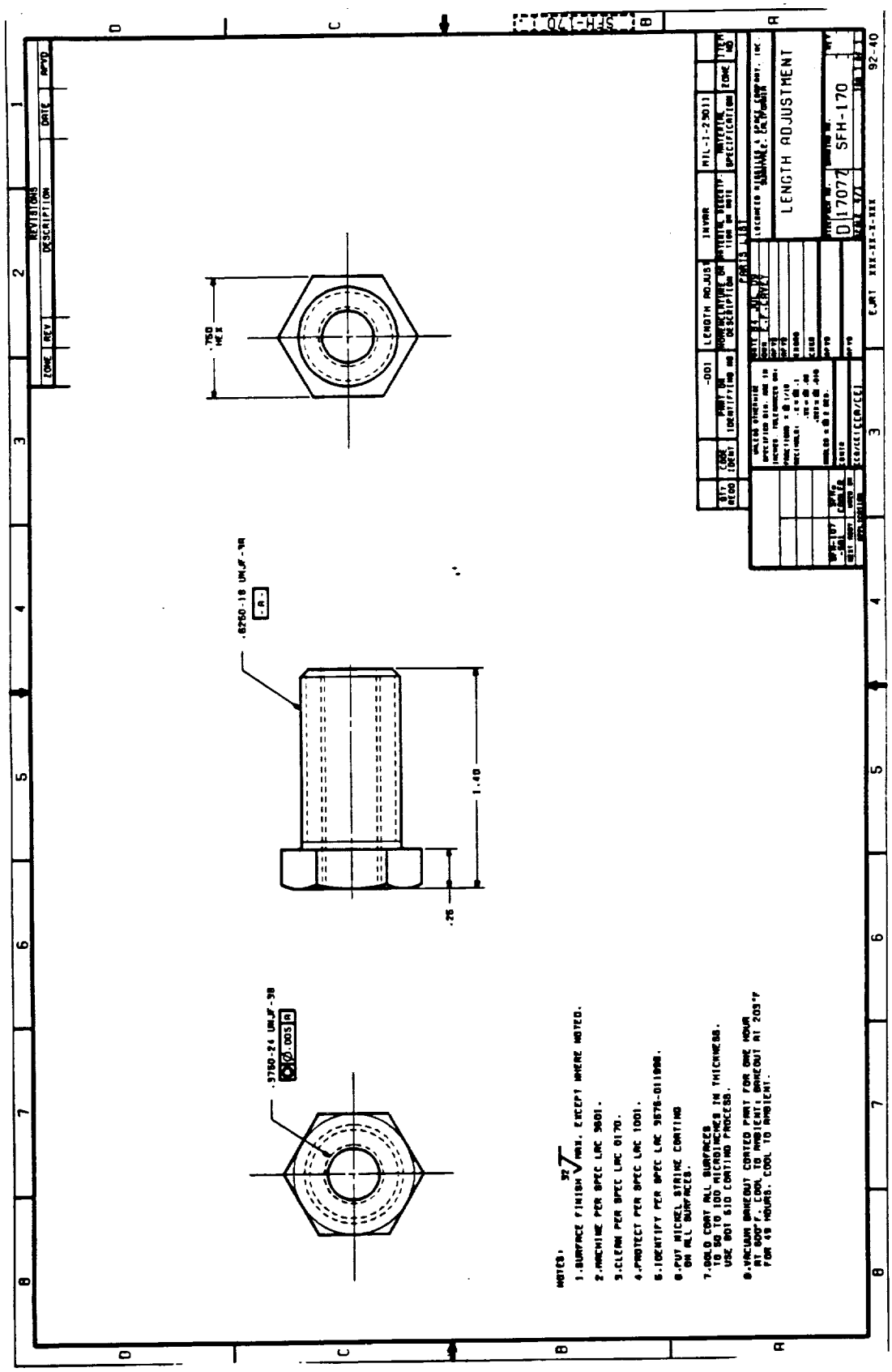

Fig. 3-11 Length Adjustment

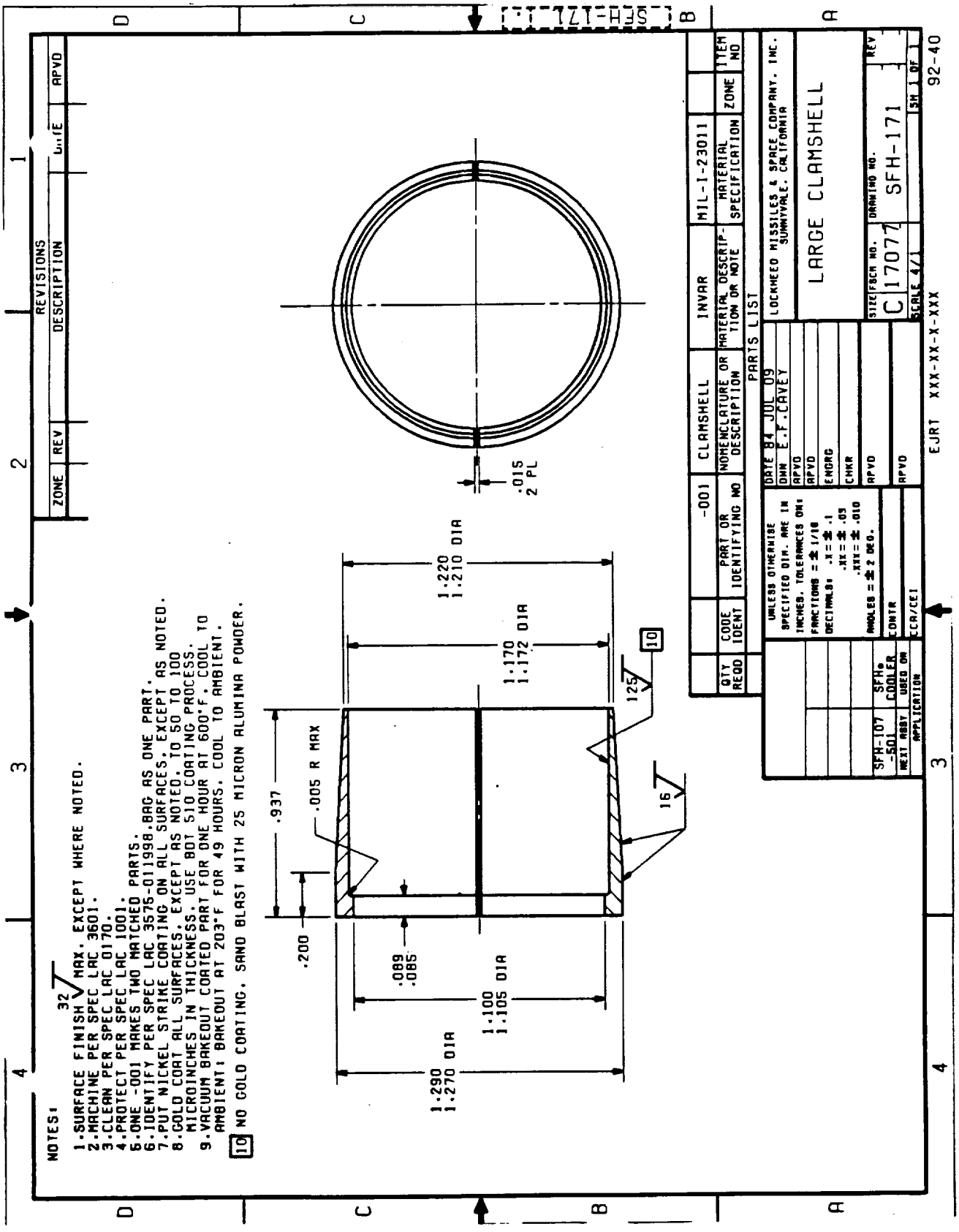

Fig. 3-12 Large Clamshell

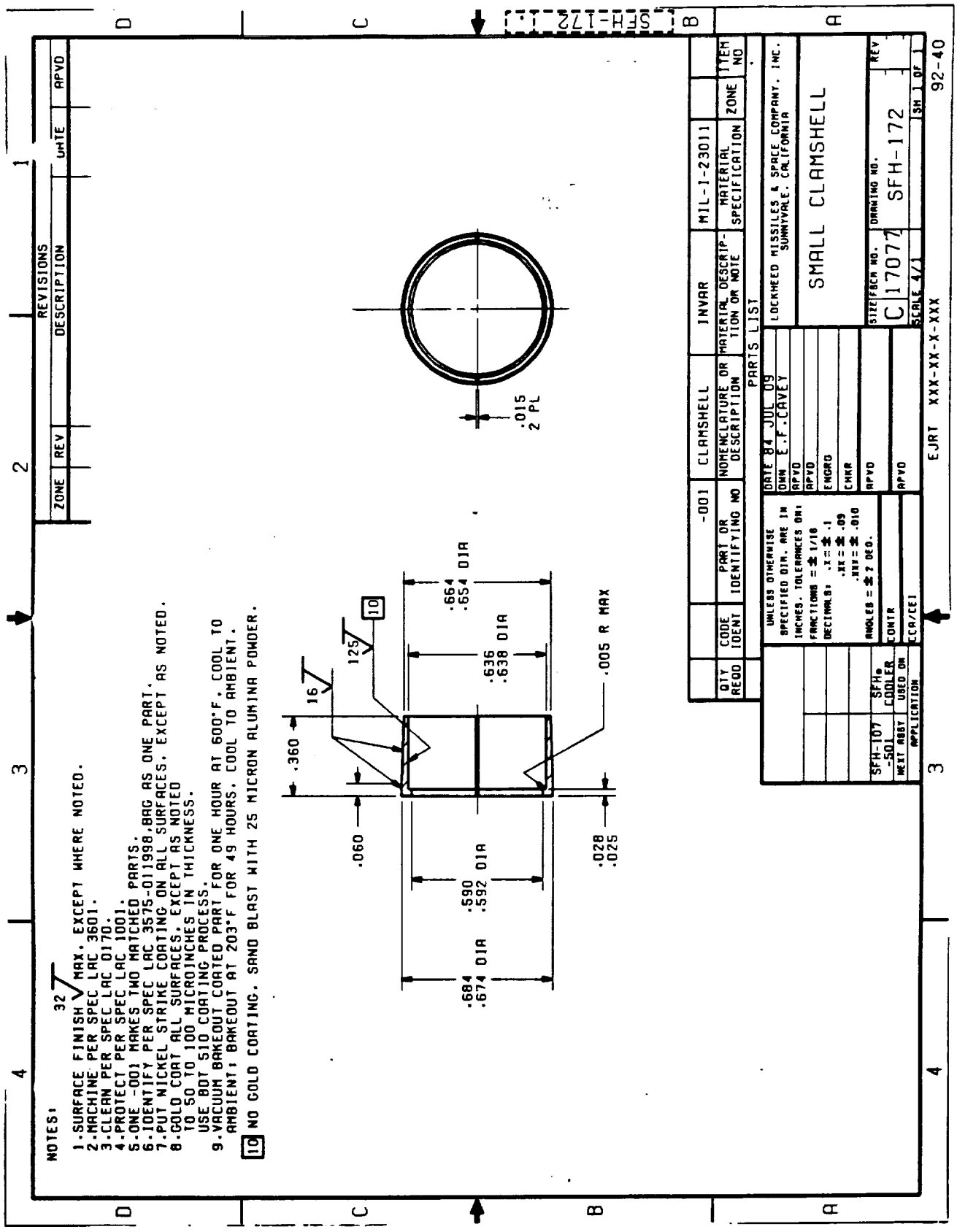

Fig. 3-13 Small Clamshell

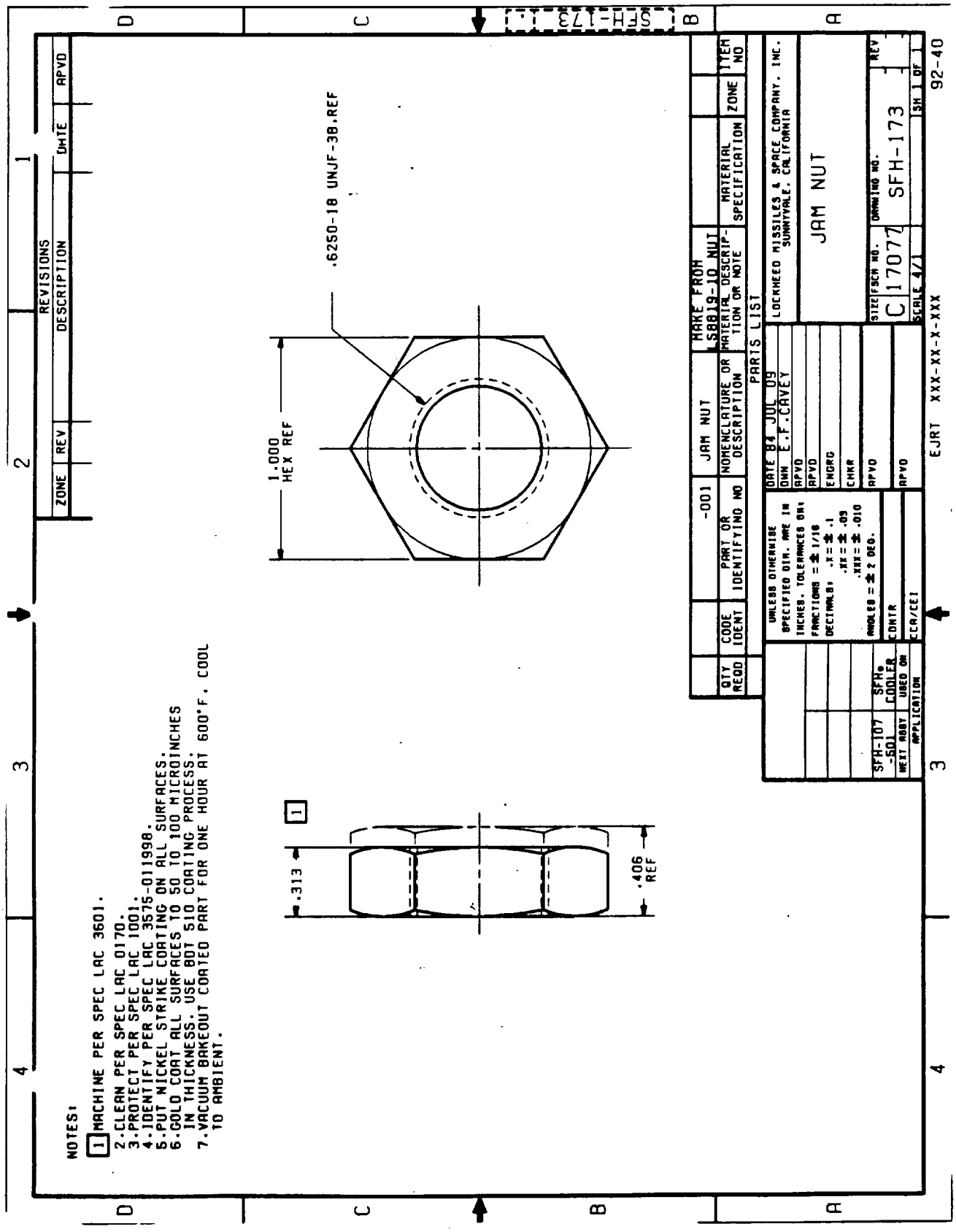

Fig. 3-14 Jam Nut

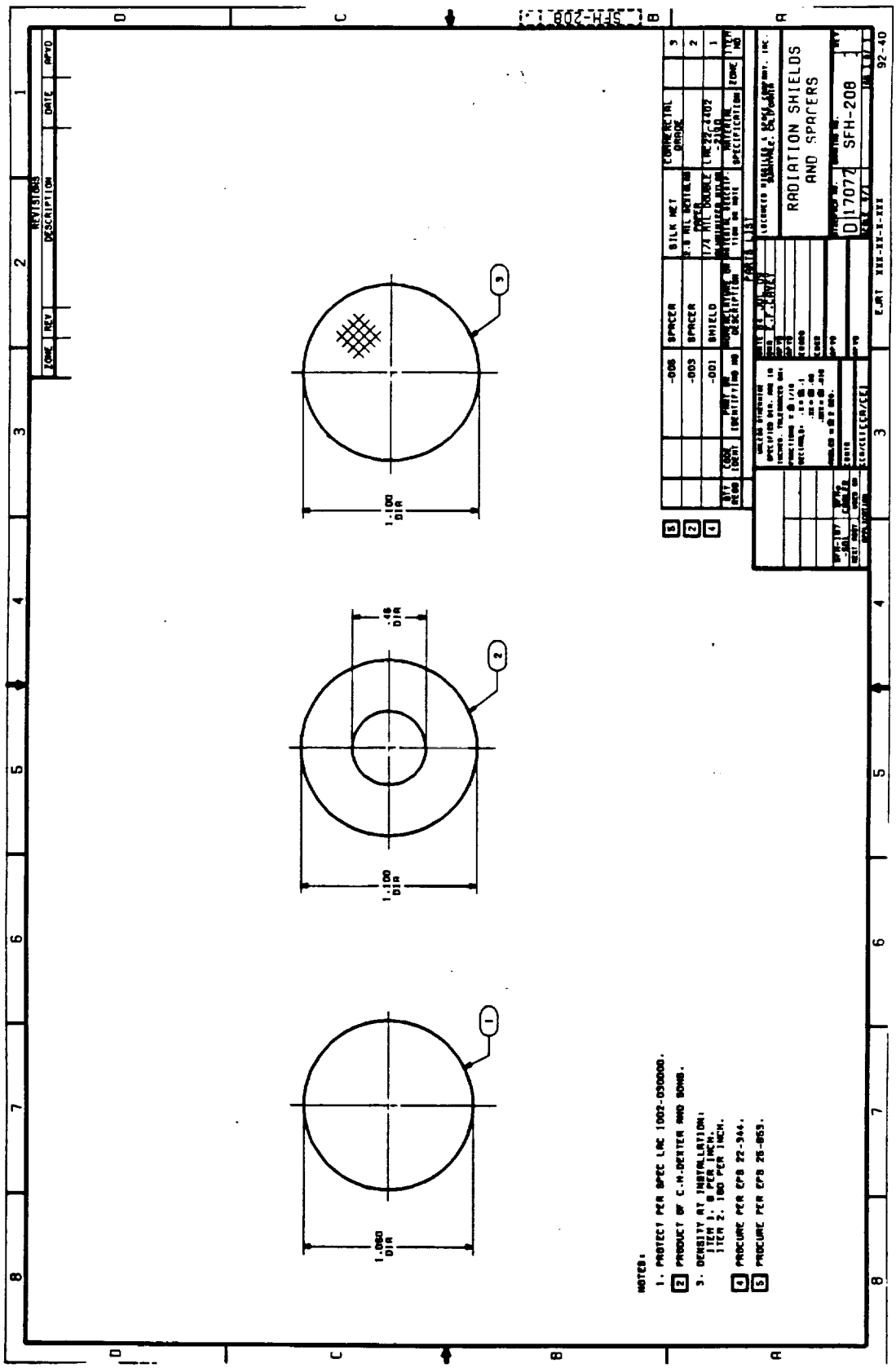

Fig. 3-15 Radiation Shields and Spacers

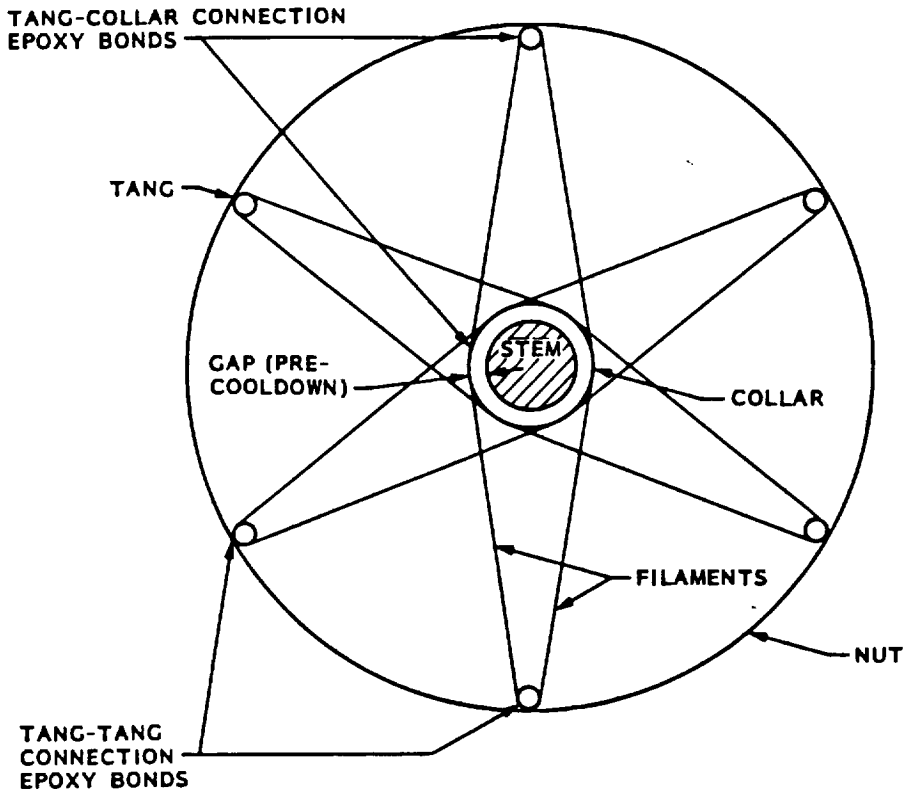

Fig. 3-16 PODS-IV Side-Load Mechanism

3.2.1 Structural Model

A computer model was developed to analyze the interaction of the filaments when the PODS-IV mechanism shorts out. Since small angles and displacements occur, the code was written in double precision FORTRAN, minimizing angle errors. Figure 3-17 and Tables 3-1 and 3-2 show the properties used. The model takes into account the shrinkage or elongation of the nut cold rod/stem assembly during cooldown (Fig. 3-18). Side loads displace the nut with respect to the collar-stem assembly, causing some of the filaments to elastically deform. A three-tang system is shown in Fig. 3-19. Filament angles are accounted for depending upon the bonding, component properties, and displacements. Equalibrium is checked by summing the moments around the collar and nut to zero and comparing the resultant filament force angle to the displacement angle.

Table 3-1 TYPICAL PROPERTIES OF FILAMENT

Properties	S-2 Glass (Ref. 6)	Graphite Thornel 300 WYP 30 I/O (Ref. 7)
Tensile Strength GN/m^2 (ksi)	4.6 (665)	3.10 (450)
Tensile Modulus GN/m^2 (10^6 psi)	87 (12.6)	230 (33.2)
Density g/cm^3 ($lb/in.^3$)	2.49 (0.090)	1.77 (0.064)
Filament Diameter μm (mil)	10 (0.39)	7 (0.28)
Minimum Bend Radius cm (in.)	0.01 (0.004	0.1 (0.04)

Table 3-2 COMPOSITE ELASTIC MODULUS VALUES GN/m^2 (10^6 psi)

Composite	Temperature			
	300 K	77 K	20 K	4 K
Epoxy	2.4 (Ref. 7) (0.35)			8.5 (Ref. 8) (1.24)
S-2 Glass (Ref. 6)	87 (12.6)			
Graphite (Thornel 300) (Ref. 7)	230 (33)			
S-2 Glass/Epoxy (10-deg wind angle, 64 vol percent)	54 (7.8)	54 (7.8)	54 (7.8)	54 (7.8)
S-2 Glass/Epoxy (30-deg wind angle, 64 vol percent) (Ref. 2)	34 (5.0)	52 (7.5)	52 (7.5)*	52 (7.5)*
Graphite/Epoxy (15-deg wind angle, 60 vol percent)	110 (15.9)	104 (15.1)	104 (15.1)*	104 (15.1)*

* Extrapolated

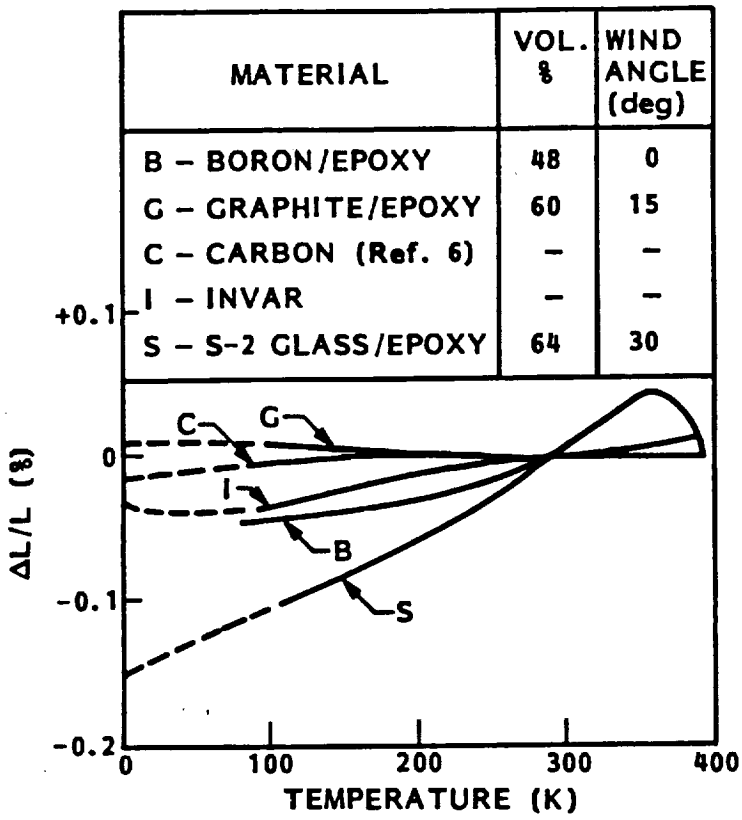

Fig. 3-17 Comparison of Composite and Invar Thermal Expansion Values

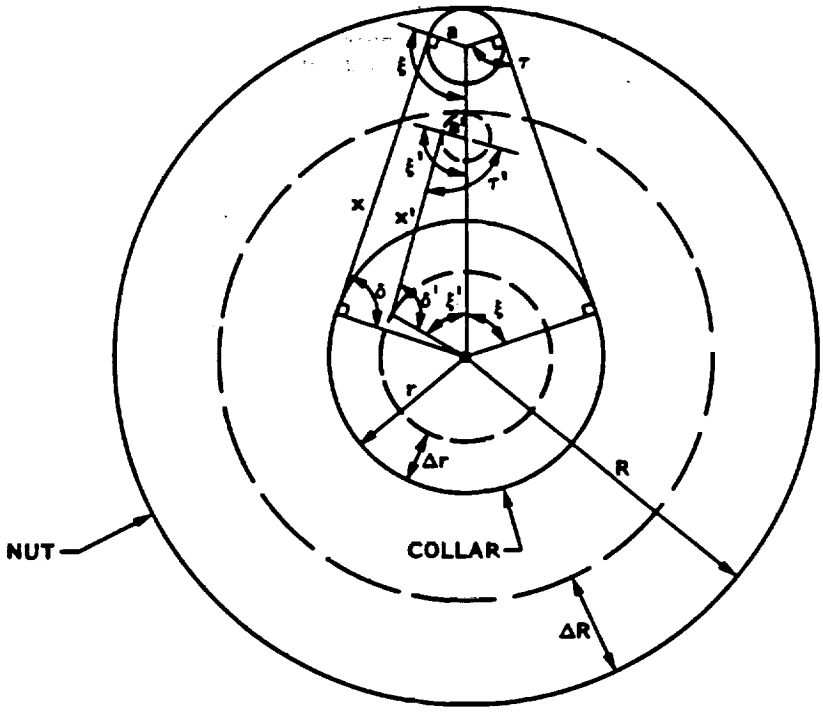

Fig. 3-18 PODS-IV Cooldown

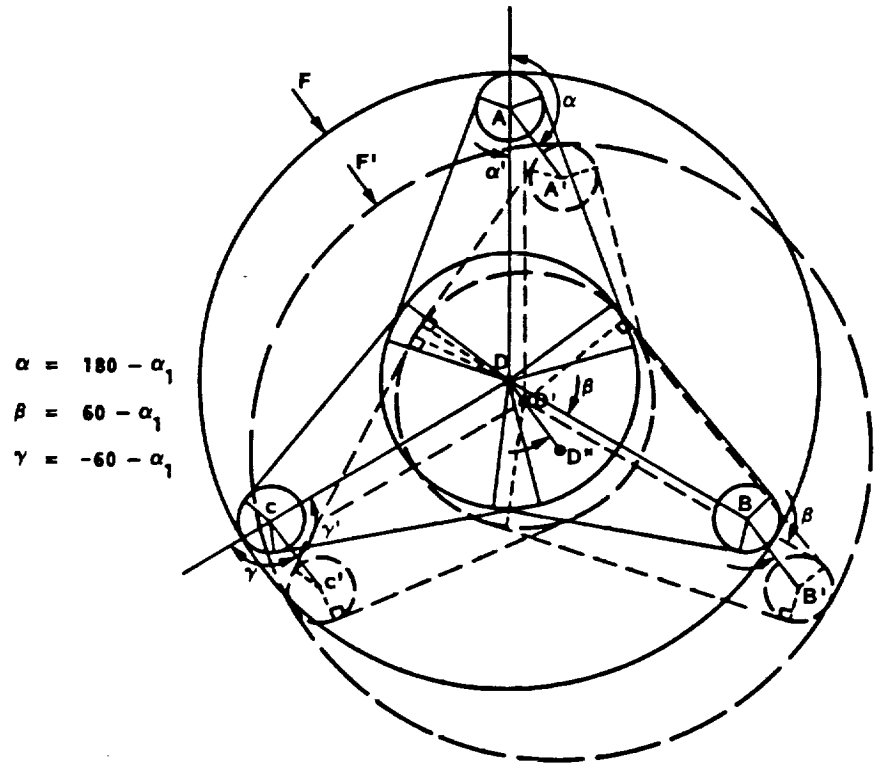

Fig. 3-19 PODS-IV System Displacement Due to Load F

The model was first used to study a three-tang filament support system. Nonuniform side-load resistance was determined to occur around the nut perimeter. A six-tang model was then developed which demonstrated a more uniform loading. Figure 3-20 compares the two systems.

Figure 3-20 also compares two six-tang systems using two different bonding techniques: tang-to-collar and tang-to-tang. The tang-to-collar bonding system bonds a filament that has been wrapped around the collar between two adjacent tangs at the tangs and collar. The tang-to-tang system bonds the filament only at the tangs and not at the collar. This effectively increases the filament strand length while decreasing filament strain. Figure 3-6 illustrates these two bonding systems. The tang-to-collar system developed larger side-load resistance than the tang-to-tang system due to the shorter filament lengths that resulted in more filament strain. Due to the uncertainty in how the epoxy-graphite bonds would behave under load, the tang-to-tang system was chosen to test initially. However, both systems were

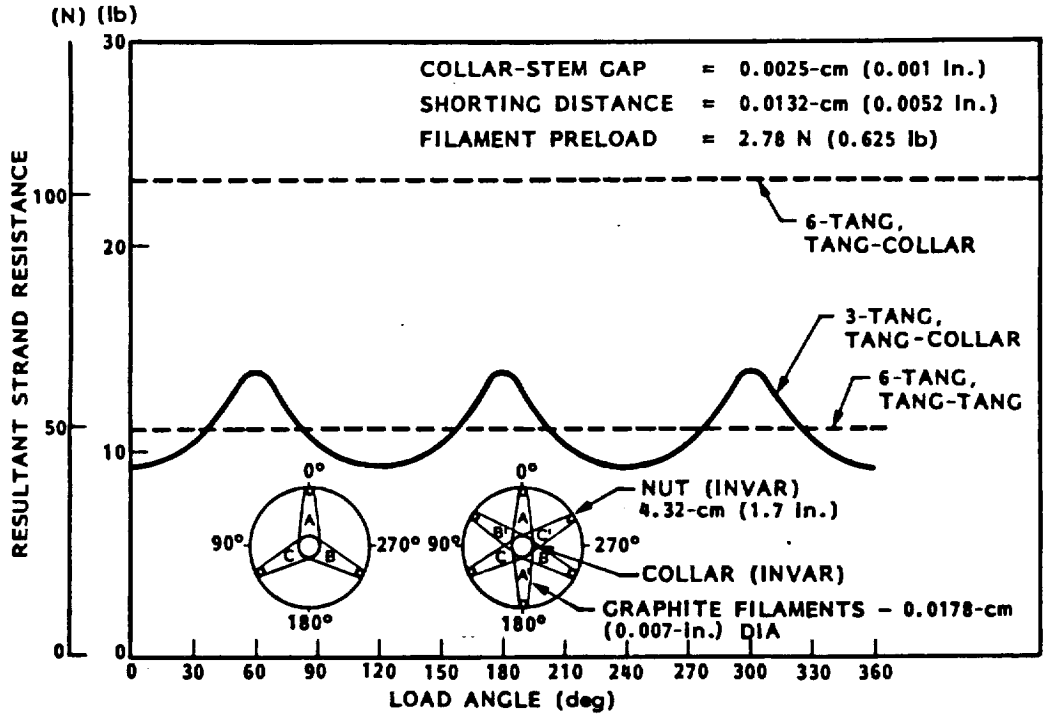

Fig. 3-20 Predicted Strand Resistance at Operating Temperature

compared, since the tang-to-tang system could behave like the tang-to-collar due to filament-collar friction and we planned to test the tang-to-collar bonded system if the first test was successful. (This was eventually done on the PODS-IV side-load tests.) A filament size of 0.018 cm (0.007 in.) was chosen to increase the orbital heat load by 10 percent for the 4.3-cm (1.7-in.) ring used for testing.

3.2.2 Strain Limitations

Since the PODS-IV may short out due to larger side loads during vibrational testing, the filaments must be able to elastically deform to the maximum shorting distance without failure. Both graphite and graphite/epoxy filaments were considered; however, as shown in Fig. 3-21, the strain is too great for graphite/epoxy at these small nut diameters. Graphite/epoxy could be used if the collar-stem gap was increased; however, as shown in Fig. 3-22, the corresponding side-load resistance decreases even further and is not practical

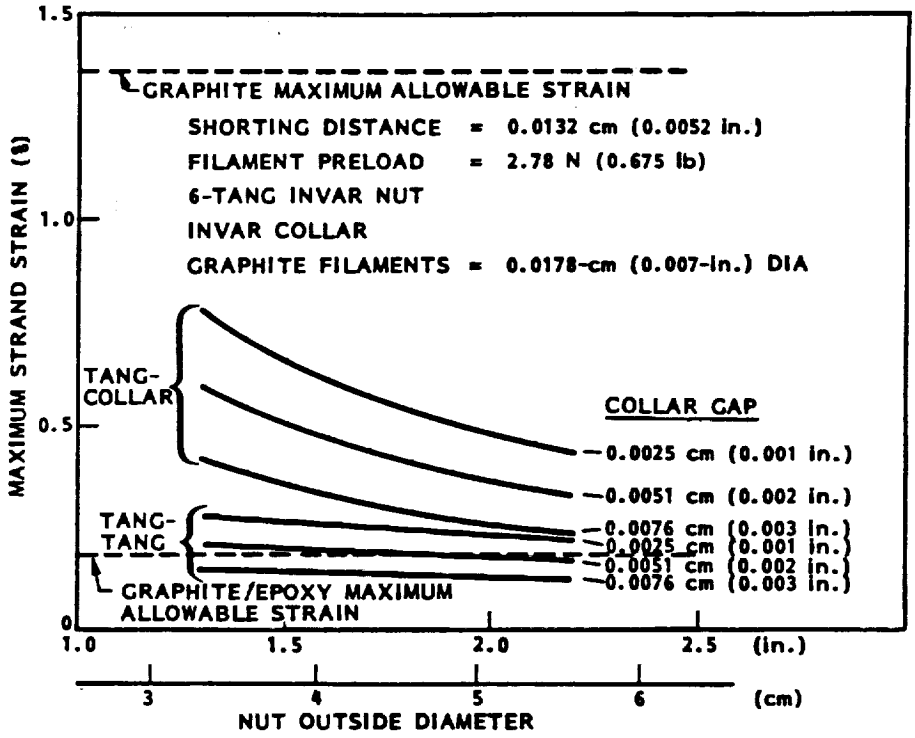

Fig. 3-21 Maximum Strand Shorting Strain

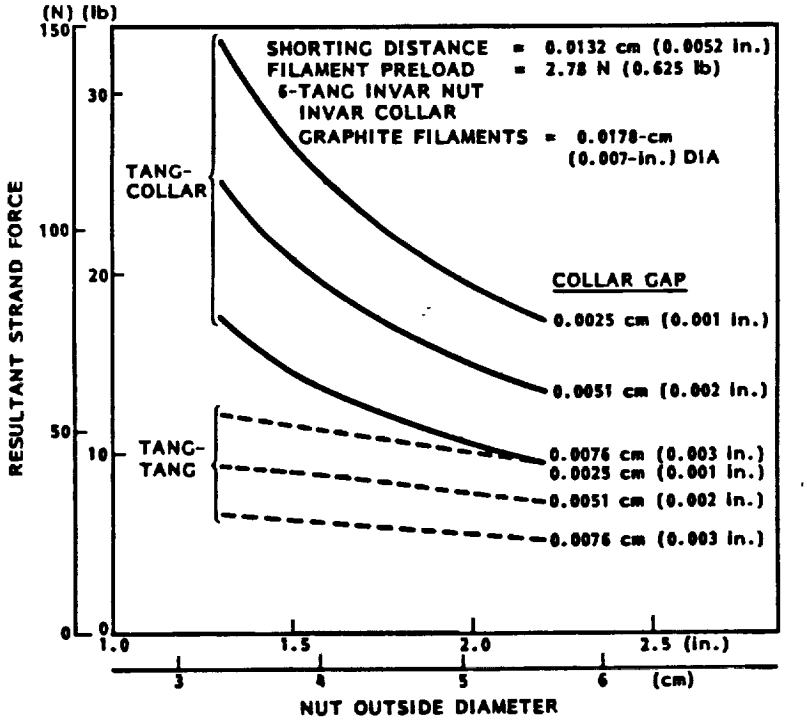

Fig. 3-22 Maximum Resultant Strand Shorting Force

due to property and tolerance uncertainties. The graphite filaments were chosen because of their larger strain tolerance. The main concern in using these filaments is that they are epoxy bonded to the tangs, and it was uncertain how the graphite/epoxy bonds would behave during loading or if the epoxy would wick up the filaments, making them brittle and fail during shear motion. Therefore, the tang-to-tang bonded system was chosen for test due to the lower strain levels. Unfortunately, side-load resistance was also reduced. Fiberglass filaments were also considered, but their lower modulus and higher thermal conductivity below 40 K made them impractical for this application. (The PODS-III support that was modified was designed for use at SFHe temperatures and utilized a graphite/epoxy orbit tube that was predicted to run between temperature boundaries of 2 and 40 K. The filaments would also run between these two temperature boundaries.) However, at higher temperatures where the thermal conductivity of fiberglass is lower than that of graphite, fiberglass should be considered for both the filaments and the orbit tube.

3.3 THERMAL ANALYSIS

During normal operation of the PODS support, the main heat resistance is conduction through the graphite/epoxy orbit tube. The PODS-IV mechanism adds to this heat load when engaged due to the parallel resistive connection of the graphite filaments. The following relationship was used to evaluate the heat load.

$$q = (T_H - T_C)/R_{EQ}$$

where

$$R_{EQ} = R_{TUBE}\, R_F/(R_{TUBE}+R_F)$$

The resistance of the filaments was determined from

$$R_F = L_F/(12\, K_F\, A_F)$$

where

L_F = effective filament length, tang to collar distance (cm)
K_F = filament conductivity (W/cm K)
A_F = filament conductive area (cm^2)

The normal operating temperature of the orbit tube was assumed to be between a hot temperature (T_H) of 20 to 40 K and a cold temperature (T_C) of 2 K. Conductivities were evaluated at average temperatures.

If heat load is the major concern, the filaments should be sized according to their effect on heat load. It is desirable to keep this effect (increase) to 10 percent due to the efficiency of the disconnect mechanism. Figure 3-23 illustrates the filament size required for a given nut diameter to limit the increase in heat load to 10 percent.

Figure 3-24 shows the effect of filament size on heat load when side load requirements drive the filament diameter above the 10 percent limit. This was a worst case for an orbit-tube hot temperature of 40 K.

3.4 SIDE-LOAD RESISTANCE

In Ref. 3, a single PODS-III support was side-load tested at 290 K and at an inclination angle of 45 deg. Figure 3-25 presents the data for this support. A modified PODS-III nut had an outer diameter of 4.3 cm (1.7 in.). A collar-stem gap of 0.0025 cm (0.001 in.) was selected to yield the largest side-load resistance. The filaments were selected to be 0.018 cm (0.007 in.) for a 10 percent increase in heat load over the PODS-III design. The predicted side-load resistances for this support are also shown in Fig. 3-25.

Usually, side-load resistance will determine PODS-IV use and therefore determine filament diameter size. Figure 3-26 was produced to help determine filament size and the effect on support heat load for various side-load requirements.

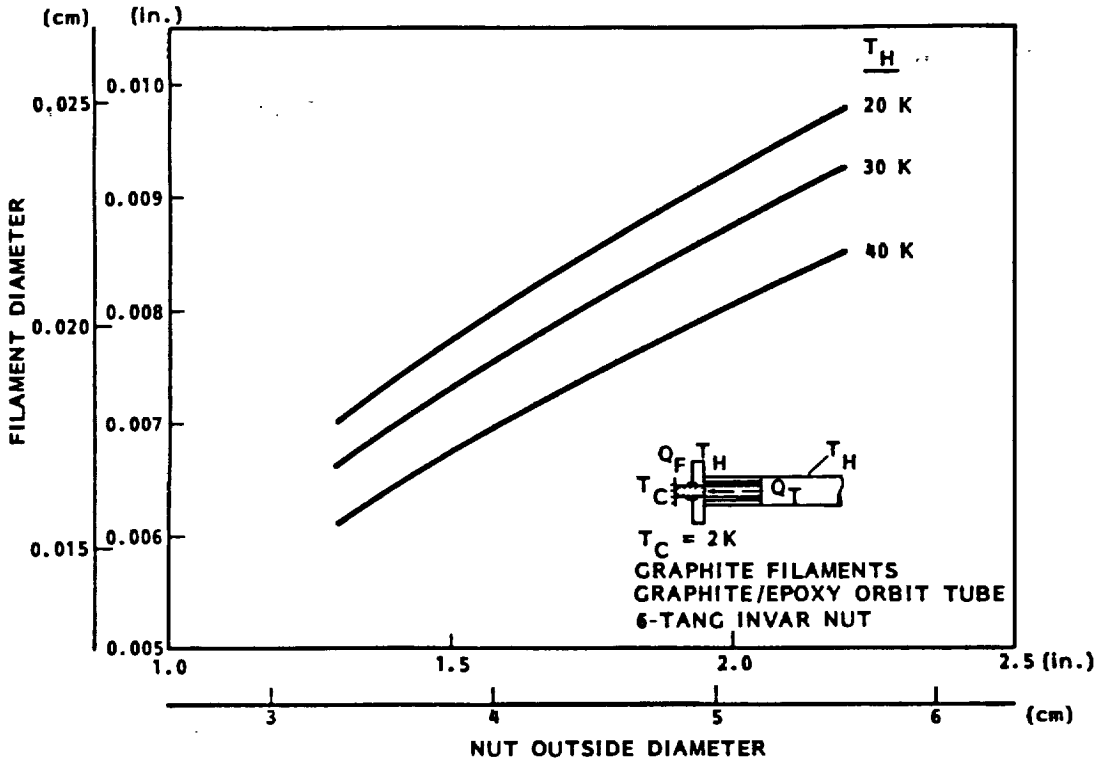

Fig. 3-23 Filament Size for a 10 Percent Increase in PODS-III Heat Rates

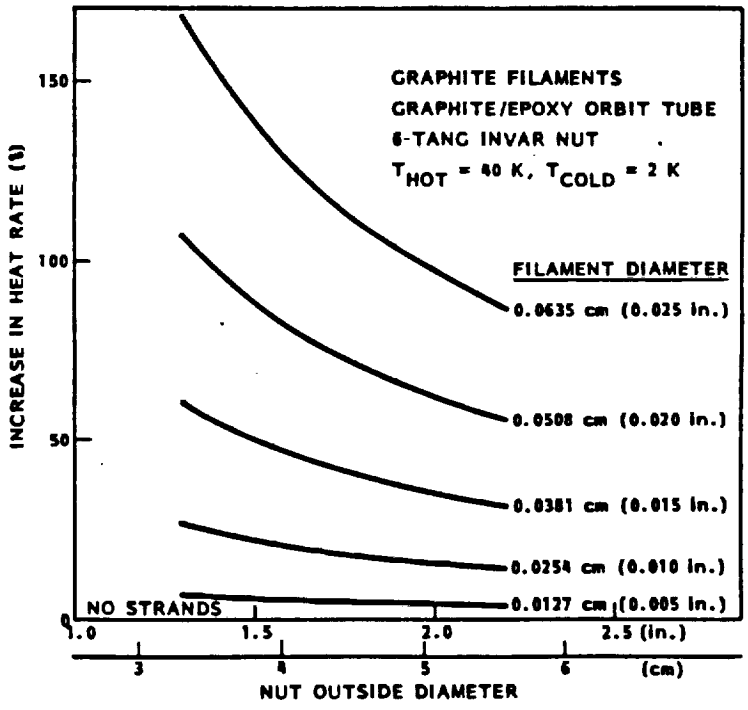

Fig. 3-24 Effect of Filament Size on Heat Rate

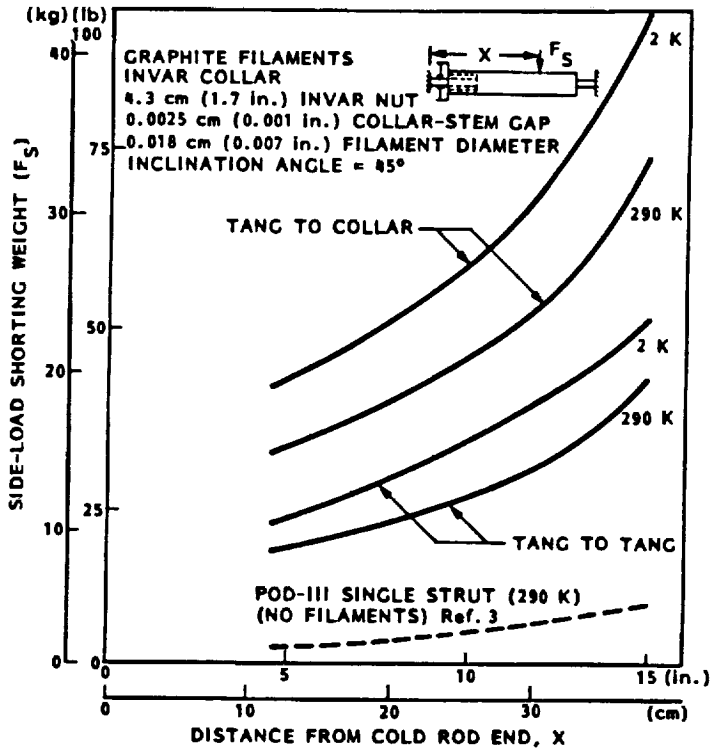

Fig. 3-25 Side-Load Resistance for a 10 Percent Increase in Heat Load

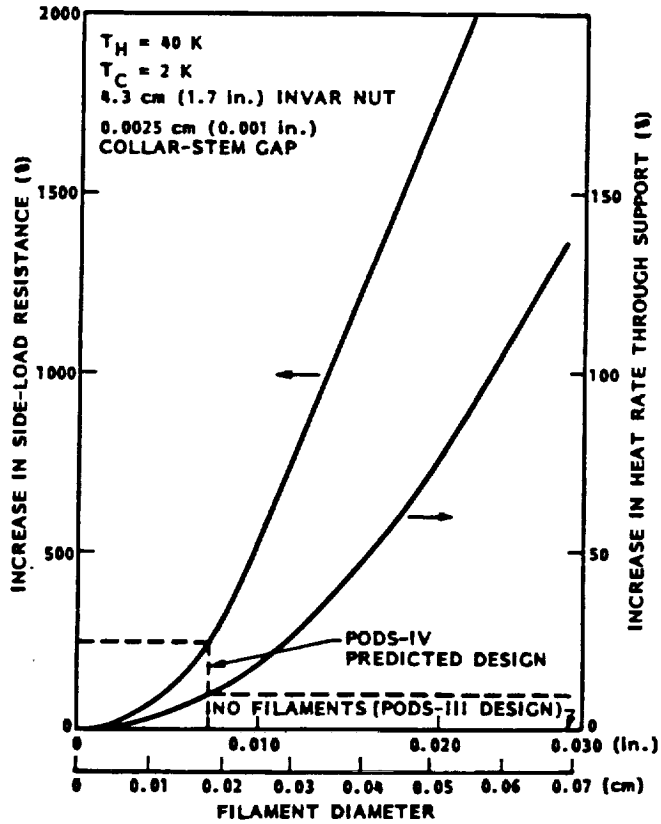

Fig. 3-26 Side-Load Filament Sizing

Section 4
TASK 2 - FABRICATION

4.1 PODS-IV COMPONENTS

A filament support ring and two collars were machined out of invar and coated with pure gold per the Sel-Hex Temperex HD coating process to lower radiation emissivity and prevent rusting. This process was different than the process used on PODS-III (BDT 510) due to the decomposition of the BDT 510 bath. The difference in the processes is that the gold in the BDT 510 bath contained a trace of arsenic. The pure gold coating was slightly duller than the BDT coating. For flight hardware, the BDT 510 bath should be reconditioned and used to provide better surface emissivity.

The filaments were sized by hand from a spool of "Thornel" 3000 filament/tow carbon fiber (WYP 30 1/0). The strands were separated into lengths of approximately 76.2 cm (30.0 in.) and weighed to obtain the desired number of fibers. The strands were then coated with a Sprayon 2000 clear acrylic to keep the strands from fraying. The strands were then twisted into a filament bundle. Some of the fibers broke during separation because of the hair-like nature of the fibers and the woven nature of the 3000 Thornel. Diameter uniformity throughout the length was not certain. Measured filament diameters ranged from 0.0076 cm (0.003 in.) to 0.0127 cm (0.005 in). The desired diameter for a 10 percent increase in heat rate was 0.0178 cm (0.007 in.). The reason for this difference is not known except for the possibility that some of the fibers were lost between the weighing and twisting stage due to fraying of the fibers. Also, there was difficulty in measuring the filament diameter because of fraying and the lack of fiber resistance to deformation caused by the micrometer measuring surfaces. This technique was necessary since the fibers could not be ordered for the desired size in a reasonable time or quantity. Once the filament was twisted, it was cut into six equal lengths and formed

into 3.8-cm (1.5-in.) ID loops. The loop ends were both tied and epoxy bonded with "blue death" (Epibond 1210 A Resin and 9615-10 Hardener).

4.2 FILAMENT ASSEMBLY

The filaments are wound around the collar and tangs in the filament assembly stand (Fig. 4-1). The stand is a whiffle-tree arrangement of pulleys, ball joints, and sliders that is designed to hold an assembled PODS and load all the filaments equally. Figure 4-2 shows the schematic of the system. Load is applied to the system through a wheel and drive screw which is connected to a load cell. The load cell (Fig. 4-3) is used to determine the amount of total load applied to the system. When load is applied to the system, it is transmitted through the load cell to a string that is looped around a pin and free to slide (Fig. 4-4). One end of the string is attached to a half-disc with a verticle rod. The other end of the string is attached to a triangular plate with a ball joint in the center. This plate is able to pivot and slide on the verticle rod. The other end of the rod is connected to another triangular plate with a ball joint that is free to pivot on the rod.

Both masses at each end of the string were balanced. Strings are hung from each corner of the plates and are attached to the top of a series of two blocks (Fig. 4-5). These blocks slide on two pins that are fixed into the assembly stand. The top block has one pulley, while the bottom contains two. The filaments are looped around the collar and tangs, up between the bottom two pulleys, and over the top pulley. The two blocks are connected together with an adjustment screw. This is used to remove any slack in the filaments when the pulleys are lined up between the tangs of the nut. As shown in Fig. 4-2, the actual load to the filaments is one-twelfth of the total load.

The filament loops are wrapped around the collar and tangs in a criss-cross pattern to balance the loading on the collar. The tangs are precoated with blue death epoxy to electrically insulate the nut from the collar. Once the loops have been installed and the assembly stand adjusted to remove slack, load is applied. For the nut-collar test specimen, this value was 11.1 N

Fig. 4-1 Filament Assembly Stand

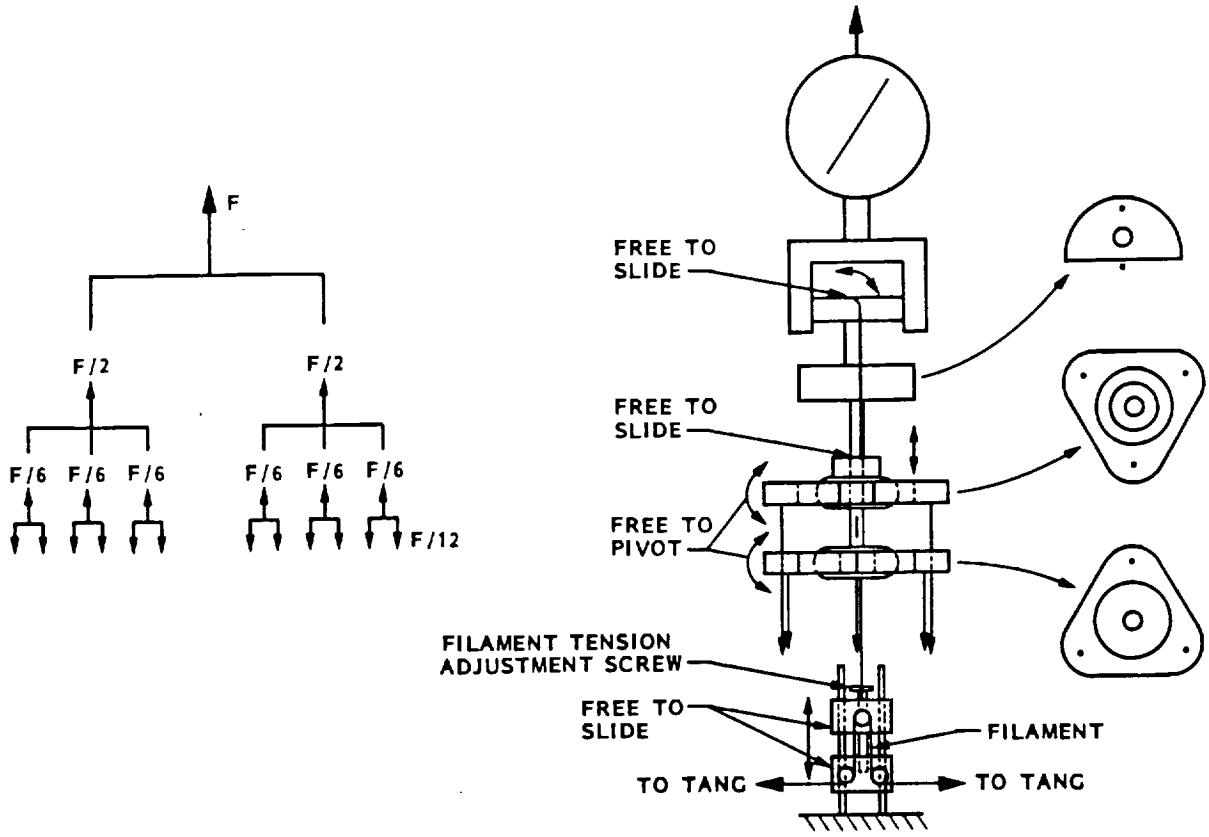

Fig. 4-2 Whiffle-Tree Schematic

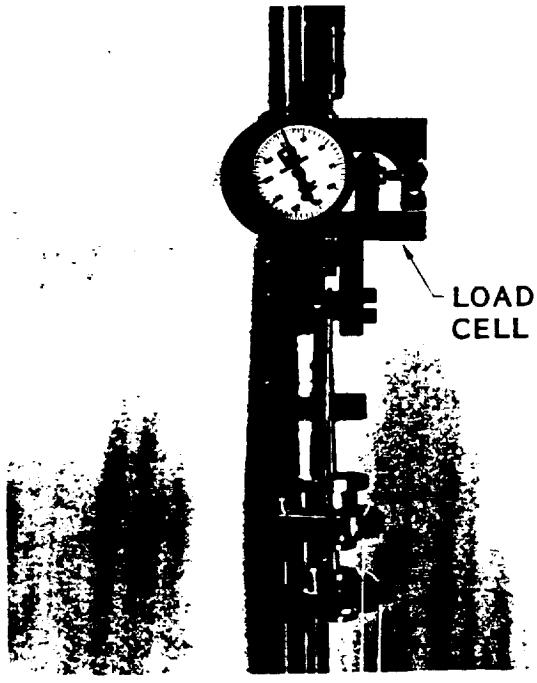

Fig. 4-3 Load Cell

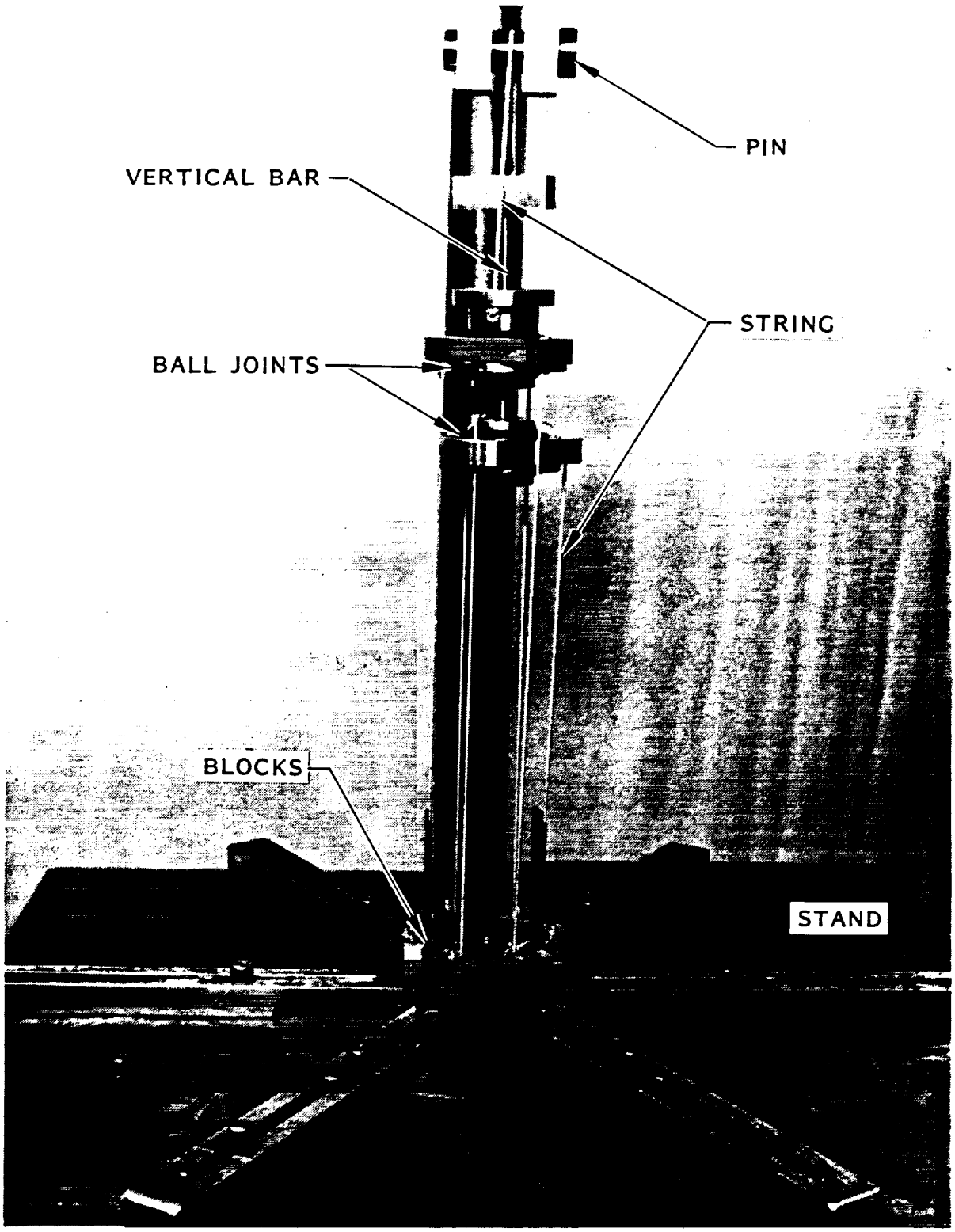

Fig. 4-4 Actual Whiffle-Tree Assembly

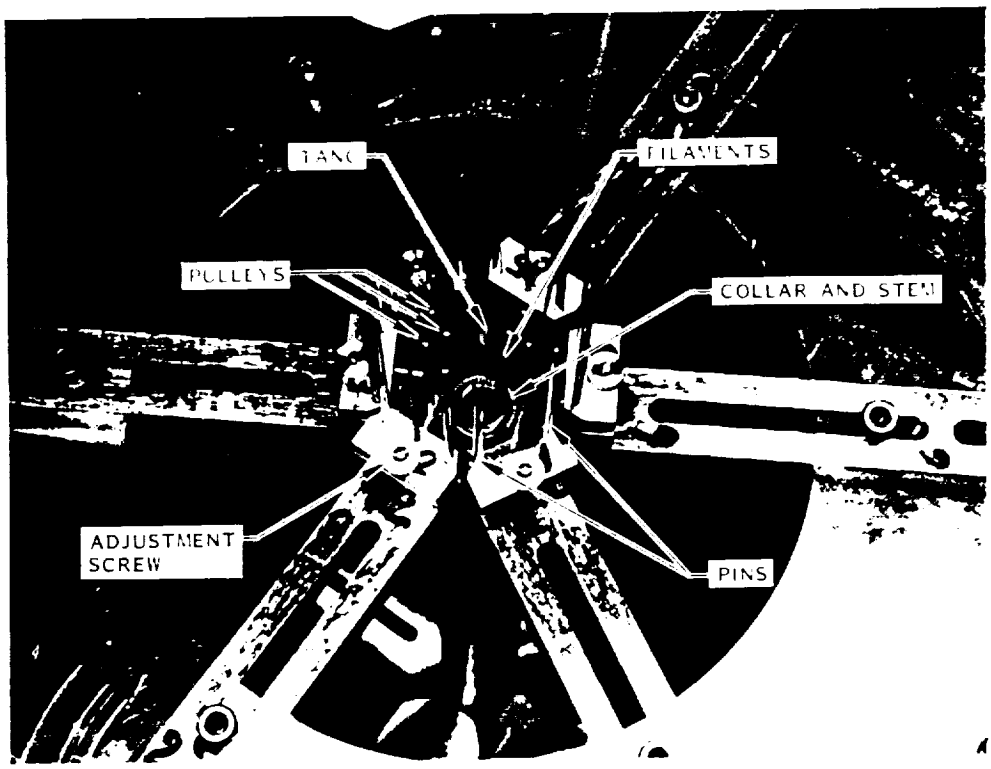

Fig. 4-5 Filament Assembly

(2.5 lb). This was later changed to 33.4 N (7.5 lb) for the assembled PODS to stretch the strings and better load the filaments. (On the first test specimen, the applied load kept dropping off until the system was fully stretched and all the minute kinks had been worked out.) Possible stem shorting is checked by an ohmmeter measurement between the stem and the launch tube body. Once the system has stabilized and both triangular plates are balanced horizontal, blue death epoxy is applied to the tangs. The epoxy is allowed to cure for 24 h before load is removed and the filaments are trimmed, completing the wrap.

4.3 NUT/COLLAR ASSEMBLY

The above procedure was used to assemble the initial nut-collar test specimen except for the initial coat of epoxy on the tangs. This was not done because shorting was not a concern on this assembly, only relative displacement and load characteristics. Figure 4-6 shows the assembly. The filaments varied

from 0.0076 cm (0.003 in.) to 0.0127 cm (0.005 in.) in diameter. This variation was again due to the separation of the fibers and difficulty in measuring the filaments which tended to fray when touched. The filament support ring was pressed on to the nut prior to filament wrapping and screwed on to the strut from which it was removed (strut 4, Ref. 3).

4.4 STRUT ASSEMBLY

PODS-III support 4 was supposed to be used for this assembly, but it was damaged when it was disassembled and inspected during testing described in Ref. 3. This damage caused the support axial load gap offset to be misaligned. This could not be corrected without disassembling the entire strut and rebuilding it.

Another support (strut 2) was chosen for its average values obtained during Ref. 3 testing. This support was modified to the PODS-IV configuration by pressing the filament support ring onto the nut and assembling the filaments according to the procedures in Sections 4.1 and 4.2. Figure 4-7 shows the assembled strut. Figure 4-8 shows the side-load mechanism.

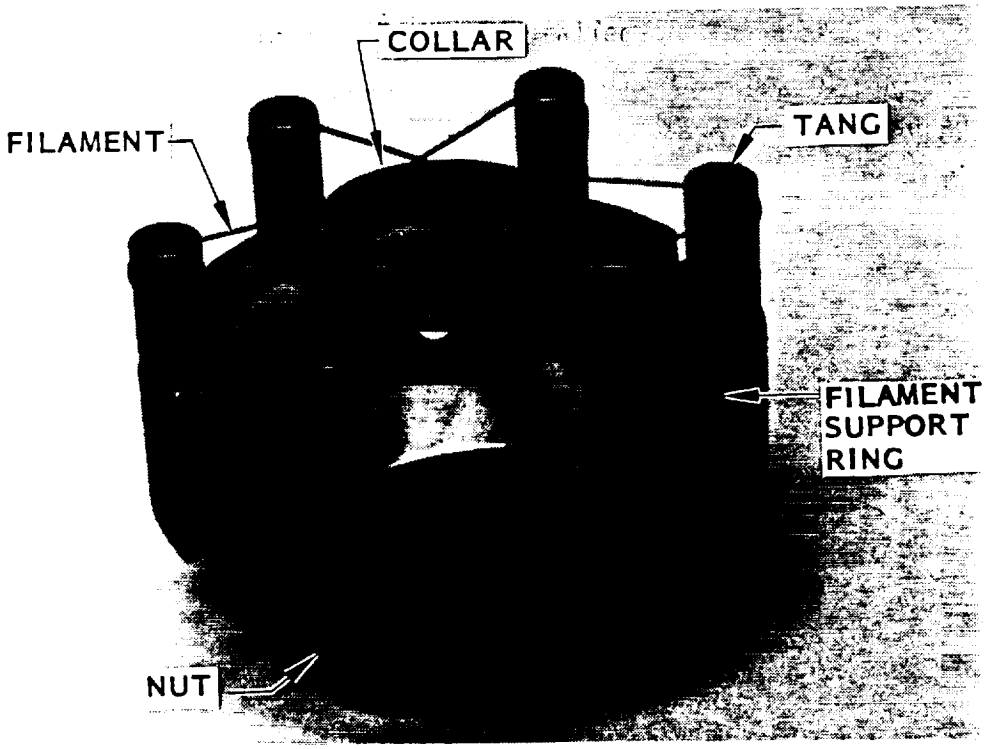

Fig. 4-6 Nut/Collar Assembly

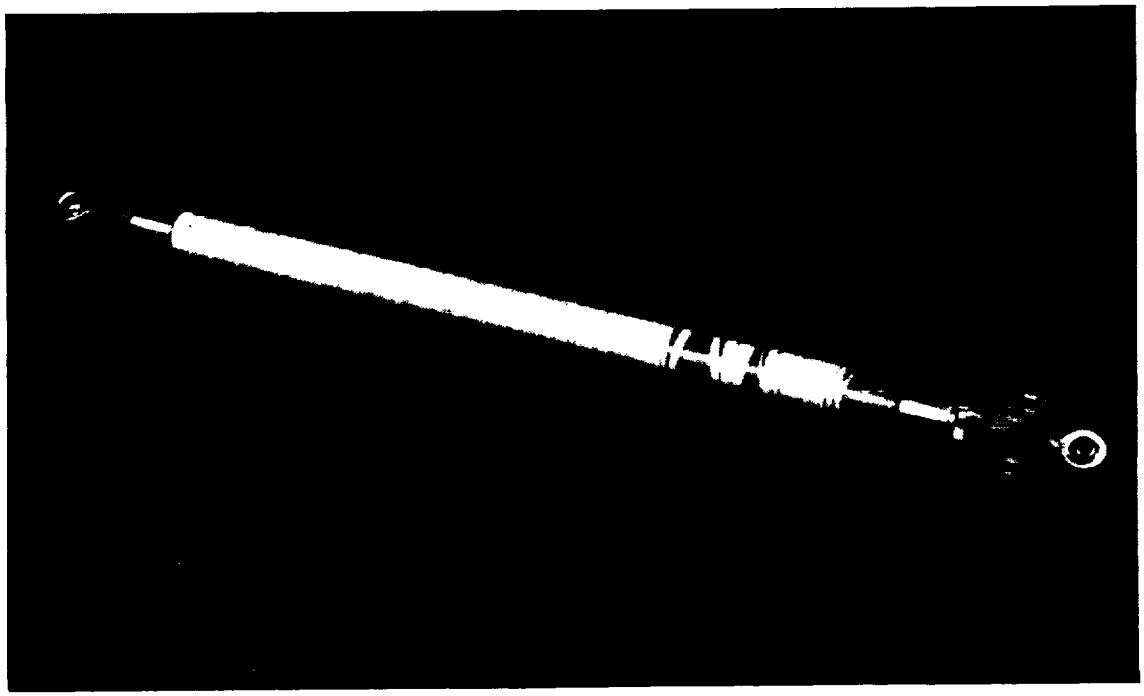

Fig. 4-7 PODS-IV Support

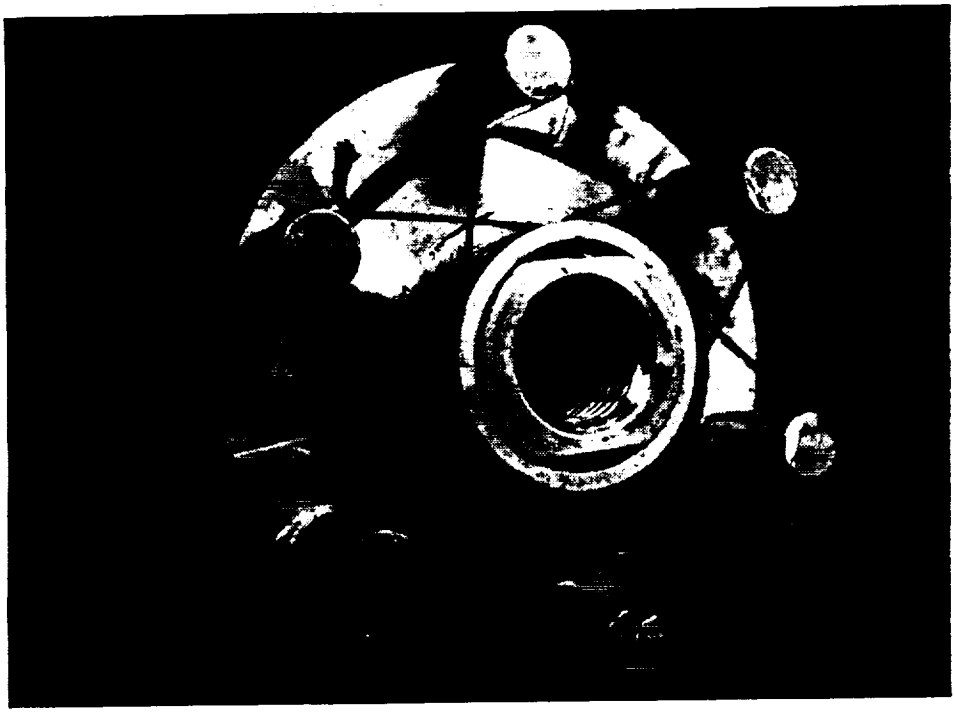

Fig. 4-8 PODS-IV Side-Load Mechanism

Section 5
TASK 3 TESTING

5.1 TEST ARTICLES

Four test specimens were assembled: a single nut/collar assembly and three PODS-IV supports. The nut/collar specimen was assembled using 700-fiber filaments that were hand separated from a 3000-fiber filament and used the tang-to-tang bonding technique. This specimen was used in the load-deflection tests and the ultimate test. The first strut was also assembled with 700-fiber, hand-separated filaments and tang-to-tang bonded. The first strut was modified after initial side-load tests to the tang-to-collar bonded system by bonding the filaments to the collar. After side-load testing of this strut, the filaments were cut and replaced with manufacturer-supplied 1000-fiber (1-K) filaments that were also tang-to-collar bonded and side-load resistance tested. The nut/collar, load-deflection tests and the ultimate test were not conducted for the last two configurations due to time constraints and the fact that the 1-K fiber was not available until the end of strut testing. This was unfortunate, because the 1-K strut dramatically increased the side-load resistance (> 1440 percent) over the PODS-III strut and over the hand-separated, 700-fiber PODS-IV assemblies.

5.2 NUT/COLLAR TESTING

Load-deflection tests were performed on a nut/collar assembly at room temperature. A single ultimate test was conducted at liquid-nitrogen temperatures.

5.2.1 Test Article and Setup

Figure 4-6 shows the nut/collar assembly. The assembly was installed into the load test setup shown in Fig. 5-1 to measure load as a function of

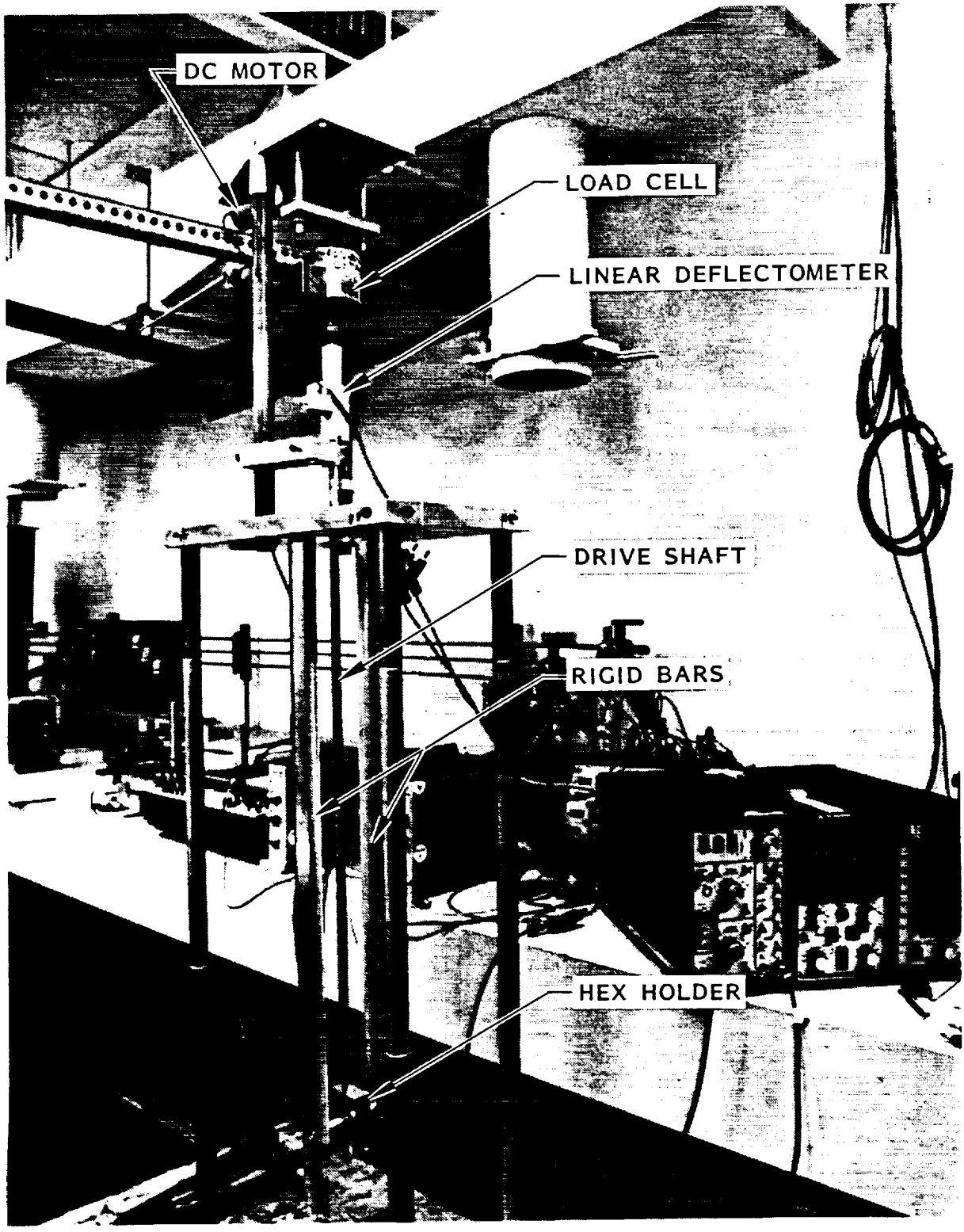

Fig. 5-1 Load-Deflection Test Setup

displacement. A linear deflectometer was installed on the drive shaft and was referenced to the test stand to measure relative displacement of the nut. A DC motor applied the load to cause displacement. This load was measured with a load cell.

Figure 5-2 shows the nut/collar assembly and the hex holder. A brass pin slides through the collar and is supported at each end by two rigid bars. It is held in place by two set screws. The collar and tangs are centered to the drive shaft and held in place with a large set screw.

The same test setup was used to conduct the ultimate stress test on the assembly. The dewar shown in Fig. 5-3 was used to submerge the assembly and adjoining parts in liquid nitrogen.

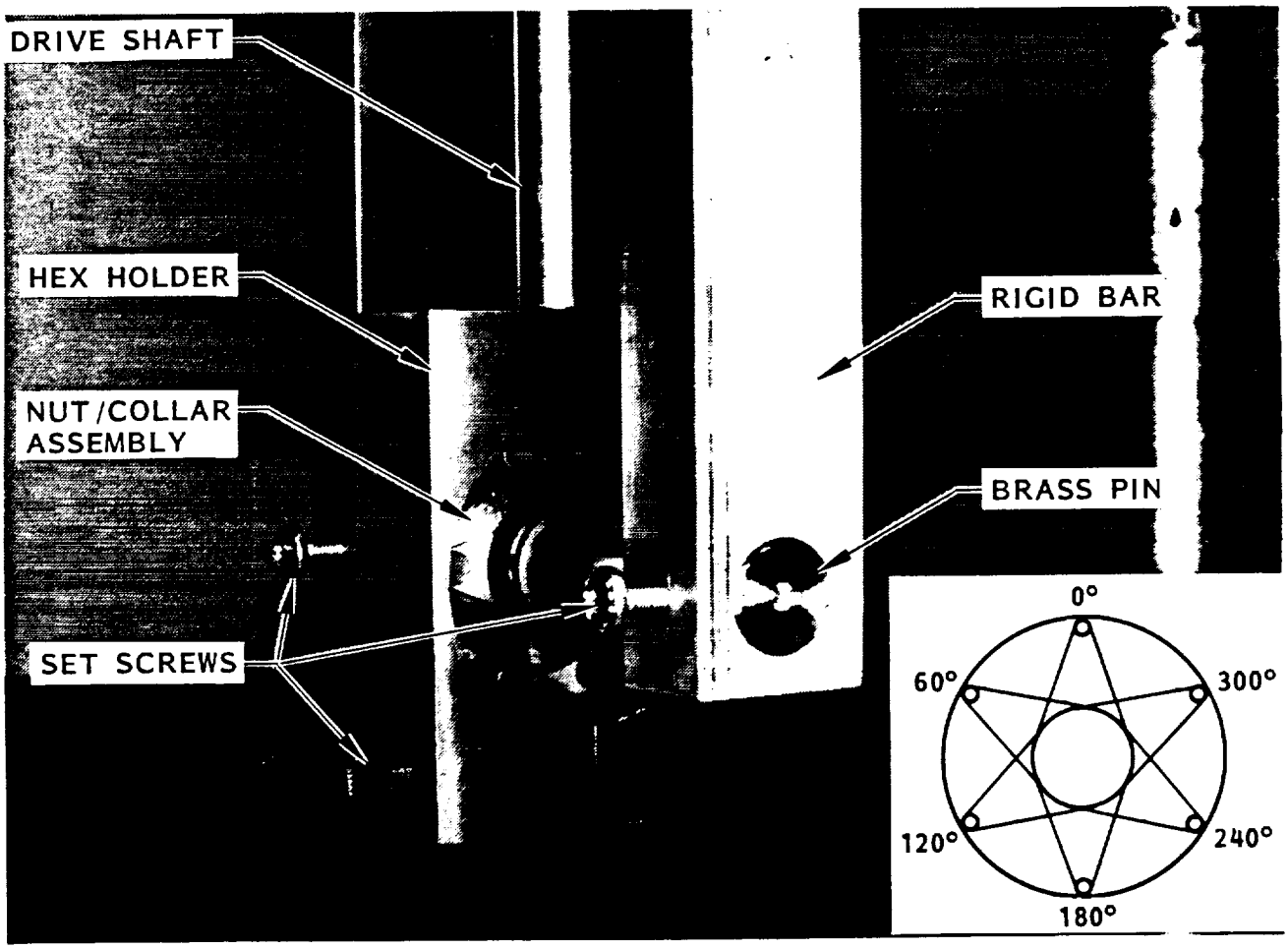

Fig. 5-2 Nut/Collar Assembly in Hex Holder

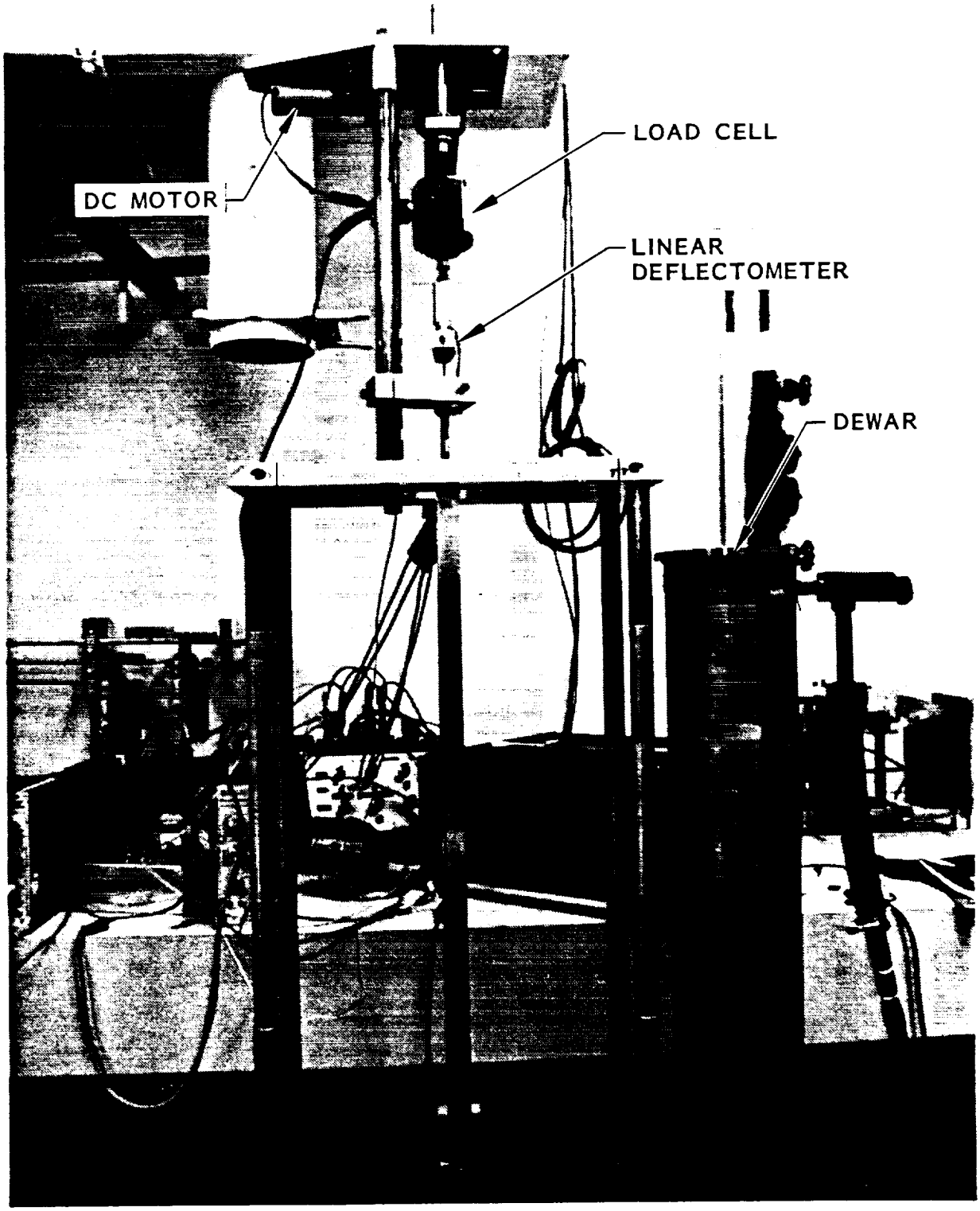

Fig. 5-3 Filament Ultimate Load Test Setup

5.2.2 Nut/Collar Test Procedure

The nut/collar assembly is placed in the hex holder, and the entire assembly is screwed on to the drive shaft. The brass pin is inserted into the collar which is supported by two rigid bars and held in place by two set screws. The collar and tangs are centered to the drive shaft and held with a large set screw. The no-load position is established, and the load and deflection scales are calibrated. The motor is engaged, and the drive shaft moves the nut with respect to the collar. Both force and deflection are recorded. The nut is displaced a maximum of 0.030 cm (0.012 in.). The motor is then reversed, and the nut is moved in the opposite direction, back through the no-load position, to a maximum of 0.030 cm (0.012 in.). The motor is then reversed again and stopped at the no-load position. The test is then repeated 12 times at 30-deg increments around the circumference of the nut.

Once the load-deflection tests are complete, the entire nut/collar assembly and holder is lowered into the dewar. Liquid nitrogen is poured in, covering the assembly. The no-load position is established, and the force and deflection scales are set. The motor is engaged, and the drive shaft moves the nut with respect to the collar. Both force and deflection are recorded until failure occurs.

5.2.3 Nut/Collar Test Results

Appendix A presents the force-deflection curves. Table 5-1 lists the data. The load varies quite a bit, 80 percent to 48 percent from 0.0025 cm (0.001 in.) to 0.0152 cm (0.006 in.) of nut deflection. The reason for the variation is not readily known, since the variation occurs even at the same positions. The collar slipped (turned) during testing and may have changed the conditions from test to test by straining the strands differently. The mean average of the data is shown in Fig. 5-4 compared to the range predicted by the computer model. (The range of values was used, since the diameter was not accurately determined.) The assembly appears to behave similarly to the tang-to-collar system between 4 and 6 mils, possibly due to filament-collar

Table 5-1 NUT/COLLAR LOAD-DEFLECTION DATA

Displacement cm (in.)	0° kg (lb)	30° kg (lb)	60° kg (lb)	90° kg (lb)	120° kg (lb)	150° kg (lb)	180° kg (lb)	210° kg (lb)	240° kg (lb)	270° kg (lb)	300° kg (lb)	330° kg (lb)	Average kg (lb)
0.0025 (0.001)	0.14 (0.3) 0.09 (0.2) 0.05 (0.1)	0.14 (0.3) 0.05 (0.1)	0.14 (0.3) 0.09 (0.2)	0.05 (0.1) 0.09 (0.2)	0.36 (0.8) 0.05 (0.1)	0.27 (0.6) 0.36 (0.8)	0.09 (0.2) 0.09 (0.2)	0.09 (0.2) 0.18 (0.4)	0.14 (0.3) 0.05 (0.1)	0.05 (0.1) 0.05 (0.1)	0.05 (0.1) 0.05 (0.1)	0.09 (0.2) 0.05 (0.1)	0.112 ± 0.09 (0.248 ± 0.20)
0.0051 (0.002)	0.32 (0.7) 0.45 (1.0) 0.09 (0.2)	0.18 (0.4) 0.14 (0.3)	0.27 (0.6) 0.64 (1.4)	0.05 (0.1) 0.73 (1.6)	0.91 (2.0) 1.45 (3.2)	0.77 (1.7) 1.45 (3.2)	0.09 (0.2) 0.45 (1.0)	0.18 (0.4) 1.36 (3.0)	0.32 (0.7) 0.05 (0.1)	0.09 (0.2) 0.27 (0.6)	0.05 (0.1) 0.05 (0.1)	0.09 (0.2) 0.05 (0.1)	0.288 ± 0.27 (0.636 ± 0.60)
0.0076 (0.003)	0.51 (1.13) 1.09 (2.4) 0.32 (0.7)	0.41 (0.9) 0.14 (0.3)	0.32 (0.7) 0.64 (1.4)	0.05 (0.1) 0.73 (1.6)	1.63 (3.6) 1.45 (3.2)	0.41* (0.9) 1.45 (3.2)	0.18 (0.4) 0.45 (1.0)	0.41 (0.9) 1.36 (3.0)	0.86 (1.9) 0.05 (0.1)	0.41 (0.9) 0.27 (0.6)	0.09 (0.2) 0.05 (0.1)	0.09 (0.2) 0.05 (0.1)	0.535 ± 0.485 (1.8 ± 1.07)
0.0102 (0.004)	0.73 (1.6) 1.81 (4.0) 0.91 (2.0)	0.73 (1.6) 0.27 (0.6)	0.36 (0.8) 1.27 (2.8)	0.23 (0.5) 1.27 (2.8)	2.40 (5.3) 2.36 (5.2)	0.32 (0.7) 2.18 (4.8)	0.36 (0.8) 0.91 (2.0)	0.86 (1.9) 2.18 (4.8)	1.59 (3.5) 0.09 (0.2)	0.86 (1.9) 0.73 (1.6)	0.18 (0.4) 0.09 (0.2)	0.36 (0.8) 0.14 (0.3)	0.925 ± 0.744 (2.04 ± 1.64)
0.0127 (0.005)	1.13 (2.5) 2.63 (5.8) 1.63 (3.6)	1.09 (2.4) 0.86 (1.9)	0.77 (1.7) 2.04 (4.5)	0.64 (1.4) 2.00 (4.4)	3.36 (7.4) 3.27 (7.2)	0.73 (1.6) 2.90 (6.4)	0.68 (1.5) 1.63 (3.6)	1.54 (3.4) 3.08 (6.8)	2.45 (5.4) 0.36 (0.8)	1.45 (3.2) 1.27 (2.8)	0.64 (1.4) 0.09 (0.2)	0.91 (2.0) 0.36 (0.8)	1.50 ± 1.03 (3.31 ± 2.10)
0.0152 (0.006)	1.72 (3.8) 3.49 (7.7) 2.45 (5.4)	1.63 (3.6) 1.54 (3.4)	1.45 (3.2) 2.90 (6.4)	1.18 (2.6) 2.86 (6.3)	2.54* (5.6) 43.17 (9.2)	1.18 (2.6) 3.76 (8.3)	1.27 (2.8) 2.54 (5.6)	2.36 (5.2) 3.95 (8.7)	3.40 (7.5) 0.77 (1.7)	2.09 (4.6) 2.00 (4.4)	1.32 (2.9) 0.32 (0.7)	1.63 (3.6) 0.91 (2.0)	2.14 ± 1.03 (4.71 ± 2.27)

* Collar slipped, causing load to decrease

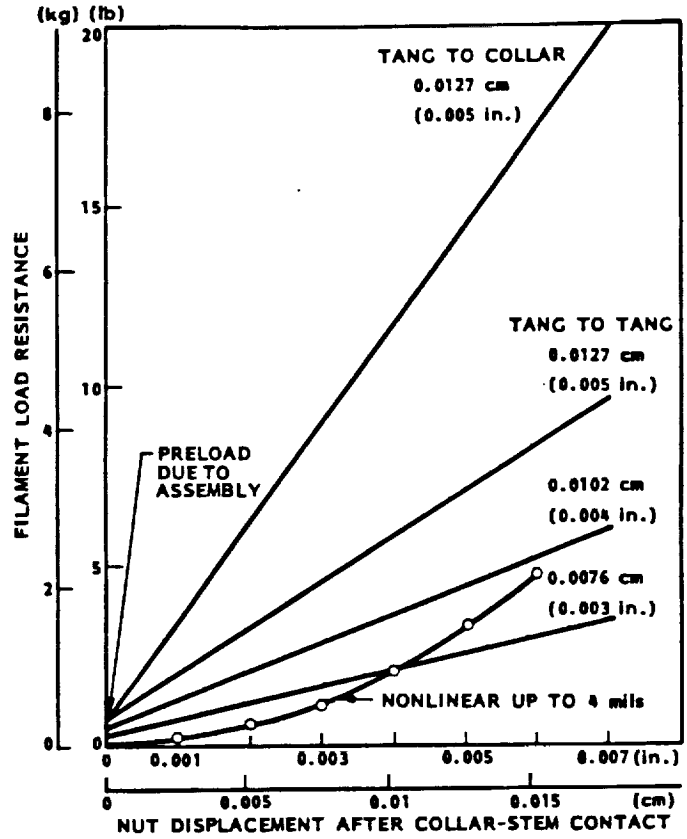

Fig. 5-4 Filament Load Versus Displacement Results (290 K)

friction. At the position 330 deg around the nut, a failure in one of the epoxy-tang joints occurred. Inspection of the joint indicated that the epoxy did not adhere to the tang, possibly due to the surface smoothness. No indication of epoxy-graphite or other bond failure was noticed.

The nut/collar assembly was positioned in the holder to place the broken filament in compression and negate its affect on the system. The force-displacement data are also shown in Appendix A. The filaments failed at 20.32 kg (44.8 lb) and a deflection of 0.0569 cm (0.0224 in.). The first 6 mils of the load-deflection curve are shown in Fig. 5-5 compared to the computer model range. Preload drops off due to contraction of the invar nut/ring assembly which is shown by the curves being displaced to the right. The curve effectively represents a stress-strain curve for the system and shows that the slope is nonlinear for the first 4 mils of deflection. Figure 5-4 showed a similar nonlinearity. Perhaps there was some slack in the

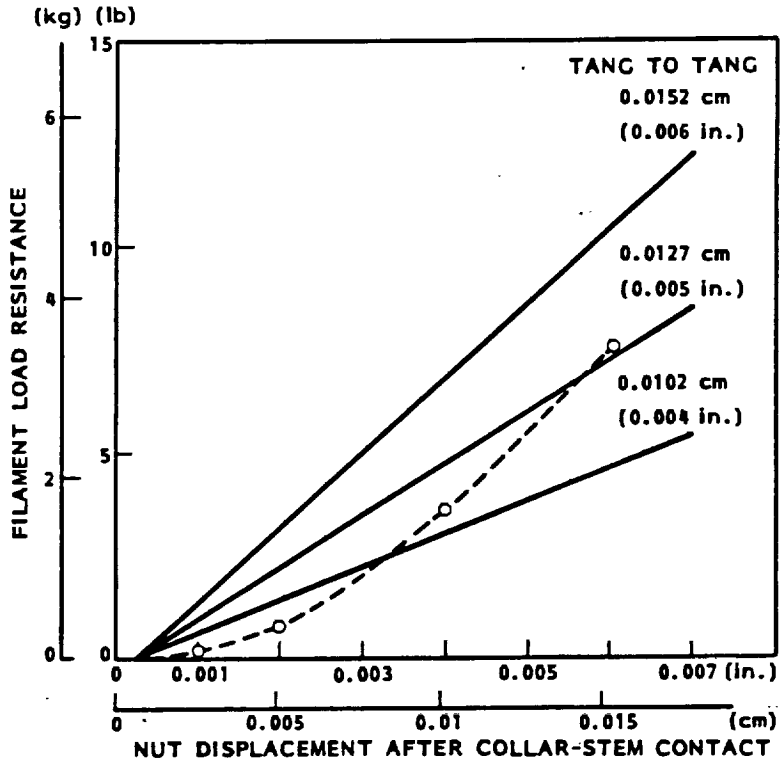

Fig. 5-5 Filament Load Versus Displacement Results (77 K)

filaments from only loading the filament assembly to 11.1 N (2.5 lb). The assembly load was increased to 33.4 N (7.5 lb) for the strut assembly.

5.3 SINGLE STRUT SIDE-LOAD TESTING

A complete PODS-IV was assembled from PODS-III strut 2. Sections 4.1 and 4.2 describe the procedure for wrapping the filaments. An axial load gap offset of 0.020 cm (0.008 in.) and a collar-stem gap of 0.0025 cm (0.001 in.) were used. The strut is 59.07 cm (23.256 in.) long from center to center of the rod end fittings and was tested on the same test setup used in Ref. 3.

5.3.1 Side-Load Tests

Vapor-cooled shields attached to the struts plus installed multilayer insulation (MLI) place side loads on the struts in 1-g. The side-load tests determine the maximum loads that can be tolerated as a function of load

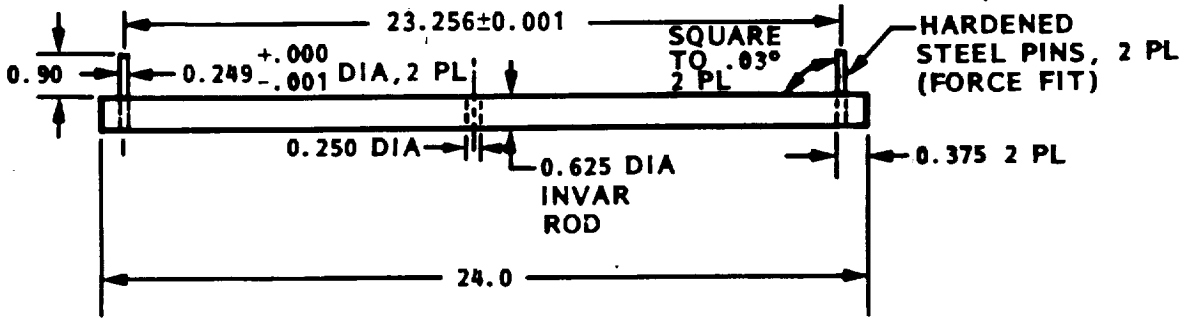

Fig. 5-6 Length Adjustment Bar

(inclination) angle and location without shorting out the strut on the ground. In orbit, weight is no longer a factor.

5.3.2 Test Setup

The length adjustment bar (Fig. 5-6) supports the strut for these tests. The invar bar has two 0.64-cm (0.250-in.) diameter press fit pins located 59.07 cm (23.256 in.) apart that slip into the rod end fittings. The bar is supported off a plate at 0 (horizontal), 15, 30, 45, 60, and 75 deg as shown in Fig. 5-7. Figure 5-8 shows the setup with strut supported. Weights are hung on the strut at different locations (including lead shot for fine weight adjustment) until the PODS-IV mechanism shorts as determined by an ohmmeter measurement between the body and stem. Figure 5-9 shows a close-up of the mechanism. The strut can be rotated so that the shorting loads are measured at 30-deg increments around the circumference to determine how well the collar is centered between the body and nut and how uniformly the strands are loaded.

5.3.3 Single Strut Test Results

Table 5-2 presents the test results and compares them to the results obtained in Ref. 3. The shorting measurements around the circumference with the

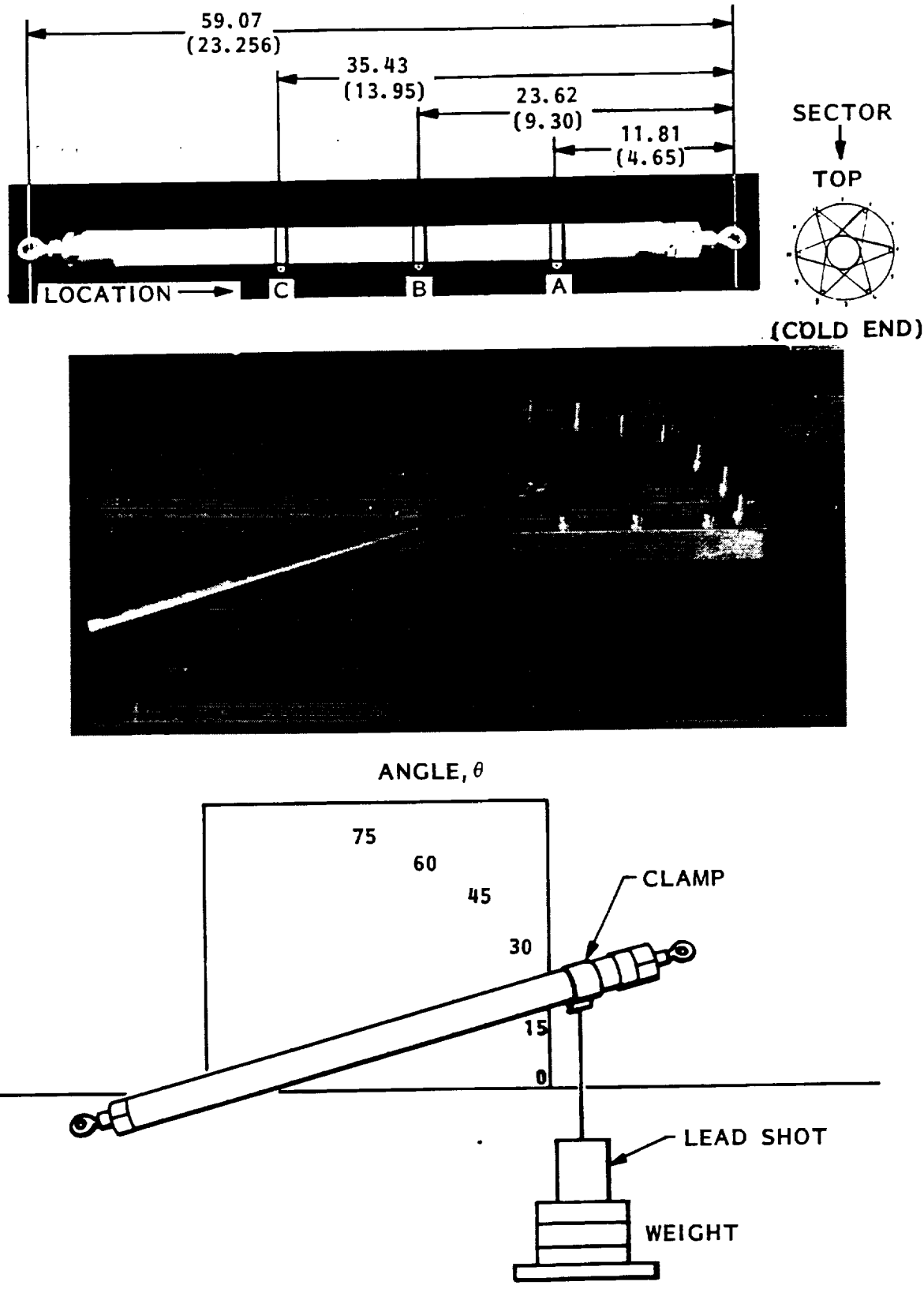

Fig. 5-7 Side-Load Test Setup

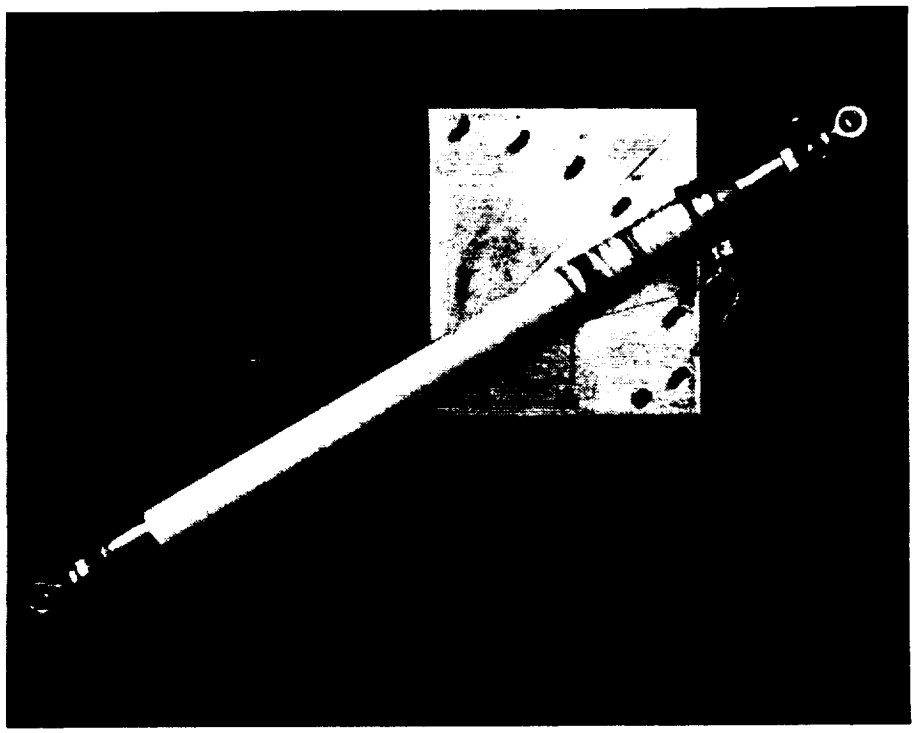

Fig. 5-8 Test Setup With PODS-IV Installed

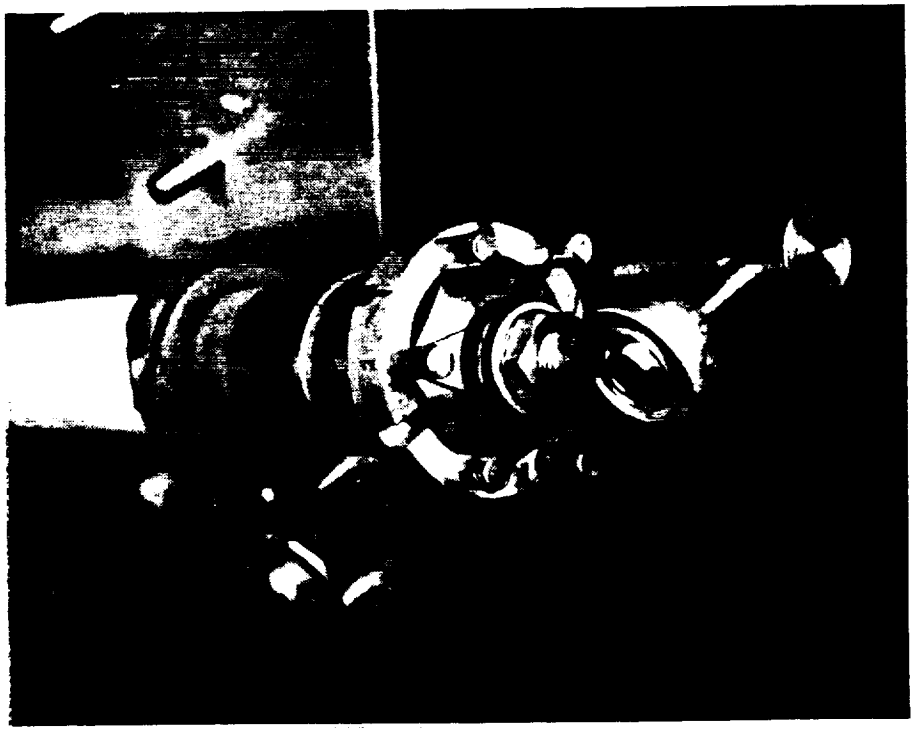

Fig. 5-9 PODS-IV Support Side-Load Mechanism

Table 5-2 PODS-IV SIDE-LOAD DATA

Strut Inclination Angle (deg)	PODS-III Single Strut (Ref. 3) kg (lb)	Sector													Average kg (lb)
		1 kg (lb)	1*	2 kg (lb)	3 kg (lb)	4 kg (lb)	5 kg (lb)	6 kg (lb)	7 kg (lb)	8 kg (lb)	9 kg (lb)	10 kg (lb)	11 kg (lb)	12 kg (lb)	
		Location A: 11.81 cm (4.65 in.)													
0	1.76 (3.88)	3.11 (6.85)	4.60 (10.15)	3.13 (6.90)	3.63 (8.00)	3.81 (8.40)	4.47 (9.85)	4.22 (9.30)	3.65 (8.05)	4.06 (8.95)	3.54 (7.80)	2.61 (5.75)	2.49 (5.50)	2.56 (5.65)	3.44 ± 0.64 (7.58 ± 1.40)
30	2.13 (4.70)	3.49 (7.70)	5.38 (11.85)												
45	2.67 (5.88)	4.35 (9.60)	6.12 (13.50)												
60	3.65 (8.05)	6.19 (13.65)	9.34 (20.60)												
		Location B: 23.62 cm (9.3 in.)													
0	2.34 (5.15)	3.90 (8.60)	5.99 (13.20)	4.31 (9.50)	4.92 (10.85)	5.31 (11.70)	5.99 (13.20)	5.65 (12.45)	4.85 (10.70)	5.15 (11.35)	4.74 (10.45)	3.38 (7.45)	3.31 (7.30)	3.38 (7.45)	4.57 ± 0.88 (10.08 ± 1.93)
30	2.69 (5.94)	4.60 (10.15)	7.17 (15.80)												
45	3.54 (7.80)	5.58 (12.30)	8.78 (19.35)												
60	4.96 (10.93)	8.07 (17.80)	12.41 (27.35)												
		Location C: 35.43 cm (13.95 in.)													
0	3.54 (7.80)	6.19 (13.65)	8.85 (19.50)	6.60 (14.55)	7.55 (16.65)	7.55 (16.65)	7.80 (17.20)	8.62 (19.00)	7.17 (15.80)	6.80 (15.00)	6.67 (14.70)	5.08 (11.20)	4.85 (10.70)	5.10 (11.25)	6.67 ± 1.13 (14.70 ± 2.50)
30	4.06 (8.95)	7.14 (15.75)	10.39 (22.90)												
45	5.21 (11.48)	8.78 (19.35)	12.47 (27.50)												
60	7.03 (15.50)	11.95 (26.35)	17.85 (39.35)												

*Filaments epoxy bonded to collar to produce a tang-to-collar system

support horizontal had a standard deviation variation of +17 percent to 19 percent, indicating that the increase in assembly load helped to equally load the filaments.

Figure 5-10 plots the effects of load location and inclination angle. The PODS-III single strut data are also plotted. The filaments effectively increased the side-load resistance by 68 percent over the PODS-III design in the tang-to-tang system. The increase was 152 percent for the tang-to-collar bonding. The equations in Fig. 5-10 give the strut angle and length relationships. The empirical constants will change with load gap setting, stem angle, filament dimensions, and graphite tube dimensions and properties.

Since the filament diameter was not known due to the difficulty in measuring the filaments and the uncertainties in the separation process, the data were compared to a range of model values shown in Fig. 5-11. The data appear to fall between 0.0076 cm (0.003 in.) and 0.0102 cm (0.004 in.). The measured values obtained were between 0.0076 cm (0.003 in.) and 0.0127 cm (0.005 in.).

The data for an inclination angle of 45 deg was also compared in Fig. 5-12 to a six-strut system tested in Ref. 3. The equations in Fig. 5-10 were multiplied by 6 to approximate a six-strut system. Curves were also produced for normal support operation by scaling the data according to the change in load gap setting from 290 K down to 2 K.

The support was also wrapped with 1-K, 0.0218-cm (0.0086-in.) diameter filaments that were used as supplied by the manufacturer. Since this filament was not available until the end of testing, it was not used in the previous load-deflection and ultimate tests. The filaments were epoxy bonded between the tangs and collar. The strut was side-loaded in the horizontal position up to 27.2 kg (60.0 lb) at location A with no shorting. The strut was placed in tension during the horizontal side-load test to even out the two gaps on each side of the stem to simulate actual operating conditions between 20-40 K. Since one end of the strut has left-handed threads and the other right-handed, the strut was placed in tension by turning the fiberglass launch tube after the strut was positioned in the test fixture between the two fixed pins of the

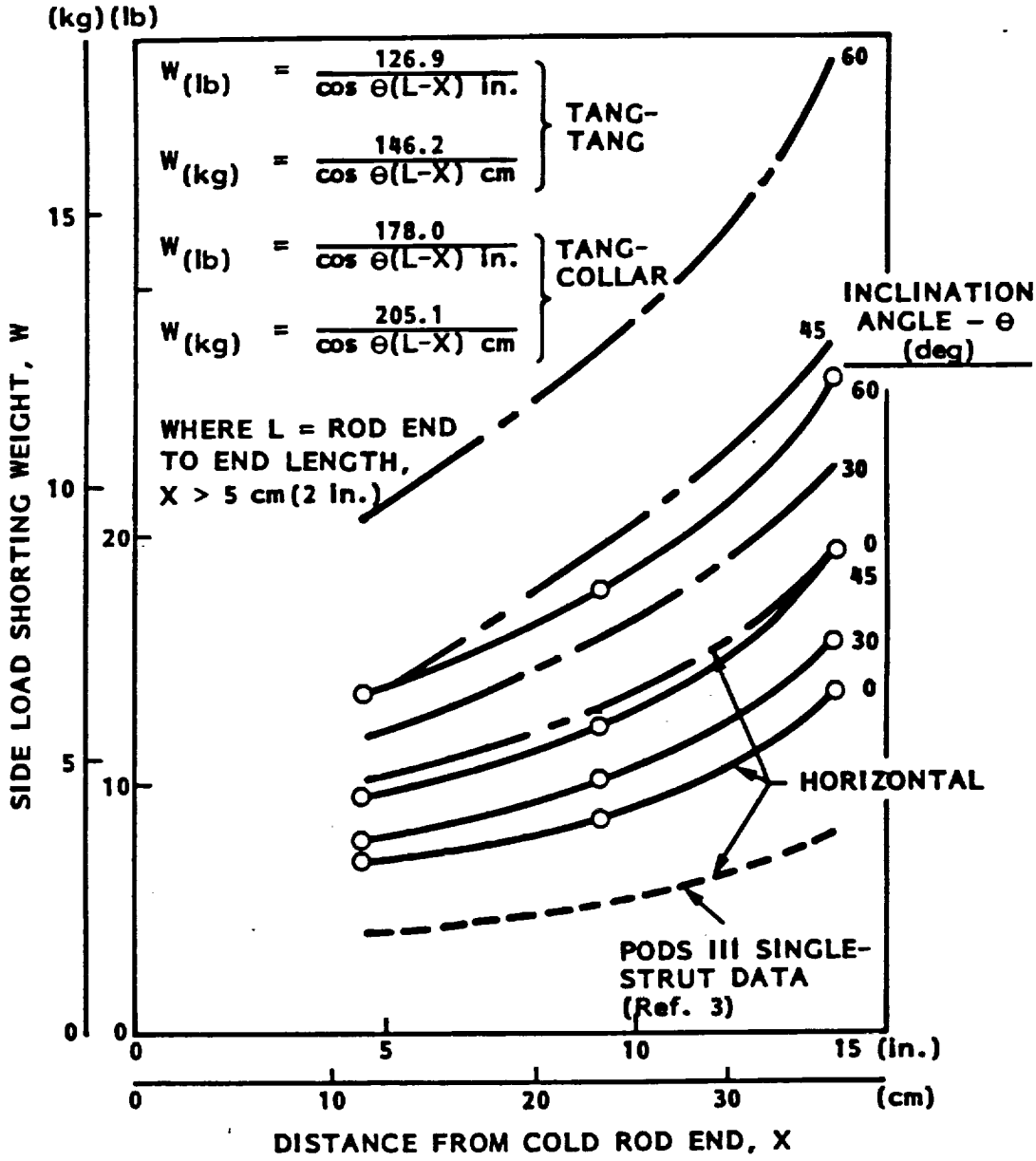

Fig. 5-10 Shorting Side Loads as a Function of Location and Angle

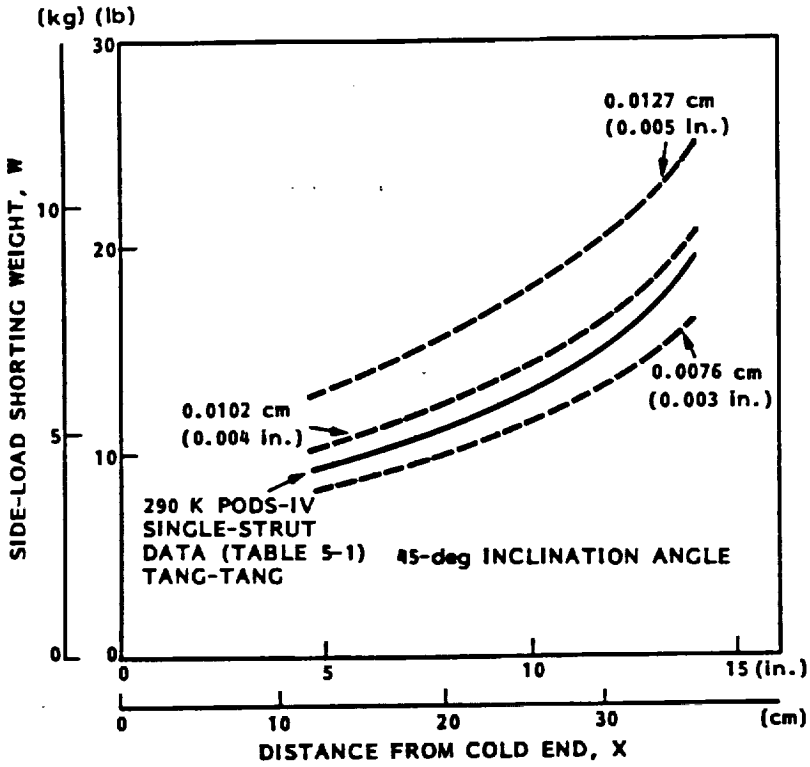

Fig. 5-11 Shorting Side-Load Model-Data Comparison

length adjustment bar. This caused the graphite/epoxy orbit tube to elongate and increase the limiting disconnect gap. The strut was side-loaded in this position to 27.2 kg (60.0 lb) at location A with no shorting. The test was stopped at this point due to safety concerns over the deflection of the fiberglass launch tube.

The support was checked by applying force directly over the filaments and electrically shorting it out. The side-load test was repeated around the nut circumference at location A with no shorting observed up to 27.2 kg (60.0 lb). Repeated checking of the support confirmed that the strut would short out if the nut was displaced. The filaments were not adversely affected by this displacement. The increase in side-load resistance was > 1440 percent over the PODS-III design. The predicted increase in support conductance is 15 percent. This > 1440 percent increase represents a major advance over the PODS-III support, not only in side-load resistance but also in design, since the increase largely removes the maximum length criterion of the graphite/epoxy orbit tube that was established due to PODS-III side-load limitations.

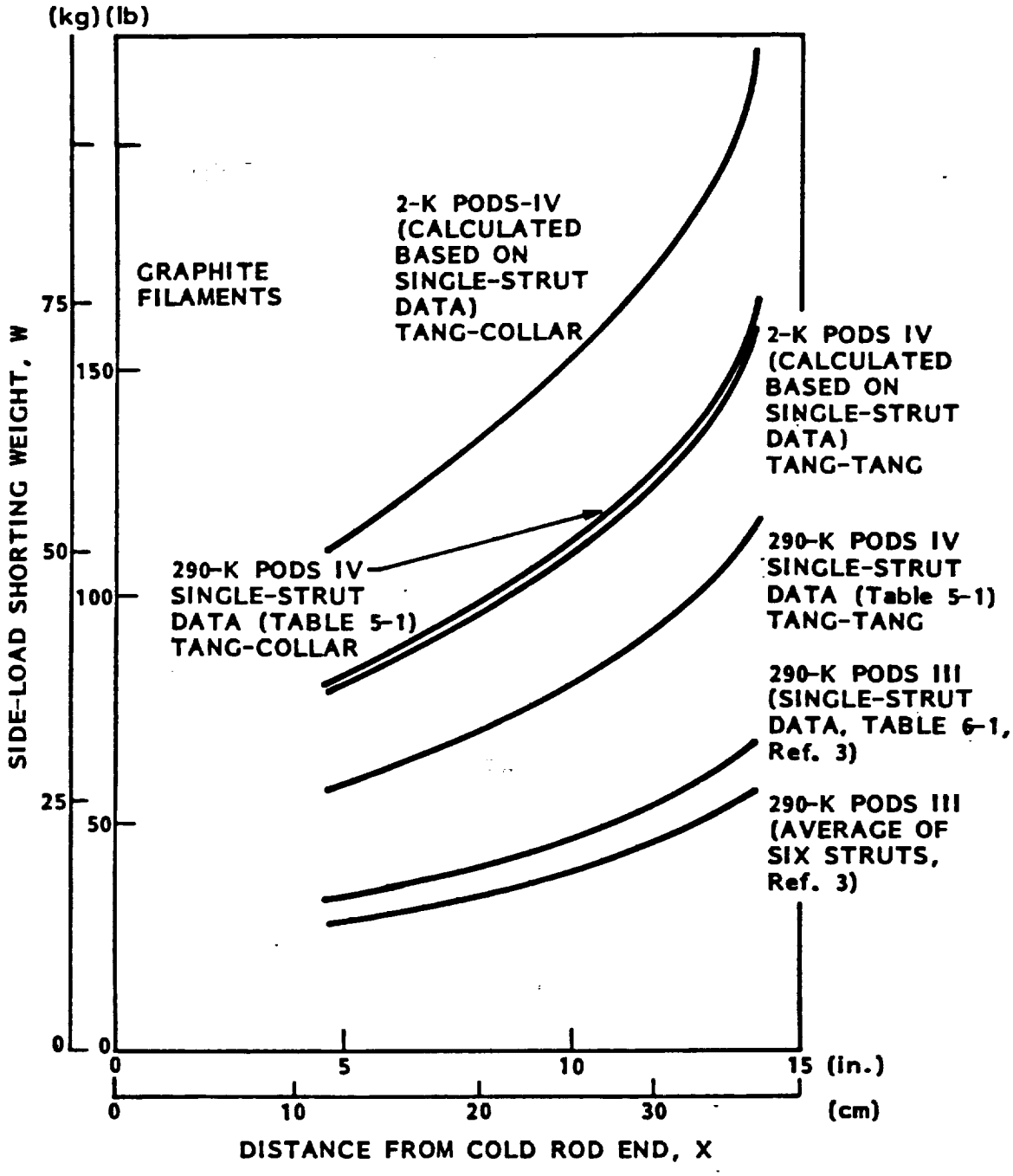

Fig. 5-12 Side-Load Shorting for a Six-Support System

Section 6
CONCLUSIONS AND RECOMMENDATIONS

6.1 CONCLUSIONS

Load-deflection tests on a PODS-IV nut/collar assembly established the ability of the graphite filaments to elastically deform over the shorting gap range. Uniform loading was not conclusively established because of collar slippage caused by filament-collar friction.

Load-deflection tests on a PODS-IV nut/collar assembly established the ability of the graphite filaments to elastically deform over the shorting gap range. Uniform loading was not conclusively established due to collar slippage caused by filament-collar friction.

Side-load tests were done on three assembled PODS-IV supports. Circumferential loading of the first support verified the adequacy of the whiffle-tree assembly and the six-tang design to provide uniform load resistance. Resistance to side-loads was increased 68 percent (tang-to-tang bonding) to 152 percent (tang-to-collar bonding) over the PODS-III design, with only marginal predicted increase in support conductance by using hand-separated 700-fiber filaments from supplied 3000-fiber strands. A larger side-load resistance can be realized by eliminating fiber damage during separation.

A >1440-percent increase in side-load resistance was obtained (using a standard 1000-fiber filament from the supplier) on a strut that was tensioned to simulate orbital conditions. Unfortunately, this fiber bundle was obtained at the end of the test program and was not available for the initial load-deflection and ultimate load tests. A 15-percent increase in support conductance is predicted for this strut if the orbital tube length is kept the same. This >1440-percent increase represents a major advance over the

PODS-III support, not only in side-load resistance but also in design, since the increase largely removes the maximum length criterion of the graphite/epoxy orbit tube that was established due to PODS-III side-load limitations. Consequently, the total conductance of a PODS-IV design can actually be lower than PODS-III, due to the higher resistance of the longer orbit tube.

6.2 RECOMMENDATIONS

The following recommendations resulted from this test program:

1. Use the PODS-IV design concept shown in Section 3 if the PODS-III side-load shorting capacity is inadequate.
2. Modify the PODS-IV concept by epoxy-bonding the filaments to the collar to generate higher filament strains and corresponding side-load resistance. This can also be accomplished by increasing assembly filament preload.
3. Use the assembly procedure specified in Section 4.2 to assemble the PODS-IV mechanism.
4. Use standard fiber bundles from suppliers; separation of fibers appears to damage and lower fiber strength.
5. Since the 1000-fiber filament was only available at the end of testing, repeat series of nut/collar load-deflection tests using the fiber to better characterize mechanism performance.

Section 7
REFERENCES

1. R. T. Parmley, Feasibility Study for Long Lifetime Helium Dewar, NASA CR 166254, Dec 1981.

2. R. T. Parmley, Passive Orbital Disconnect Strut (PODS-III) Structural and Thermal Test Program, NASA CR 166473, Mar 1983.

3. R. T. Parmley, Passive Orbital Disconnect Strut (PODS-III) Structural Test Program, NASA CR 177325, Jan 1985.

4. R. T. Parmley, Test and Evaluate Passive Orbital Disconnect Struts (PODS-III), NASA CR 177368, Aug 1985.

5. S. Nishijima, T. Okada, and M. Takano, "Thermal and Mechanical Properties of Advanced Composite Materials At Low Temperatures," ICMC, 12-16 Aug 1985, DX-5.

6. Owens/Corning Fiberglas Data Sheet on E, S, and S2 glass.

7. Union Carbide Technical Bulletin 465-227 on Thornel 300 carbon fiber, Grade WYP 15 1/0.

8. J. V. Gauchel, J. L. Olinger, and D. C. Lupton, "Characterization of Glass Reinforced Composites for Cryogenic Applications," Advances in Cryogenic Engineering, Vol. 28, 1982, p. 214.

Appendix A
LOAD-DEFLECTION TEST RESULTS

The load-deflection plots given here are test data from Section 5.1. The curves are labeled according to angle position and refer to Table 5-1. The loads were recorded up to + 12 mils from the zero datum. Abrupt changes in slope represent collar-stem slippage and corresponding ease in filament strain.

5-29-1986
Pods 4 Modified
Cycle 1
Position D
0/93:30
Capt. Holmes
Lt. Gardner
Scales:
Horiz: .001"/inch
Vert: 2 lbs/inch
Down
Δ=.045"
Δ=.045" @ 25 lbs
Δ=.045" @ 50 lbs
Δ=.045" @ 75 lbs
Δ=.045" @ 100 lbs
Δ=.045" @ 125 lbs
Δ=.045" @ 150 lbs
Δ=.045" @ 175 lbs
Δ=.045" @ 200 lbs
Δ=.045" @ 225 lbs
Δ=.045" @ 250 lbs
Δ=.045" @ 275 lbs
Δ=.045" @ 300 lbs
Δ=.045" @ 325 lbs
Δ=.045" @ 350 lbs
Δ=.045" @ 375 lbs
Δ=.045" @ 400 lbs
Δ=.045" @ 425 lbs
Δ=.045" @ 450 lbs
Δ=.045" @ 475 lbs
Δ=.045" @ 500 lbs
Δ=.045" @ 525 lbs
Δ=.045" @ 550 lbs
Δ=.045" @ 575 lbs
Δ=.045" @ 600 lbs
Δ=.045" @ 625 lbs
Δ=.045" @ 650 lbs
Δ=.045" @ 675 lbs
Δ=.045" @ 700 lbs
Δ=.045" @ 725 lbs
Δ=.045" @ 750 lbs
Δ=.045" @ 775 lbs
Δ=.045" @ 800 lbs
Δ=.045" @ 825 lbs
Δ=.045" @ 850 lbs
Δ=.045" @ 875 lbs
Δ=.045" @ 900 lbs
Δ=.045" @ 925 lbs
Δ=.045" @ 950 lbs
Δ=.045" @ 975 lbs
Δ=.045" @ 1000 lbs
Δ=.045" @ 1025 lbs
Δ=.045" @ 1050 lbs
Δ=.045" @ 1075 lbs
Δ=.045" @ 1100 lbs
Δ=.045" @ 1125 lbs
Δ=.045" @ 1150 lbs
Δ=.045" @ 1175 lbs
Δ=.045" @ 1200 lbs
Δ=.045" @ 1225 lbs
Δ=.045" @ 1250 lbs
Δ=.045" @ 1275 lbs
Δ=.045" @ 1300 lbs
Δ=.045" @ 1325 lbs
Δ=.045" @ 1350 lbs
Δ=.045" @ 1375 lbs
Δ=.045" @ 1400 lbs
Δ=.045" @ 1425 lbs
Δ=.045" @ 1450 lbs
Δ=.045" @ 1475 lbs
Δ=.045" @ 1500 lbs
Δ=.045" @ 1525 lbs
Δ=.045" @ 1550 lbs
Δ=.045" @ 1575 lbs
Δ=.045" @ 1600 lbs
Δ=.045" @ 1625 lbs
Δ=.045" @ 1650 lbs
Δ=.045" @ 1675 lbs
Δ=.045" @ 1700 lbs
Δ=.045" @ 1725 lbs
Δ=.045" @ 1750 lbs
Δ=.045" @ 1775 lbs
Δ=.045" @ 1800 lbs
Δ=.045" @ 1825 lbs
Δ=.045" @ 1850 lbs
Δ=.045" @ 1875 lbs
Δ=.045" @ 1900 lbs
Δ=.045" @ 1925 lbs
Δ=.045" @ 1950 lbs
Δ=.045" @ 1975 lbs
Δ=.045" @ 2000 lbs
Δ=.045" @ 2025 lbs
Δ=.045" @ 2050 lbs
Δ=.045" @ 2075 lbs
Δ=.045" @ 2100 lbs
Δ=.045" @ 2125 lbs
Δ=.045" @ 2150 lbs
Δ=.045" @ 2175 lbs
Δ=.045" @ 2200 lbs
Δ=.045" @ 2225 lbs
Δ=.045" @ 2250 lbs
Δ=.045" @ 2275 lbs
Δ=.045" @ 2300 lbs
Δ=.045" @ 2325 lbs
Δ=.045" @ 2350 lbs
Δ=.045" @ 2375 lbs
Δ=.045" @ 2400 lbs
Δ=.045" @ 2425 lbs
Δ=.045" @ 2450 lbs
Δ=.045" @ 2475 lbs
Δ=.045" @ 2500 lbs
Δ=.045" @ 2525 lbs
Δ=.045" @ 2550 lbs
Δ=.045" @ 2575 lbs
Δ=.045" @ 2600 lbs
Δ=.045" @ 2625 lbs
Δ=.045" @ 2650 lbs
Δ=.045" @ 2675 lbs
Δ=.045" @ 2700 lbs
Δ=.045" @ 2725 lbs
Δ=.045" @ 2750 lbs
Δ=.045" @ 2775 lbs
Δ=.045" @ 2800 lbs
Δ=.045" @ 2825 lbs
Δ=.045" @ 2850 lbs
Δ=.045" @ 2875 lbs
Δ=.045" @ 2900 lbs
Δ=.045" @ 2925 lbs
Δ=.045" @ 2950 lbs
Δ=.045" @ 2975 lbs
Δ=.045" @ 3000 lbs
Δ=.045" @ 3025 lbs
Δ=.045" @ 3050 lbs
Δ=.045" @ 3075 lbs
Δ=.045" @ 3100 lbs
Δ=.045" @ 3125 lbs
Δ=.045" @ 3150 lbs
Δ=.045" @ 3175 lbs
Δ=.045" @ 3200 lbs
Δ=.045" @ 3225 lbs
Δ=.045" @ 3250 lbs
Δ=.045" @ 3275 lbs
Δ=.045" @ 3300 lbs
Δ=.045" @ 3325 lbs
Δ=.045" @ 3350 lbs
Δ=.045" @ 3375 lbs
Δ=.045" @ 3400 lbs
Δ=.045" @ 3425 lbs
Δ=.045" @ 3450 lbs
Δ=.045" @ 3475 lbs
Δ=.045" @ 3500 lbs
Δ=.045" @ 3525 lbs
Δ=.045" @ 3550 lbs
Δ=.045" @ 3575 lbs
Δ=.045" @ 3600 lbs
Δ=.045" @ 3625 lbs
Δ=.045" @ 3650 lbs
Δ=.045" @ 3675 lbs
Δ=.045" @ 3700 lbs
Δ=.045" @ 3725 lbs
Δ=.045" @ 3750 lbs
Δ=.045" @ 3775 lbs
Δ=.045" @ 3800 lbs
Δ=.045" @ 3825 lbs
Δ=.045" @ 3850 lbs
Δ=.045" @ 3875 lbs
Δ=.045" @ 3900 lbs
Δ=.045" @ 3925 lbs
Δ=.045" @ 3950 lbs
Δ=.045" @ 3975 lbs
Δ=.045" @ 4000 lbs
Δ=.045" @ 4025 lbs
Δ=.045" @ 4050 lbs
Δ=.045" @ 4075 lbs
Δ=.045" @ 4100 lbs
Δ=.045" @ 4125 lbs
Δ=.045" @ 4150 lbs
Δ=.045" @ 4175 lbs
Δ=.045" @ 4200 lbs
Δ=.045" @ 4225 lbs
Δ=.045" @ 4250 lbs
Δ=.045" @ 4275 lbs
Δ=.045" @ 4300 lbs
Δ=.045" @ 4325 lbs
Δ=.045" @ 4350 lbs
Δ=.045" @ 4375 lbs
Δ=.045" @ 4400 lbs
Δ=.045" @ 4425 lbs
Δ=.045" @ 4450 lbs
Δ=.045" @ 4475 lbs
Δ=.045" @ 4500 lbs
Δ=.045" @ 4525 lbs
Δ=.045" @ 4550 lbs
Δ=.045" @ 4575 lbs
Δ=.045" @ 4600 lbs
Δ=.045" @ 4625 lbs
Δ=.045" @ 4650 lbs
Δ=.045" @ 4675 lbs
Δ=.045" @ 4700 lbs
Δ=.045" @ 4725 lbs
Δ=.045" @ 4750 lbs
Δ=.045" @ 4775 lbs
Δ=.045" @ 4800 lbs
Δ=.045" @ 4825 lbs
Δ=.045" @ 4850 lbs
Δ=.045" @ 4875 lbs
Δ=.045" @ 4900 lbs
Δ=.045" @ 4925 lbs
Δ=.045" @ 4950 lbs
Δ=.045" @ 4975 lbs
Δ=.045" @ 5000 lbs

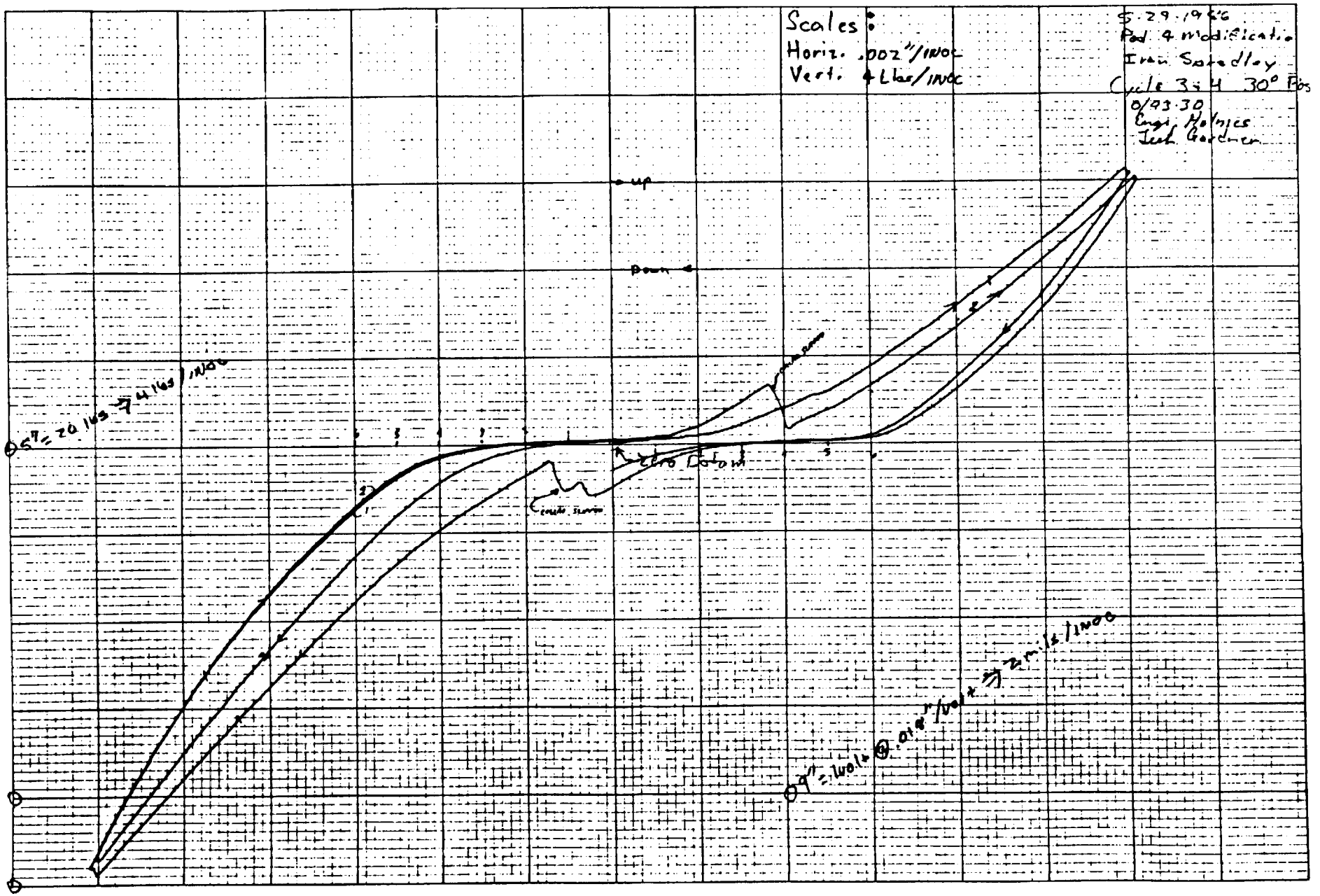
Scales:
Horiz. .002"/INOC
Vert. 4 Lbs/INOC
5-29-1966
Pad 4 Modification
Iron Spredley
Cycle 3 & 4 30° Pos
0/93-30
Engr. Holmes
Jack Gardner
up
down
Zero Datum
5" = 20 lbs → 4 lbs/INOC
9" = 1 volt @ .018"/volt → 2 mils/INOC

Sept. 1956
Pads 4 Modification
Iron Spradley
Cycles 546 60°P
± .012"
0/93-30
Engr. Holmes
Inst. Gardner
Scales
Horiz. .002"/inch
Vert. 4 Lbs/inch
Pads
Load Decrease
Talc Slurry
Talc Slurry
Pads
Load Decrease
Talc Slurry
Talc Slurry
Pads
Load Decrease
Talc Slurry
Talc Slurry

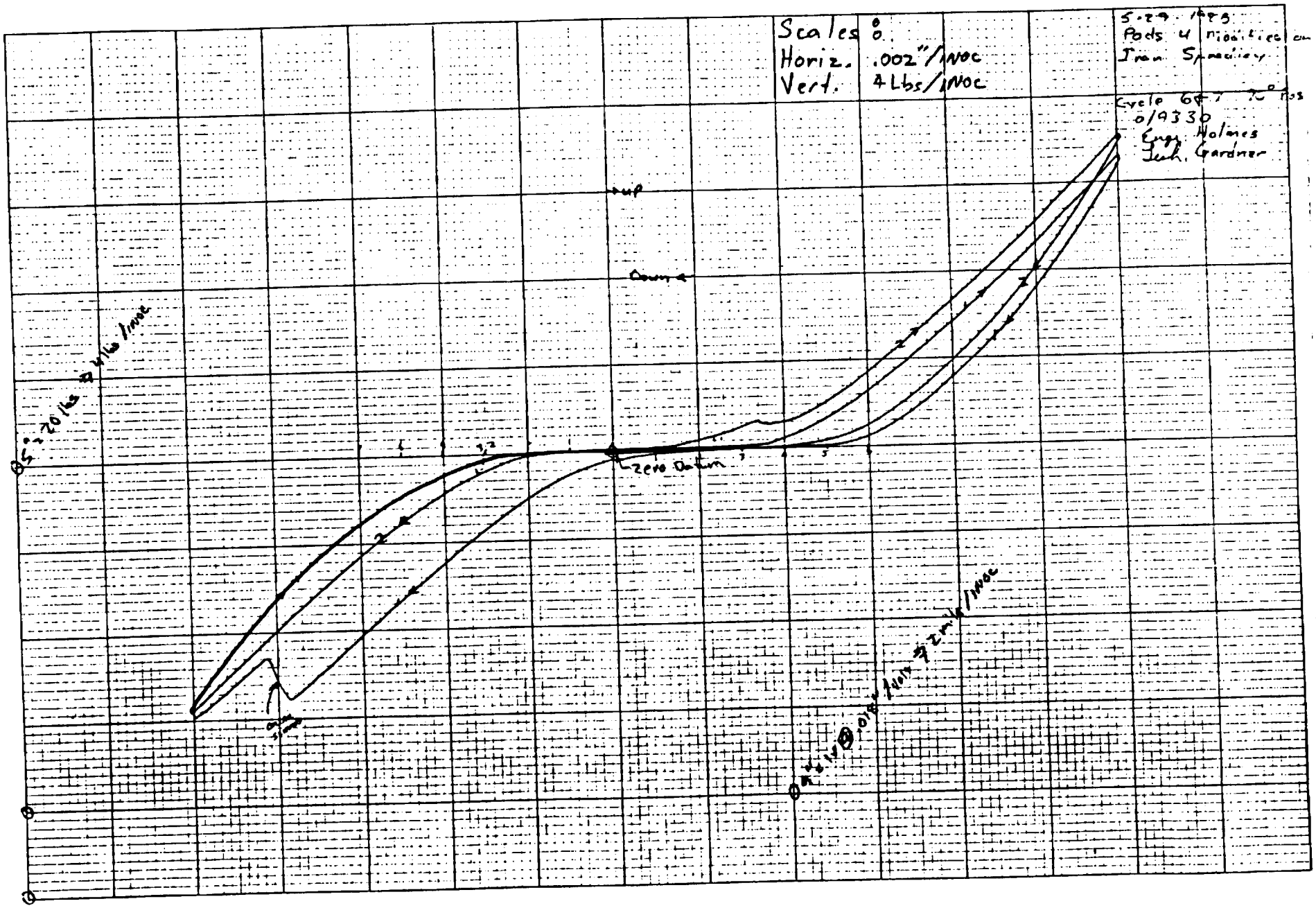
Scales
Horiz. .002"/INOC
Vert. 4 Lbs/INOC
5-29-1983
Pads 4 Modification
Iron Spreading
Cycle 6 & 7
0/9330
Engr. Holmes
Tech. Gardner
up
Down
Zero Datum
5° = 20 lbs @ 4 lbs/INOC
.018"/Volt @ 2 mils/INOC

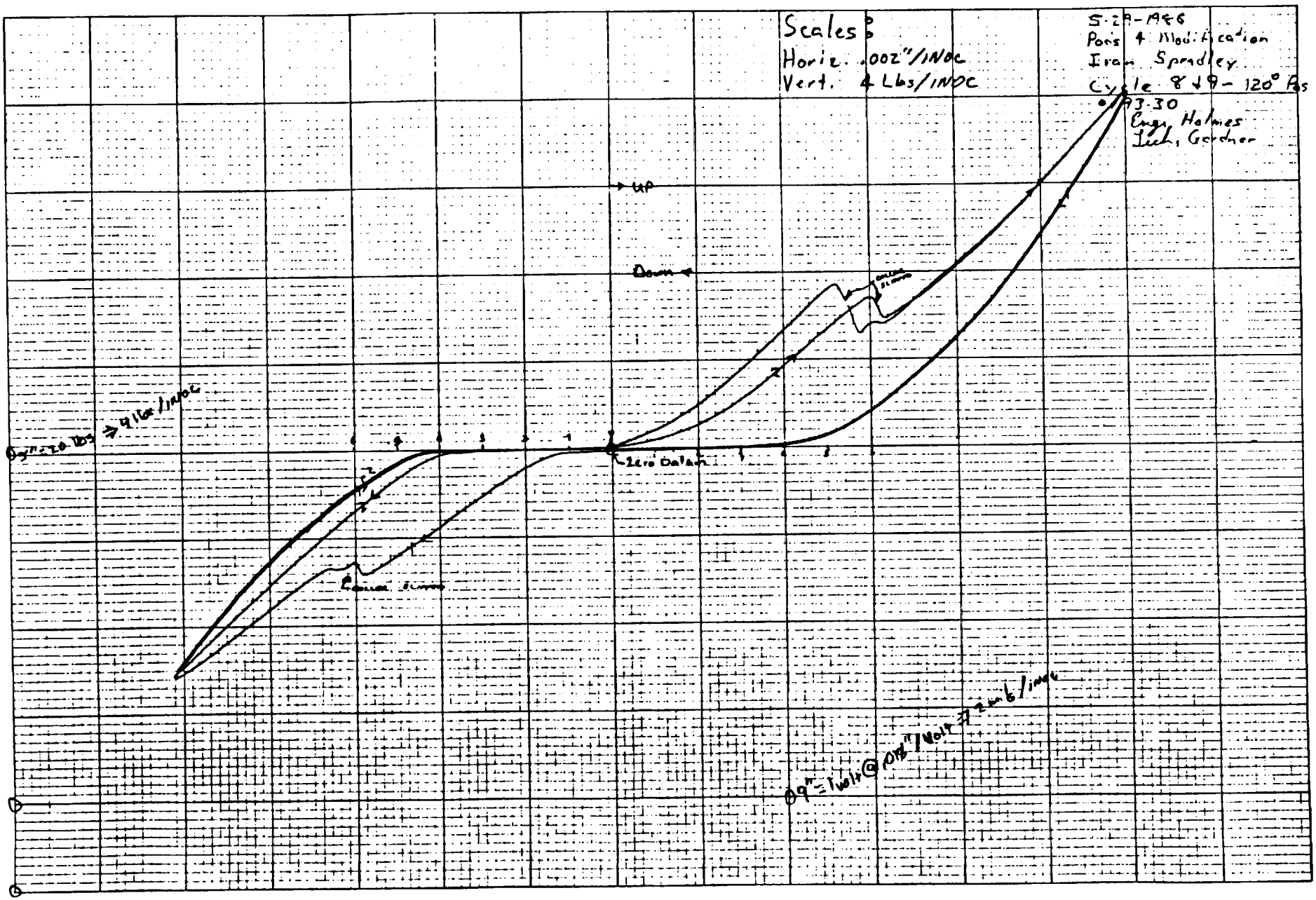
Scales:
Horiz. .002"/INOC
Vert. 4 Lbs/INOC
5-29-1986
Pods 4 Modification
Iran Spradley
Cycle 8 & 9 - 120° Pos
93.30
Engr. Holmes
Tech. Gardner
UP
Down
Zero Datum
9" = 20 lbs ⇒ 9 lbs/INOC
9" = 1 volt @ .018"/volt ⇒ 2 mb/INOC

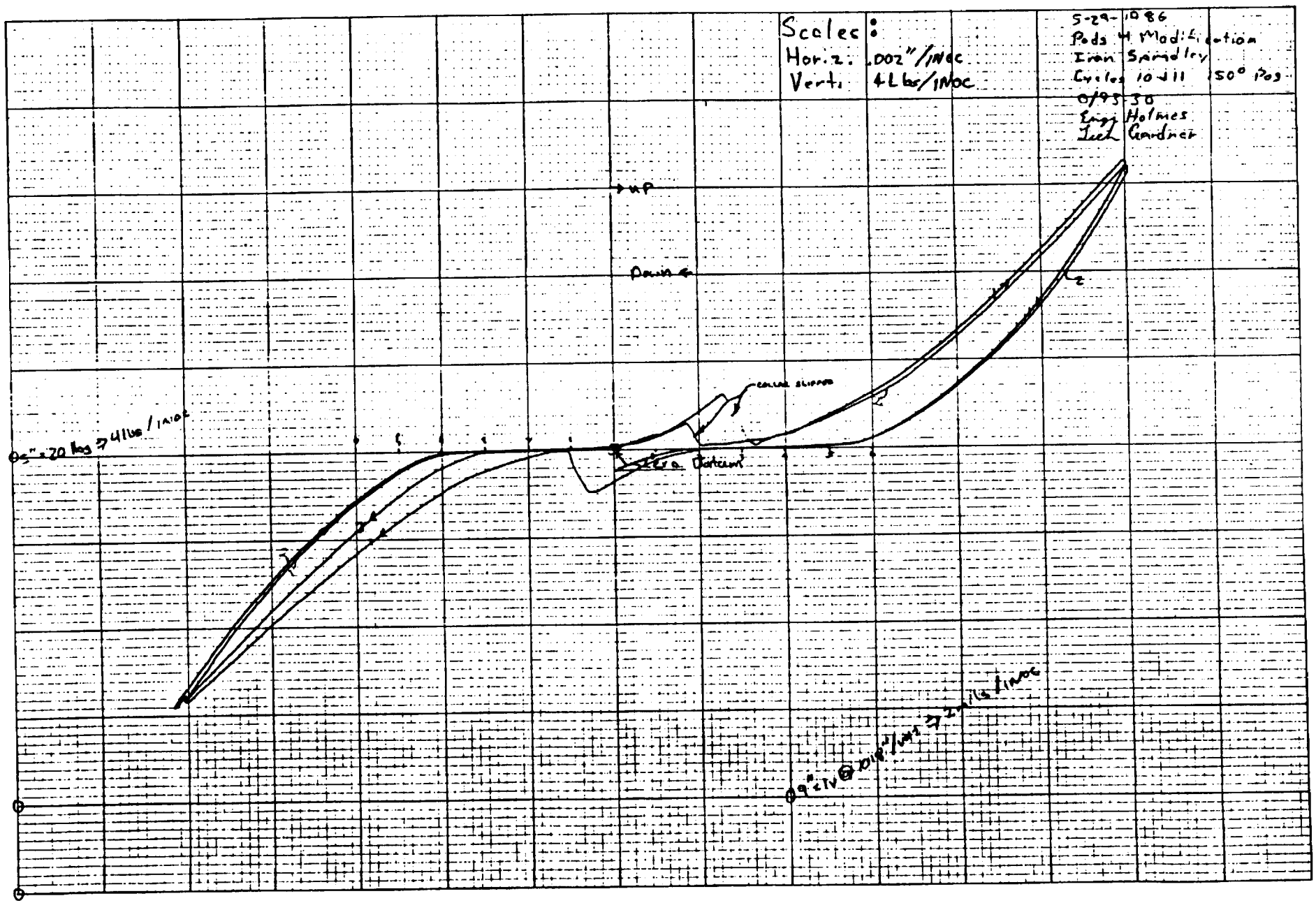
Scales:
Horiz. .002"/INOC
Vert. 4Lbs/INOC
5-29-1986
Pads 4 Modification
Iron Sandley
Cycles 10 & 11 150° Pos
0/93-30
Engr Holmes
Tech Gardner
UP
Down
Collar slipped
Zero Datum
5" = 20 lbs ⇒ 4lbs/INOC
9" = 1V @ .018"/volt ⇒ 2 mils/INOC

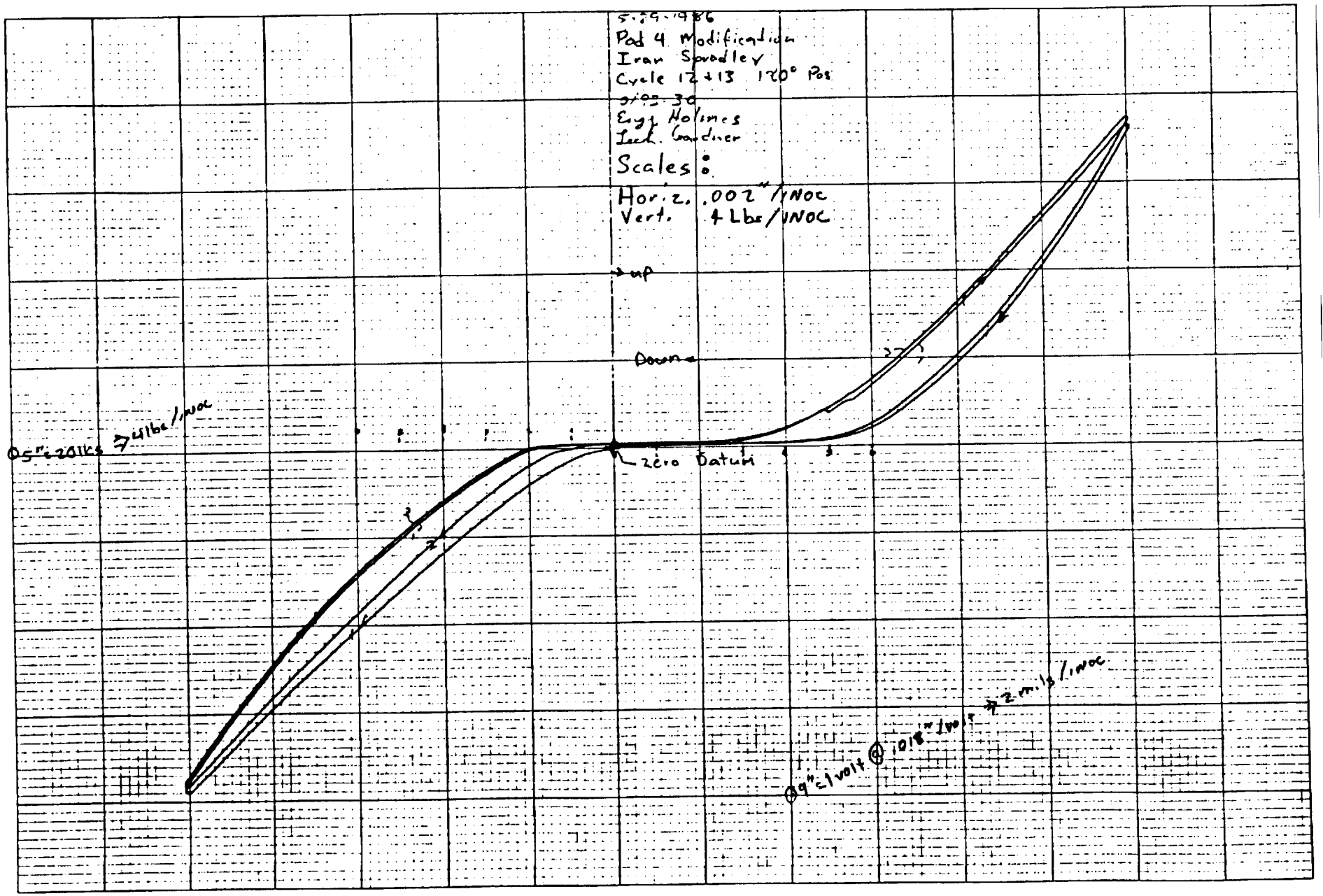
5-29-1986
Pad 4 Modification
Iran Spradley
Cycle 12+13 120° Pos
Eng. Holmes
Tech. Gardner
Scales:
Horiz. .002"/INOC
Vert. 4 Lbs/INOC
up
Down
zero Datum
5" = 20 lbs → 4 lbs/INOC
9" = 1 volt @ .018"/volt → 2 mils/INOC

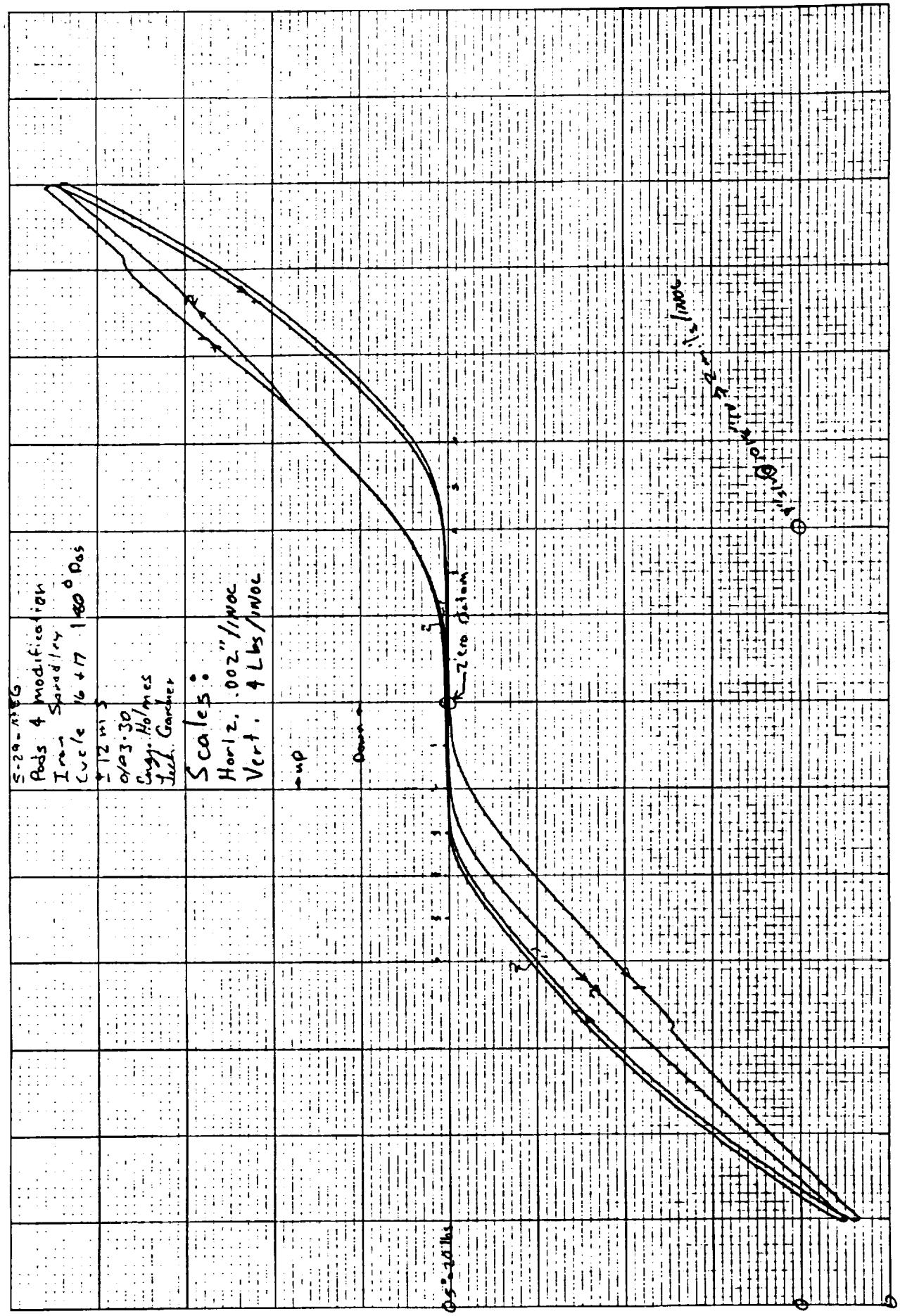
Pods 4 modification
Iron Spradley
Cycle 16+17 180° Pos
Scales:
Horiz. .002"/INOC
Vert. 4 Lbs/INOC
up
Down
Zero Datum

5-29-86
Pods 4 modification
Imah Spradley
Cycle 14 to 210°
1.012"
0/93-39
Hoimes
Gordon
Scales:
Horiz. .002"/inch
Vert. 4 Lbs/inch
Top
Panel
Zero
Zero
Zero

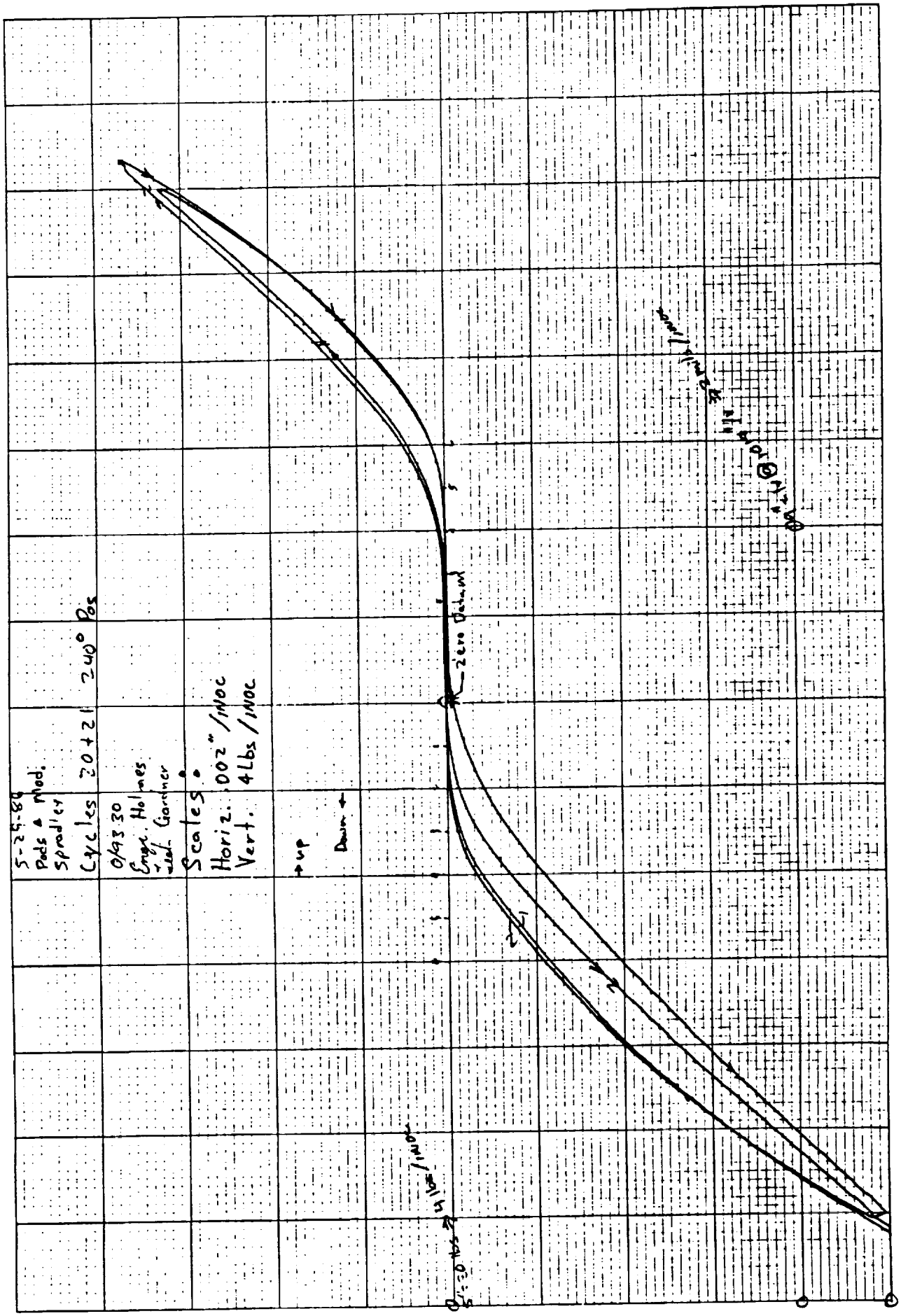
5-29-86
Pads & Mod.
Spradley
Cycles 20+21 240° Pos
0/93 30
Engr. Holmes
Gardner
Scales:
Horiz. .002"/INOC
Vert. 4Lbs/INOC
up
Down
zero Datum
4 lbs/INOC

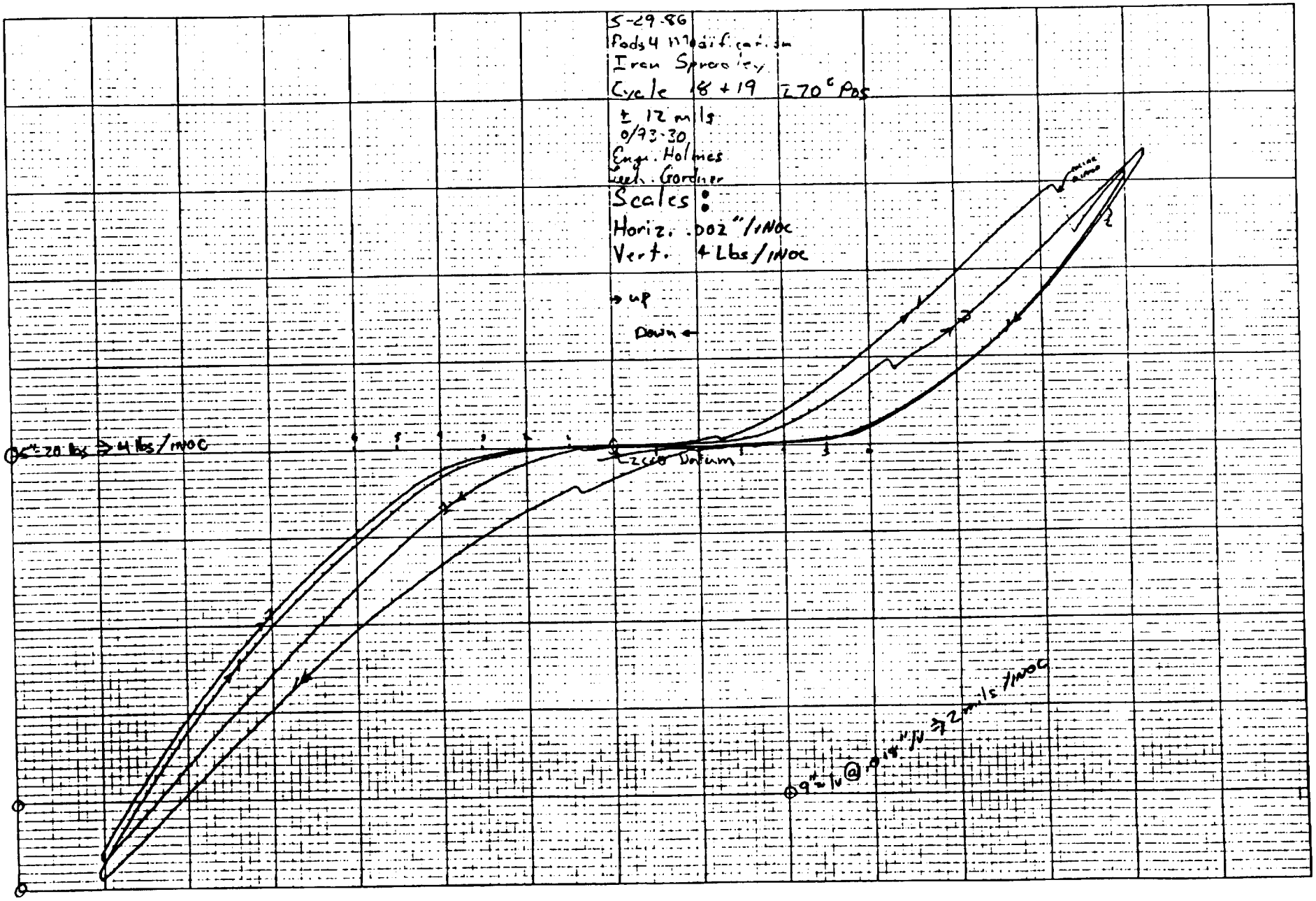
5-29-86
Pads 4 Modification
Iron Sprocket
Cycle 18 + 19 ≈ 70° Pos
± 12 mils
0/93-30
Engr. Holmes
Tech. Gardner
Scales:
Horiz. .002"/INOC
Vert. 4 Lbs/INOC
→ up
Down ←
5" = 20 lbs ⇒ 4 lbs/INOC
Zero Datum
9" = 1v @ .018"/v ⇒ 2 mils/INOC

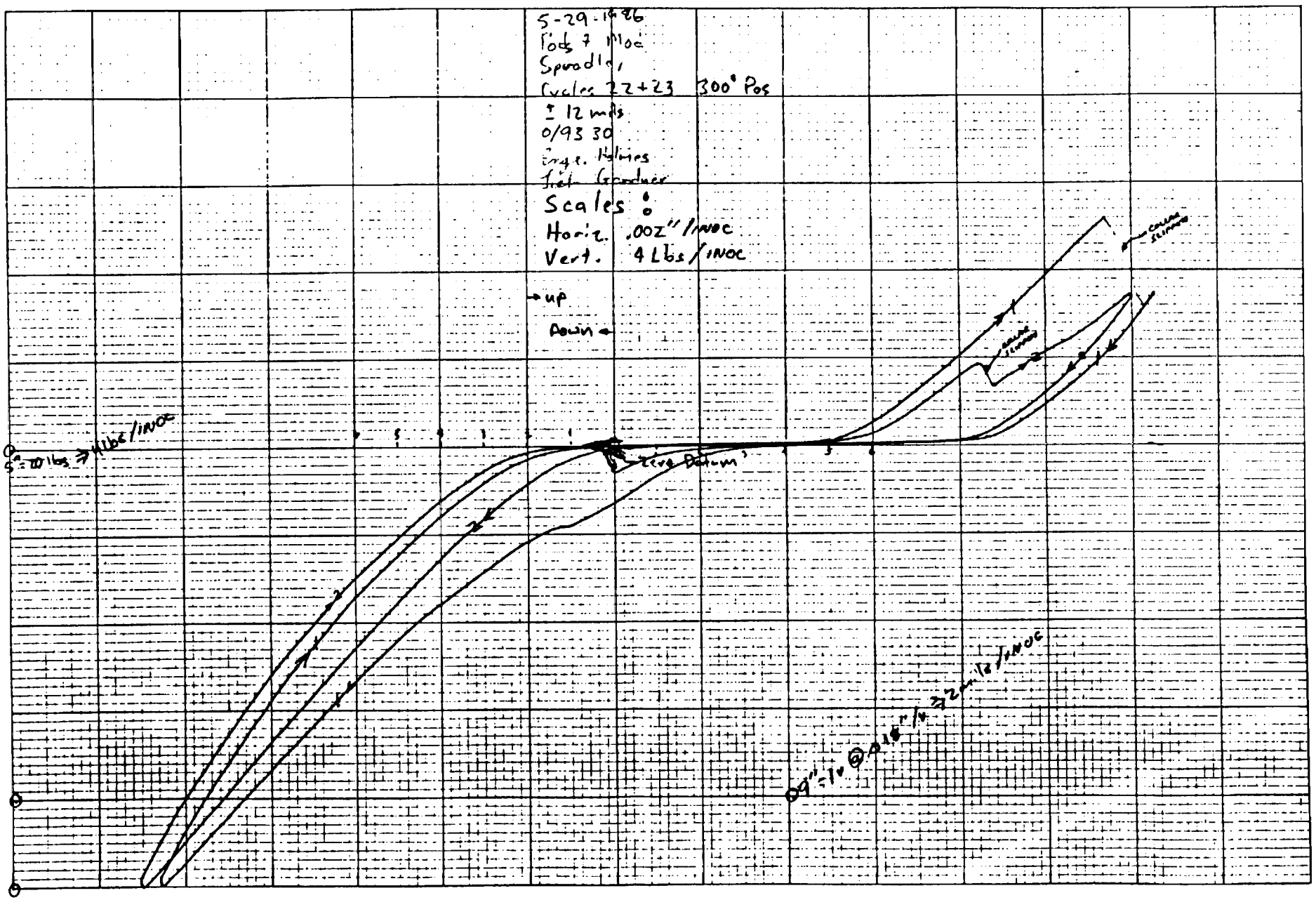
5-29-1986
Pods 7 Mod
Spreadley
Cycles 22+23 300° Pos
± 12 mils
0/93 30
Scales:
Horiz. .002"/INOC
Vert. 4 Lbs/INOC
up
Down
Zero Datum

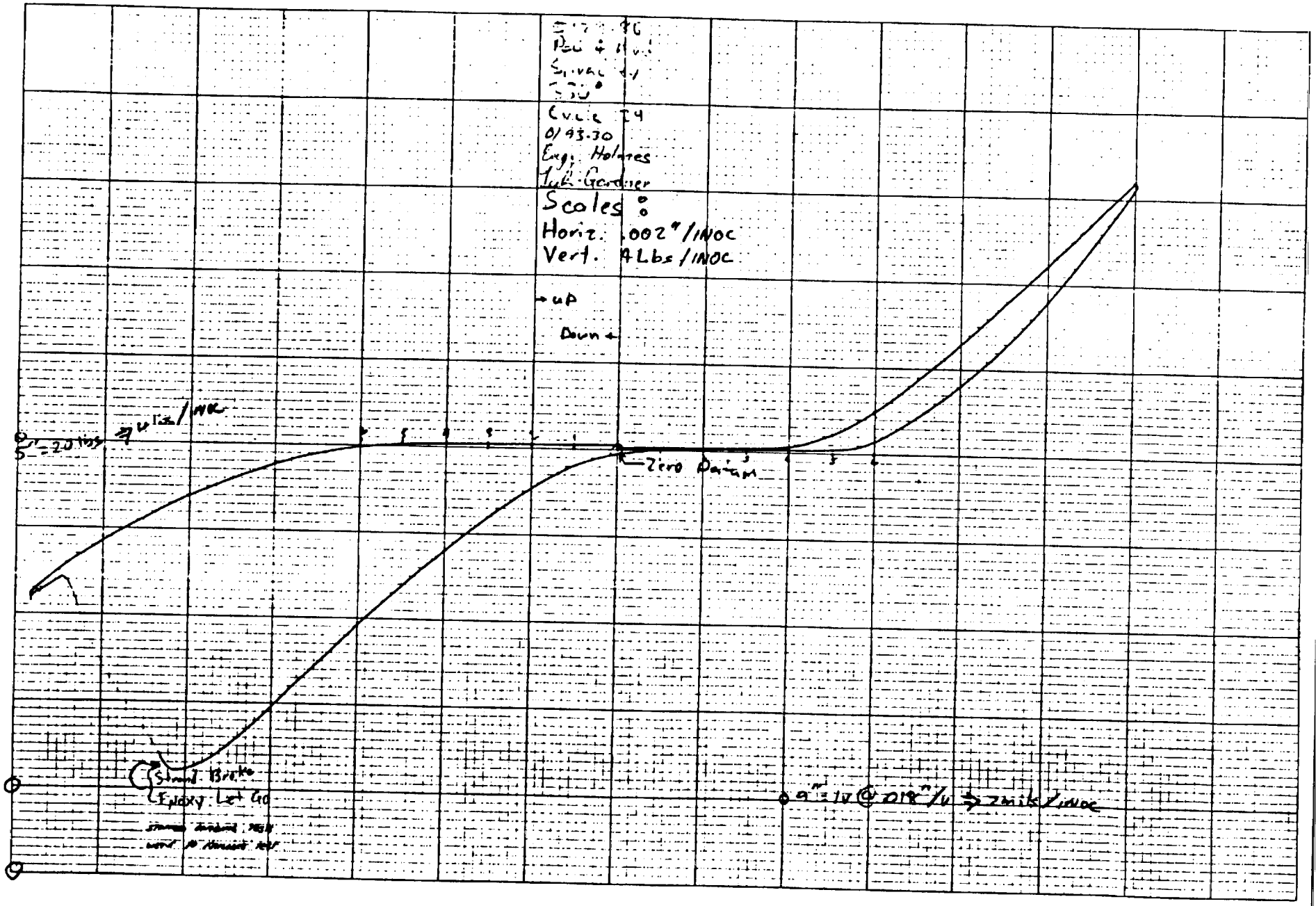
Cycle 24
0/93-30
Eng. Holmes
Tech. Gardner
Scales:
Horiz. .002"/INOC
Vert. 4Lbs/INOC
→ up
Down ←
5" = 20 lbs ⇒ 4 lbs/INOC
Zero Datum
Strand Broke
Epoxy Let Go
9" = 1V @ .018"/V ⇒ 2 mils/INOC

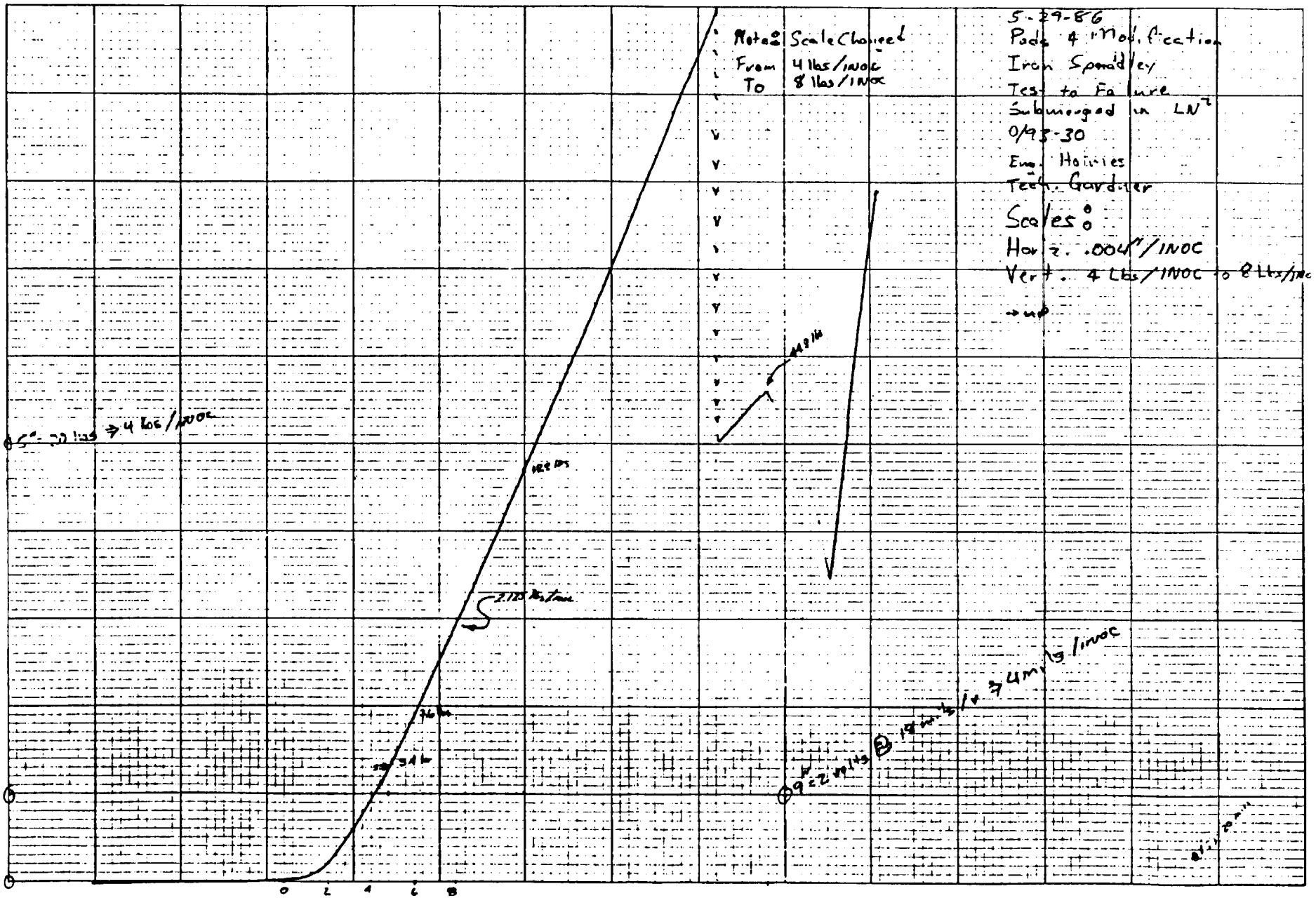
Note: Scale Changed
From 4 lbs/INOC
To 8 lbs/INOC
5-29-86
Pads 4 Modification
Iron Spindley
Test to Failure
Submerged in LN2
0193-30
Engr. Haines
Tech. Gardner
Scales
Horiz. .004"/INOC
Vert. 4 Lbs/INOC to 8 Lbs/INOC
→up

DISTRIBUTION LIST

National Aeronautics and Space Administration
Attn: L. B. Holcomb/RC
Washington, D.C. 20546

National Aeronautics and Space Administration
Attn: M. Sokoloski/RC
Washington, D.C. 20546

National Aeronautics and Space Administration
Attn: John DiBattista/RC
Washington, D.C. 20546

National Aeronautics and Space Administration
Attn: Wayne Hudson/RS
Washington, D.C. 20546

National Aeronautics and Space Administration
Attn: N. W. Boggess/EZB
Washington, D.C. 20546

National Aeronautics and Space Administration
Attn: G. P. Newton/EZA
Washington, D.C. 20546

National Aeronautics and Space Administration
Attn: R. E. Halpern/EN
Washington, D.C. 20546

National Aeronautics and Space Administration
Attn: E. Reeves/EM
Washington, D.C. 20546

National Aeronautics and Space Administration
Attn: C. Pellerin/EZ
Washington, D.C. 20546

National Aeronautics and Space Administration
Attn: J. W. Moore/M
Washington, D.C. 20546

National Aeronautics and Space Administration
Attn: D. H. Herman/SE
Washington, D.C. 20546

National Aeronautics and Space Administration
Attn: Dr. W. P.Raney/SU
Washington, D.C. 20546

Goddard Space Flight Center
National Aeronautics and Space Administration
Attn: A. Sherman/Code 713
Greenbelt, MD 20771

Goddard Space Flight Center
National Aeronautics and Space Administration
Attn: M. Sedlazek/Code 400.6
Greenbelt, MD 20771

Goddard Space Flight Center
National Aeronautics and Space Administration
Attn: S. Castles, Code 713
Greenbelt, MD 20771

Lewis Research Center
National Aeronautics and Space Administration
Attn: E. P. Symons/501-6
21000 Brookpark Drive
Cleveland, OH 44135

George C. Marshall Space Flight Center
National Aeronautics and Space Administration
Attn: L. Hastings/EP43
E. Urban/ES63
Huntsville, AL 35812

Jet Propulsion Laboratory
Attn: D. D. Elleman 183-401
D. G. Elliott 125-224
4800 Oak Grove Drive
Pasadena, CA 91109

National Bureau of Standards
Attn: P. Ludtke
325 Broadway
Boulder, CO 80303

AFWAL/Flight Dynamics Lab
Attn: Mr. Haskins
Wright-Patterson AFB, OH 45433

Air Force Space Division
Kevin O'Brian
P. O. Box 92960
Worldway Postal Center
Los Angeles, CA 90009

BMD/ATCO
Attn: Mr. W. O. Davies
P. O. Box 1500
Huntsville, AL 35807

AFRPL
Attn: R. A. Silver
Edwards AFB, CA 93523

Hughes Aircraft Co.
Attn: George Specke
Bldg. E51
MS A 286
2000 E. El Segundo Blvd.
P. O. Box 902
El Segundo, CA 90245

Ball Aerospace Systems Division
Attn: A. R. Urbach
P. O. Box 1062
Boulder, CO 80306

Beech Aircraft Corporation
Attn: Dr. Hal Gier
P. O. Box 9631
Boulder, CO 80301

Garrett Ai Research Company of California
Attn: C. W. Browning
2525 W. 190th Street
Torrance, CA 90509

Ames Research Center
Attn: M. Murphy/244-5
C. McCreight/244-10
J. H. Lee/244-10
W. Brooks/244-15
J. Mansfield/244-15
J. M. Lee/244-10

Technology Utilization Office/240-2
Patent Counsel/200-11A
P. Kittel/244-10 (11 copies)

Martin Marietta Aerospace
Attn: D. A. Fester
P. O. Box 179
Denver, CO 80201

Johnson Space Center
National Aeronautics and Space Administration
Attn: R. Kahl/EP4
Houston, TX 77058

1. Report No.	2. Government Accession No.	3. Recipient's Catalog No.
NASA CR 177426		

4. Title and Subtitle	5. Report Date
Passive Orbital Disconnect Strut (PODS-IV) Development	Sep 1986
	6. Performing Organization Code
7. Author(s)	8. Performing Organization Report No.
I. Spradley	
	10. Work Unit No.
9. Performing Organization Name and Address	T7459
Lockheed Missiles & Space Company Palo Alto, CA 94304	11. Contract or Grant No.
	NAS2-11946
	13. Type of Report and Period Covered
12. Sponsoring Agency Name and Address	Contractor Report
National Aeronautics and Space Administration Washington, D. C. 20546	14. Sponsoring Agency Code
	506-45-31

15. Supplementary Notes

Point of Contact: Technical Monitor, Peter Kittel, MS 244-10, Ames Research Center, Moffett Field, CA 94035
415-694-6525 or FTS 8-464-6525

16. Abstract

The objectives are: (1) design structurally and thermally a mechanism to increase PODS resistance to side loads; (2) fabricate the mechanism and modify a PODS-III strut (PODS-IV); (3) structurally test mechanism and strut to determine improvement in side-load resistance.

Task 1 – Design. A mechanism was designed to modify existing PODS-III struts to withstand greater side loads (PODS-IV). The design consists of a collar suspended around the PODS-III cold end stem by graphite filaments that are attached to the PODS-III nut via a filament support ring. Side-load "shorting" is resisted by filament strain. An analytic model was developed to predict mechanism side-load resistance and strut thermal degradation.

Task 2 – Fabrication. An assembly fixture was constructed to wrap the filaments. A whiffle-tree was used to equally load each filament and suspend the collar.

Task 3 – Testing. Initial testing of the mechanism included circumferential loading at room temperature followed by an ultimate load test at liquid-nitrogen temperature. Side-load tests were performed on a modified strut at inclination angles from 0 to 60 degrees. Results were compared to previous PODS-III results and predicted values.

17. Key Words (Suggested by Author(s))	18. Distribution Statement
Low heat leak supports Cryogen storage Analysis, Design, Fabrication, Test	UNCLASSIFIED-UNLIMITED STAR Category - 18

19. Security Classif. (of this report)	20. Security Classif. (of this page)	21. No. of Pages	22. Price*
UNCLASSIFIED	UNCLASSIFIED	86	

*For sale by the National Technical Information Service, Springfield, Virginia 22161